UNIVERSITY OF TROMSØ UIT

FACULTY OF SCIENCE AND TECHNOLOGY
DEPARTMENT OF GEOLOGY

Late Paleozoic-Cenozoic fault correlation and characterization of fault rocks in western Troms, North Norway

Jean-Baptiste Koehl

GEO-3900 Master's Thesis in Geology

May 2013

Acknowledgement

I would like to warmly thank Prof. Steffen Bergh for the time he spent with me in the field, discussing the data and correcting my written English. His experience and geological skills, notably in the field, and his passion for structural geology and tectonics are a source of inspiration for me. Steffen, it has been a real honour to work with you.

Thank you very much to my secondary supervisor Prof. Holger Stunitz for his help in characterizing the fault rocks, his experience in the field and, above all, his great teaching skills.

I am also very thankful to Kjetil Indrevær for his constant good mood, his unlimited patience, his pedagogy and, most of all, for his constant support. You have been a really nice buddy through these two years and I feel honoured to be your friend!

Kisses to all my international friends with whom I spent so many incredible and wonderful moments in Tromsø! Thanks also to the University of Tromsø and more particularly to the geology department and the international and master students offices. Thanks to all of you I have a second place in the world I can call “Home”.

Merci à toi mon Toumou. Je n’oublierai jamais ma demande en marriage et nos fiançailles, ni tous les bons moments qu’on a pu partager entretemps… héhhhéééé! Merci aussi à Michel le pti-gros de m’avoir débarrassé de la grosse, ouaiiis… et à Coucouille pour les poumons grillés, désolé…

Enfin… merci à toute la famille Koehl & Cie, mes deux grosses, papa, maman, car chaque moment passé à vos côtés n’est que pur Bonheur et que quoiqu’il arrive on s’en sortira toujours ensemble!

Never say never

JB Koehl,

29th Mai 2013

Abstract

The present work focuses on the mapping and description of onshore brittle fault zones on the SW Barents Sea Margin, within gneisses and granitic intrusions belonging to the West Troms Basement Complex. The description of the brittle structures includes the geometry, kinematics and fault rock characteristics, using DEM satellite imaging, structural field work and a microstructural analysis of the fault rocks. As a result of the present study, two major sets of onshore brittle faults have been observed, trending NNE-SSW and ENE-WSW, and they are tentatively correlated in two, NE-SW trending fault complexes: the Rekvika and the Vestfjorden-Vanna fault complexes. These fault complexes run parallel to the Troms-Finnmark fault complex that borders major offshore sedimentary basins in the NW. On the one hand, the Vestfjorden-Vanna fault complex defines the southeastern boundary of the West Troms Basement Complex towards the Caledonian nappes, and is made of wide fault zones that have experienced major displacement (ca. 1-3km). On the other hand, the Rekvika fault complex is considered as an intra-horst fault system, composed of narrow fault zones that are thought to have accommodated low amounts of displacement (> 250 m). On a local scale, the fault zones display similarities in attitude (trend and dip) with the Caledonian and Precambrian fabrics, indicating a possible influence of pre-existing zones of weakness on brittle faulting. The dominant deformation mechanism (cataclastic flow) indicates pressure range about 0.2-0.3 GPa, i.e. 5-10 km depth for the formation of the cataclastic fault rocks, and these fault rocks contain mineral assemblages that generally indicate temperatures about 350-500°C. This suggests that the West Troms Basement Complex has been largely uplifted later on, until present level. The NNE-SSW and ENE-WSW trending fracture sets are believed to have formed synchronously due to WNW-ESE extension, during an early stage of rifting in the Permian-Early Triassic. The NNE-SSW trending faults likely represent the main fault system, orthogonal to the extension direction, and the ENE-WSW trending faults may correspond to oblique transfer zones that link the NNE-SSW fault segments. An alternative model implies NW-SE trending transfer zones to link the NNE-SSW faults. A late stage of minor reverse reactivation of the NNE-SSW and ENE-WSW trending faults, and the development of NW-SE striking fractures are tentatively correlated to ridge-push forces during the opening of the North Atlantic in the Eocene.

Contents

1 Introduction

1.1 Frame of the project

This master thesis is part of an ongoing project between the University of Tromsø (UiT) and DONG Energy (Dansk Olie og NaturGas) as the continuation of the work initiated by the UiT, Statoil, Det Norske and Front Exploration. The general goal of this project is to characterize the nature and the movement history of major brittle fault zones on the North-Norwegian Continental Shelf, from the Lofoten-Vesterålen Margin in the South to Finnmark in the North, and to correlate them with offshore structures bounding major Late Paleozoic-Cenozoic basins on the western part of the Barents Sea continental shelf offshore. The interest for the Barents Sea Margin has recently reached its climax due to the new discovery of one of the largest oil field offshore Northern Norway (Skrugard), which is located along one of the major normal/oblique faults in the central part of the Barents Sea, the NE-SW striking Bjørnerenna fault complex. This fault complex tends to parallel the Troms-Finnmark fault complex (Fig. 1) and potentially corresponds with similarly oriented onshore brittle faults in Troms (Fig. 2).

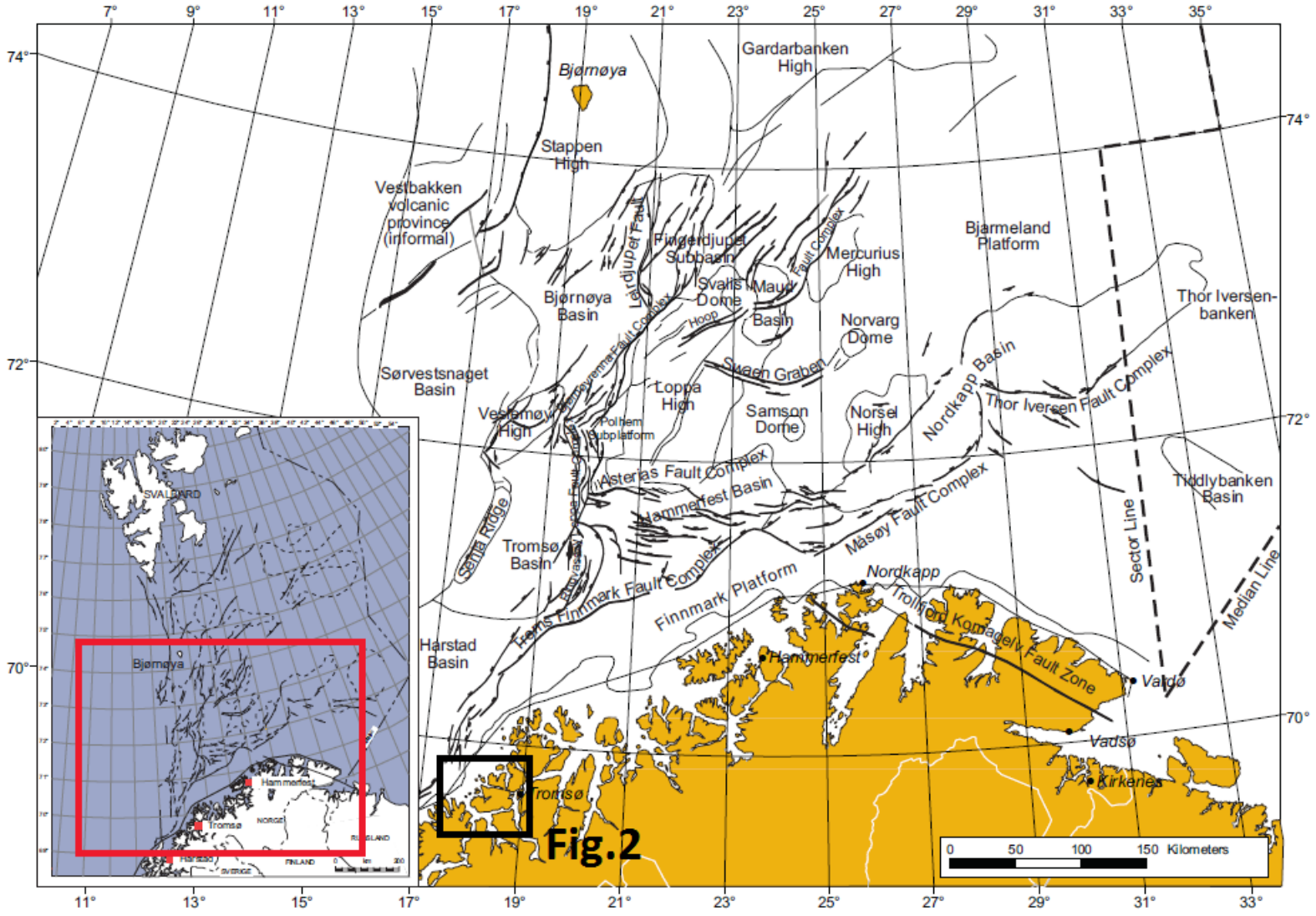

Figure 1: Structural elements of the SW Barents Sea Margin, from Larssen et al. (2002)

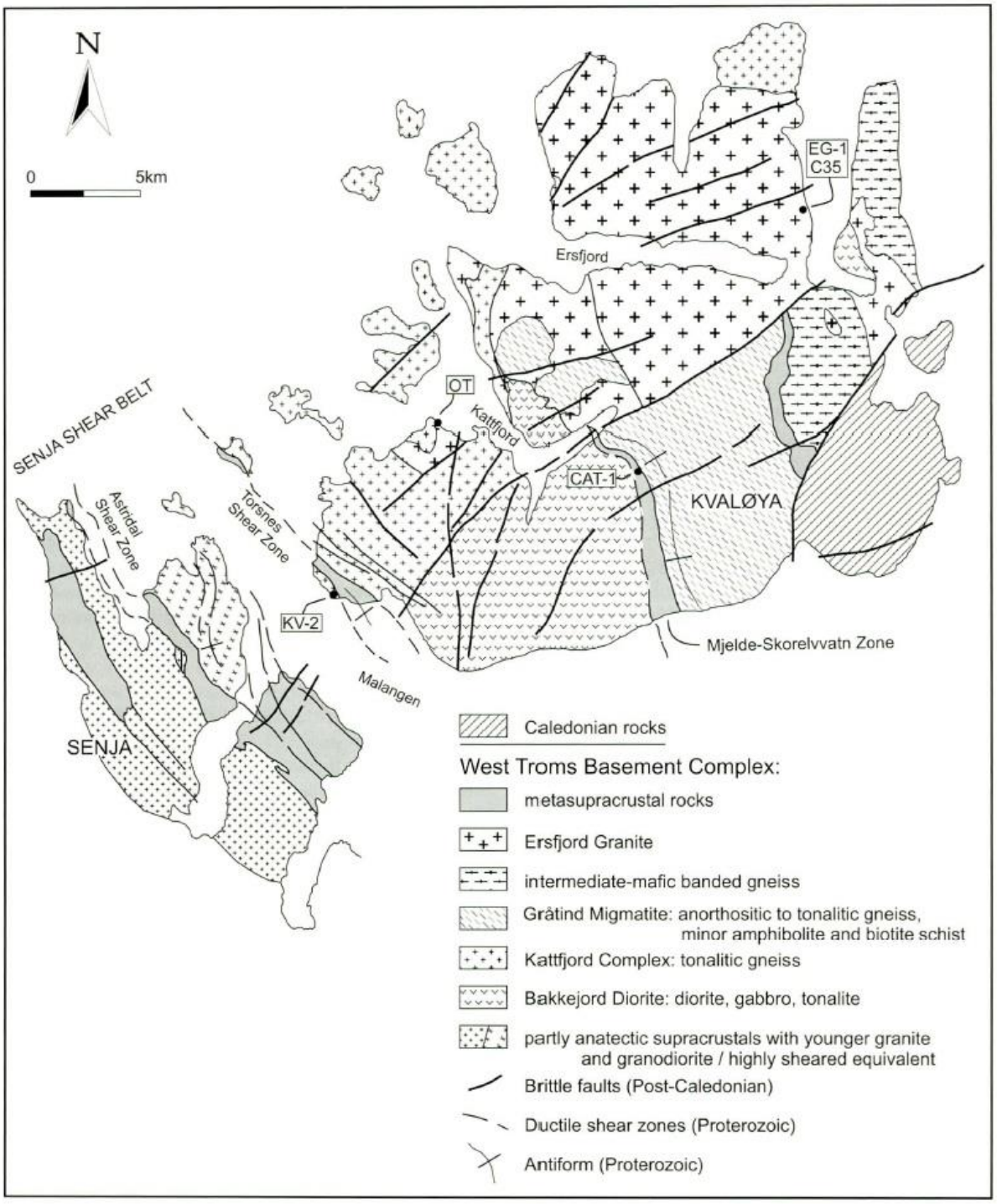

<u>Figure 2:</u> Geological Map of Kvaløya and Northernmost Senja showing the location of presumed brittle faults in addition to the basement rocks and the ductile fabrics (Corfu et al. 2003a); see location on figure 1.

1.2 Aim and goals

The continental shelf offshore western Troms is located at the transition between the extensive Mid-Norwegian Continental Shelf and the transpressional-transtensional Barents Sea and Svalbard margins. It is commonly accepted that this part of the continental shelf

underwent several post-Caledonian extensional events during the rifting of the North-Atlantic Ocean (Bergh et al. 2007a; Eig et al. 2008a; Hansen et al. 2011, 2012). Brittle faulting related to this period was comprehensive and widespread throughout the margin, and faulting may have controlled sedimentation, ridge-basin (horst-graben) formation and the structural architecture in general, as well as later leaking of oil and gas in the sedimentary strata of the basins (Gabrielsen et al. 1990; Faleide et al. 1993; Gudlaugsson et al. 1998; Brekke 2000; Larssen et al. 2002). Although onshore fault equivalents to major basin-bounding faults offshore have been recorded on the Lofoten-Vesterålen Margin (Olesen et al. 1997; Bergh et al. 2007a; Eig et al. 2008a; Hansen et al. 2011, 2012) complementary work is required for the Troms portion of the margin where only few onshore brittle fault zones have been studied in detail (Forslund 1988; Gagama 2005; Antonsdóttir 2006).

The present work focuses on the network of potentially Late Paleozoic-Cenozoic brittle faults on the islands of Kvaløya and Senja in western Troms (Fig. 2 and 3). These islands are part of a basement horst that extends from Lofoten in the south where it is referred as the Lofoten Ridge (Blystad et al. 1995; Tsikalas et al. 2005; Wilson et al. 2006; Bergh et al. 2007a; Eig et al. 2008a; Hansen et al. 2012), via the islands of Senja and Kvaløya, to Vanna in the north where the ridge of Precambrian rocks is commonly called the West Troms Basement Complex (see fig. 4; Olesen et al. 1997; Corfu et al. 2003a; Bergh et al. 2010). In the south, the Lofoten Ridge is flanked by major fault zones that border the offshore Vestfjorden and Ribban basins (Blystad et al. 1995; Bergh et al. 2007a; Hansen et al. 2012). Further north, in Troms, this basement high is bounded to the east by the Straumsbukta-Kvaløysletta fault belonging to the Vestfjorden-Vanna fault complex and that down-dropped the Caledonian nappes several kilometers to the east (Fig. 4; Forslund 1988; Olesen et al. 1997; Roberts and Lippard 2005). However, no specific major onshore fault that could correspond to the horst-bounding offshore fault (Troms-Finnmark fault complex) against the Tromsø and Hammerfest basins has yet been observed on the western edge (Fig. 1).

The main goal of this work is on a specific brittle fault system, the Rekvika fault zone (Fig. 2; Antonsdóttir 2006) in the western and interior part of the basement horst in Kvaløya (Fig. 2) that has previously not been analyzed in any detail and not even recognized (cf. Hansen et al. 2011). One of the key aims resides in providing a regional structural map

(gathering the nature of the brittle fault, the location of rock-type boundaries, and structural orientation data) of the Rekvika fault zone, including all possible subsidiary faults from the perspective of characterizing the fault pattern (geometry in map and cross-sections), discuss the kinematics (sense of shear indicators, slickensides, offsets, and potential fault association such as rotation, bending and duplex) and the fault rock behavior (characteristics of fault core and damage zone, fault rock description & classification in cross-section and lateral variations, mineral composition, type of deformation through microtextural analysis) as a framework for regional comparison with onshore fault trends on the Lofoten-Vesterålen Margin and in Troms, such as the Straumsbukta-Kvaløysletta fault zone. The relative timing of faulting can be inferred from cross-cutting relationships between fault-fracture populations, and the order of deformation succession (one or multiple events?) together with pressure/temperature estimation from microtextural analysis.

Additional fault zones have been investigated the same way on the islands of Kvaløya and Senja, including the Bremneset, Tussøya-Røkneset and Hillesøya faults in western Kvaløya, the Straumsbukta fault (southern tip of the Straumsbukta- Kvaløysletta fault zone) in eastern Kvaløya, and the Stonglandseidet fault zone in Senja (Fig. 4). Their general geometry and kinematic character suggest they belong to an *en echelon* fault pattern on both sides of the basement horst. The present work attempts to investigate and test this hypothesis further, in order to get a better understanding of the brittle faults architecture and their evolution within the basement culmination in Kvaløya and Senja.

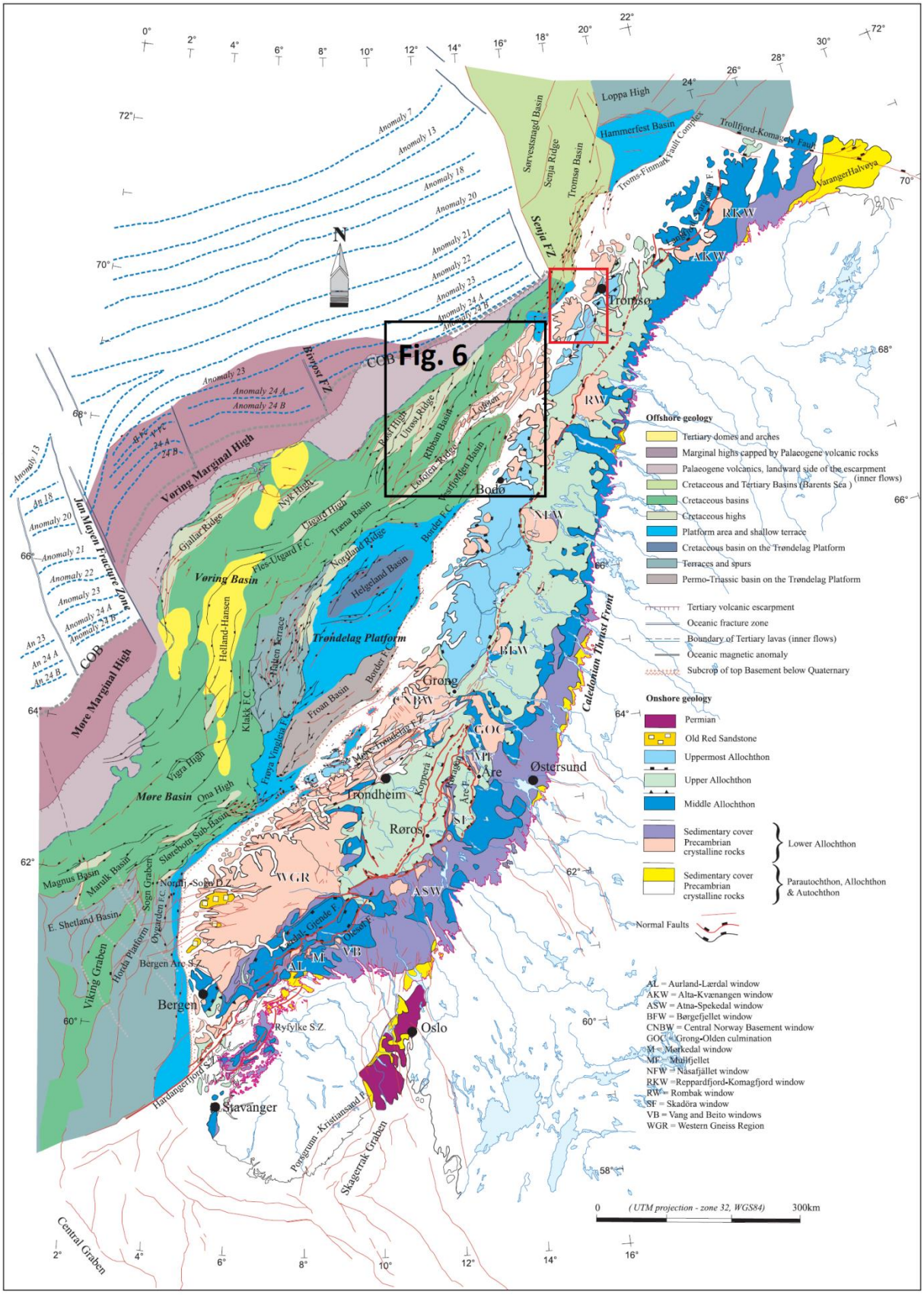

<u>Figure 3:</u> Map of the different lithological units on the Norwegian Continental Shelf. The study area is located by a red frame. From Mosar et al. (2002).

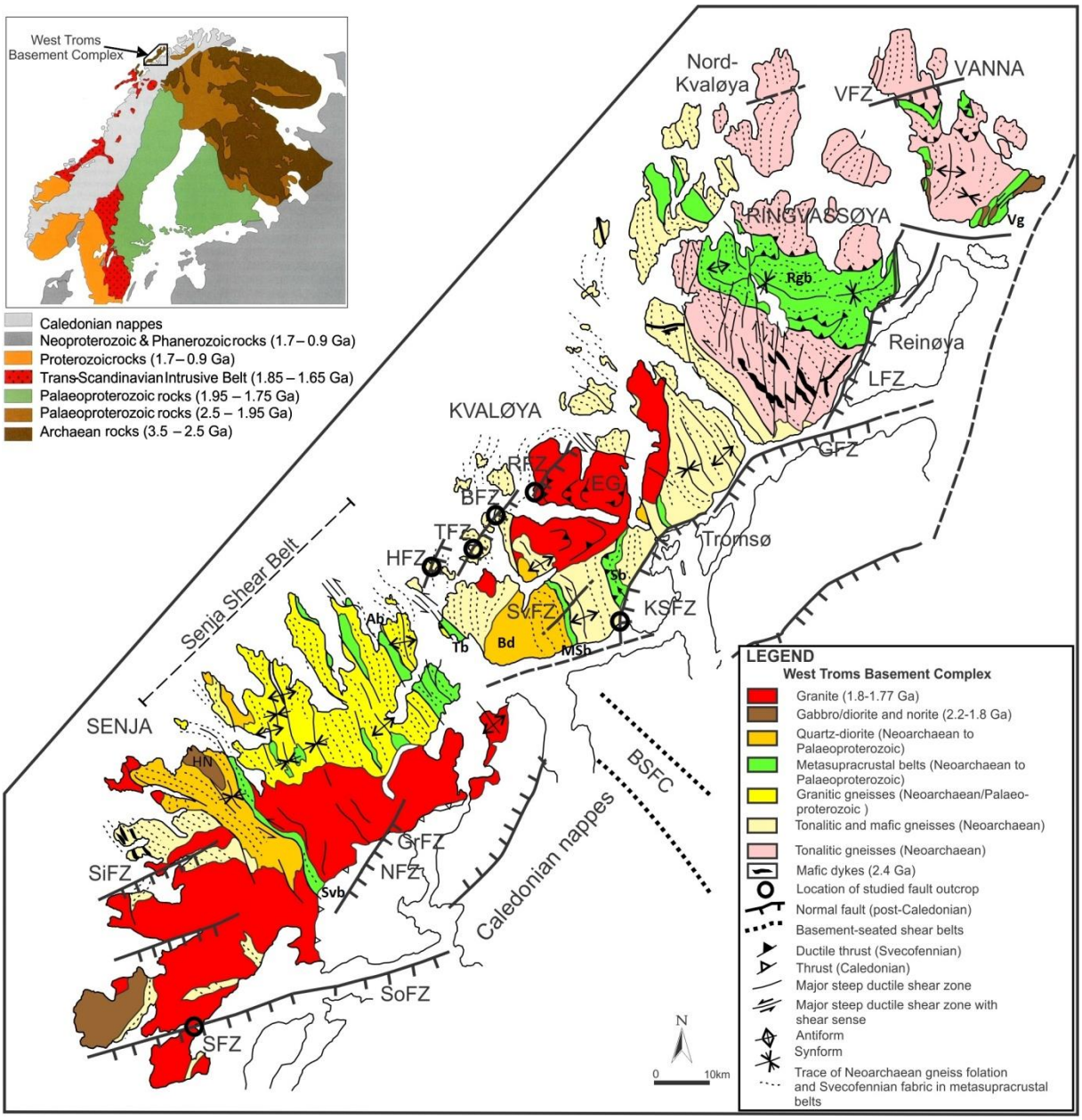

Figure 4: Regional geologic-tectonic map of the West Troms Basement Complex showing the Precambrian fabrics and the post-Caledonian brittle fault zones investigated in this study, and indicated by circles; modified after Bergh et al. (2010) and Indrevær et al. (2013). **Abbreviations: Ab = Astridal belt, Bd = Bakkejord diorite, BFZ = Bremneset fault zone, BSFC = Bothnian-Senja fault complex, EG = Ersfjord granite, GFZ = Grøtsundet fault zone, GrFZ=Grasmyrskogen fault zone, HFZ = Hillesøya fault zone, HN = Hamn Norite, KSFC=Kvaløysletta-Straumsbukta fault zone, LFZ = Langsundet fault zone, MSb = Mjelde-Skorelvvatn belt, NFZ=Nybygda fault zone, RFZ = Rekvika fault zone, Rgb = Ringvassøya greenstone belt, SFZ = Stonglandseidet fault zone, SiFZ = Sifjorden fault zone, SoFZ=Solbergfjorden fault zone, SvFZ = Skorelvvatn fault zone, Sb = Steinskardtind belt, Svb = Svanfjellet belt, Tb = Torsnes belt, TFZ=Tussøya-Røkneset fault zone, Vg = Vanna group, VFZ = Vannareid fault zone.**

1.3 Location of the studied fault zones

The present study was carried out in specific areas where major brittle fault zones are located, on the islands of Kvaløya and Senja in Troms, North Norway (Fig. 4). The

investigated fault zones are all fully located within Precambrian basement rocks belonging to the West Troms Basement Complex (Bergh et al. 2010). A special emphasis was ascribed to the study of the Rekvika fault zone previously described by Antonsdóttir (2006). This fault zone is located in the northwestern part of the basement horst on Kvaløya (Fig. 2) but has previously not been analyzed (even not recognized) in any detail from the perspective of characterizing the map pattern, kinematics, fault rock behavior and framework for correlation (cf. Hansen et al. 2011). Some other fault zones that may possibly be linked to the Rekvika fault zone have recently been observed in the northwestern edge of the basement high, specifically in Bremneset, Tussøya-Røkneset and Hillesøya (Fig. 4). These separate brittle fault zones are tentatively grouped together with the Rekvika fault zone and referred as the *Rekvika fault complex*.

A structural analysis of a portion of the Straumsbukta-Kvaløysletta fault zone (Andresen & Forslund 1987; Forslund 1988; Olesen et al. 1997) in Straumsbukta, on the southeastern edge of the West Troms Basement Complex (Fig. 4) was also carried out for comparison with the Rekvika fault complex. In the island of Senja the investigations were focused on the Stonglandseidet fault zone in the south, that is also located on the southeastern flank of the basement horst (Fig. 4). These faults will later be referred to as the Vestfjorden-Vanna fault complex (Forslund 1988; Olesen et al. 1997; Roberts and Lippard 2005).

1.4 Regional setting and previous work

1.4.1 General geology of Troms

The regional geology of Troms consists of two main components, the Precambrian basement provinces and the Caledonian nappe pile (Fig. 3 and 4), in addition to offshore areas, that cover Palaeozoic through Cenozoic strata (not exposed onshore but in Andøya in Vesterålen).

The Precambrian basement in the west of Troms, also called the West Troms Basement Complex, covers the most part of Kvaløya and Senja, and is composed of various Neoarchean to Palaeoproterozoic tonalitic-trondhjeimitic-granitic (TTG) gneisses, igneous-

intrusive and metasupracrustal rocks (Fig. 4). It has been divided into four units by Bergh et al. (2010): foliated Neoarchean gneisses, Neoarchean to Palaeoproterozoic supracrustal rocks, early Palaeoproterozoic mafic dykes, and Palaeoproterozoic granitic and mafic plutonic intrusions. Similar Neoarchean gneisses and Proterozoic supracrustal rocks have been encountered on the Lofoten-Vesterålen Margin (Griffin et al. 1978; Løseth & Tveten 1996; Corfu 2004). They are intruded by plutons of about the same age than in the West Troms Basement Complex (Corfu et al. 2003a). The Precambrian rock assemblage abruptly disappears under younger Caledonian units in the south-east due to normal brittle faults (Forslund 1988; Zwaan 1995; Olesen et al. 1997).

In the north-east, the Precambrian horst stands adjacent to quartzo-feldspatic gneisses and mafic migmatites from the Nakkedal Nappe Complex (Zwaan et al. 1998; Selbekk et al. 2000; Corfu et al. 2003b; Indrevær 2011), and high-grade ultramafic rocks and metasediments characteristic of the Tromsø Nappe Complex (Krogh et al. 1990; Corfu et al. 2003b; Indrevær 2011). These two nappe complexes are referred as parts of the Uppermost Allochton of the Caledonides (Corfu et al. 2003b; Indrevær 2011). In the south-east, the Precambrian rocks stand alongside ophiolites belonging to the Lyngen Nappe Complex, which is part of the Upper Allochton (Roberts 2003; Indrevær 2011). Further east on the mainland, the Precambrian rocks outcrop in the Mauken Window were they occur as granitic plutons and supracrustal rocks (Zwaan et al. 1998). These basement rocks are bordered by the Vaddas, Kåfjord and Nordmannvik Nappes from the Upper Allochthon and by the Målselv Nappe that is related to the Middle Allochtons (Anderson et al. 1992). Although well-developed over Northern Norway, the Caledonian deformation had a very weak overprint effect on the Precambrian basement (Corfu et al. 2003a; Bergh et al. 2010).

This orogeny has been followed by several pulses of sedimentation and brittle faulting from the Late Paleozoic to Late Cenozoic. Albeit the brittle structures are still well-preserved onshore the sediment succession can only be observed partly on Andøya, Vesterålen, where Jurassic and Cretaceous sediments can be found on the shore (Dalland 1981; Bøe et al. 2010). The most part of the sediment pile has been recorded offshore in large and deep sedimentary basins: the Ribban and Vestfjorden basins on the Lofoten-Vesterålen Margin (Blystad et al. 1995; Olesen et al. 1997; Brekke 2000; Bergh et al. 2007a; Eig et al. 2008a; Hansen et al. 2012), and the Harstad, Tromsø and Hammerfest basins on the

Troms margin (Gabrielsen et al. 1990; Faleide et al. 1993; Breivik et al. 1998; Larssen et al. 2002; Barrère et al. 2009). The sediment succession is believed to rest directly over the Precambrian basement. They have likely been deposited from the Late Paleozoic, as Permian sediments have been inferred from seismic data, and through the Mesozoic and Cenozoic Periods (Gudlaugsson et al. 1998; Bergh et al. 2007a; Steltenpohl et al. 2009, 2011). These basins are bounded by major normal faults that are thought to have form during Late Paleozoic-Cenozoic crustal extension and rifting (Gabrielsen et al. 1990; Faleide et al. 1993; Breivik et al. 1998; Gudlaugsson et al. 1998; Bergh et al. 2007a; Eig et al. 2008a; Aftab 2011; Hansen et al. 2012).

1.4.2 Precambrian basement provinces

The West Troms Basement Complex is mostly composed of TTG gneisses, igneous-intrusive and metasupracrustal rocks (Fig. 4). Bergh et al. (2010) split these rocks into four major rock types: Neoarchean gneisses (2.89-2.56 Ga), Neoarchean to Palaeoproterozoic supracrustal rocks (2.4-1.97 Ga), early Palaeoproterozoic mafic dykes (2.67-2.22 Ga), and Palaeoproterozoic granitic and mafic plutonic intrusions (1.80-1.75 Ga).

The Neoarchean gneisses display an amphibolitic metamorphic facies. They are dominantly tonalite or tonalitic gneisses and they show some mafic intercalations in the northeast of Kvaløya, whereas they look more granitic in the southwest, in Senja (Zwaan 1995; Motuza 1998; Bergh et al. 2010). The boundary of this compositional difference corresponds with the Senja Shear Belt that strikes NW-SE (Zwaan 1995; see fig. 4). The dominant foliation strikes N-S to NW-SE with various dips and is associated with oblique to dip-slip stretching lineations, boudinaged mafic pods and intrafolial asymmetric folds that have been interpreted as evidence for ENE-WSW to E-W contraction. Migmatitic zones are quite common and can generally be linked to foliation-parallel shear belts that are separating rocks of different composition (e.g. the Senja Shear Belt). U-Pb dating on the Bakkejord Diorite yielded an age of 2723 ± 7 Ma (Kullerud et al. 2006a) and age determinations on gneisses in Torsnes and in Senja gave respective results of 2689 ± 6 Ma (Corfu et al. 2003a) and ca. 2800-2750 Ma (Kullerud et al. 2006a).

The metasupracrustal rocks form lens-shaped belts crosscutting the Neoarchean gneiss fabric such as the Astridal, Svanfjellet and Torsnes belts in the Senja Shear Belt, and the Mjelde-Skorelvvatn and Steinskardtind belts in Kvaløya (Fig. 4; Bergh et al. 2010). They are dominantly composed of meta-conglomerates, meta-psammites, mica-schists and meta-volcanics which show a SW and NE-dipping mylonitized foliation. Greenschist to amphibolitic metamorphic conditions have been determined for the rocks composing these belts. Paleoproterozoic U-Pb zircon age constraints have been obtained for the Svanfjellet (adjacent Hamn diorite dated to 1802.3 ± 0.7 Ma by Kullerud et al. 2006a), Torsnes (max. 1970 ± 14 Ma; Myhre et al. 2009) and Mjelde-Skorelvvatn belts (1.98 Ga.; Corfu et al. 2006 and Myhre et al. 2009). A Neoarchean origin cannot be ruled out for the Astridal and Steinskardtind belts as Neoarchean ages have been proposed for similar provinces in northern Troms such as the Ringvassøya greenstone belt (2.85-2.83 Ga.; cf. Motuza et al. 2001 and Kullerud et al. 2006a) and the Vanna group (2.40-2.22 Ga.; Bergh et al. 2007b). The Astridal, Svanfjellet, Torsnes and Mjelde-Skorelvvatn belts are characterized by steep NNW-SSE to NW-SE trending, anastomosing, sinistral strike-slip shear zones and minor, NNE-SSW striking, dextral conjugate shear zones. The Steinskardtind belt, however, displays low-angle oblique-slip shearing, accompanied by foliation-parallel thrusting (Bergh et al. 2010).

Mafic dykes trending N-S to NNW-SSE have been dated from the latest Neoarchean to the early Paleoproterozoic by Kullerud et al. (2006a). U-Pb zircon dating on a mafic dyke swarm yielded an age of 2627 Ma. Younger ages were suggested for dyke swarms in Ringvassøya (2403 ± 3 Ma; Kullerud et al. 2006b) and a diorite sill on Vanna (2221 ± 3 Ma; Bergh et al. 2007b). In Senja and Kvaløya the dykes generally do not truncate the metasupracrustal rock boundaries. Their main characteristic resides in their undeformed state, apart from a weak mylonitization along the contacts that appears only locally (Kullerud et al. 2006b).

Igneous plutonic rocks intruded the West Troms Basement Complex in the late Paleoproterozoic. In Kvaløya, the Neoarchean gneisses of the Kattfjord complex have been intruded by the Ersfjord granite (Fig. 4) dated with the U-Pb method to 1792 ± 5 Ma by Corfu et al. (2003a). This igneous body is a coarse-grained homogenous granite showing steep sheared and mylonitized contacts with the surrounding gneisses (e.g. foliation S_B from Antonsdóttir 2006). In addition to this mylonitic fabric, gently-dipping ductile shear zones

trending ENE-WSW were encountered within the Ersfjord granite, with evidence for a later formation. Pegmatite dykes finally developed in and along the contact with the intruded gneisses or metasupracrustal rocks. In southwestern Senja, the basement has been intruded by granitoids very similar to the Ersfjord granite (Fig. 4). Myhre & Corfu (2008) inferred an age of approximately 1805 Ma from U-Pb age dating on this pluton. Finally, the Hamn norite in northwestern Senja (Fig. 4) contains dykes of basaltic affinity and xenoliths of granodiorite, and has been dated at 1802.3 ± 0.7 Ma with the U-Pb method by Kullerud et al. (2006a) and 1800 ± 3 Ma (unpublished age quoted in Zwaan et al. 1998).

The TTG gneisses have developed first around 2.89-2.56 Ga. The metasupracrustal rocks were deposited during the Palaeoproterozoic (2.4- 1.97 Ga.). Mafic dyke swarms were also injected from 2.67 to 2.22 Ga and later plutonic intrusions, like the Ersfjord granite in the north-west of Kvaløya and the Hamn norite in the south of Senja, deformed the gneisses and the metasupracrustal rocks ca. 1.80-1.75 Ga ago during the Svecofennian tectonic event (Corfu et al. 2003a). The metamorphic conditions reached the amphibolite-granulite facies and finally retrogressed to greenschist facies. Bergh et al. (2010) also recorded decreasing metamorphic grades from the southwest to the northeast of Troms. They proposed a northeastward accretion linked to the Svecofennian contraction. This resulted in lens-shaped, NW-trending shear zones of metasupracrustal rocks wrapped in Neoarchean gneisses, such as the Senja Shear Belt (see fig. 4; Bergh et al. 2010). Bergh et al. (2010) and Corfu et al. (2003a) argued in favor of an autochthonous origin for the rocks composing the West Troms Basement Complex. For them, these rocks clearly belong to the Baltic shield and their current exposure is the result of uplift along post-Caledonian brittle faults. This was also supported by Steltenpohl et al. (2011) on the Vesterålen Margin, where they noticed the uplift of core complexes along extensional shear zones in the Devonian and Permian, and by Davids et al. (2012a) who evidenced an exhumation stage during the Permo-Triassic in Troms. Motuza (1998) and Dallmeyer (1992), on the contrary, think this basement unit shows Laurentian affinities. Davids et al. (2012a) for the Troms area, and Steltenpohl et al. (2011) on the Lofoten-Vesterålen Margin inferred that the West Troms Basement Complex remained at high crustal levels during the Caledonian deformation event, since the regional temperature did not exceed the muscovite closure temperature, leading to Precambrian $^{40}Ar/^{39}Ar$ ages.

The rocks of the West Troms Basement Complex are bordered by the Paleozoic Caledonian nappes in the southeast. Corfu et al. (2003a) and Bergh et al. (2010) argued that the West Troms Basement Complex has not been disturbed by the Caledonian contraction, apart for some thermal overprint that has recently been studied in more details by Davids et al. (2012a). The contact is however marked by low-angle brittle-ductile thrusts that formed during the nappe stacking phase of the Caledonian orogeny, but also by post-Caledonian, high-angle, normal brittle faults that developed during the post-orogenic extension and Late Paleozoic to Cenozoic rifting episodes. The thrusts commonly exhibit mylonitic fabrics and may have experienced later reactivation as extensional faults during the opening of the North Atlantic Ocean (Doré et al. 1997) as evidenced on the Lofoten-Vesterålen Margin by Steltenpohl et al. (2011). The Vestfjorden-Vanna fault complex has already been mentioned as the northwestern limit of the Caledonian nappes against the West Troms Basement Complex rocks in Senja and Kvaløya (Forslund 1988; Olesen et al. 1997).

1.4.3 Caledonian nappes

The Caledonides are the result of the closure of the Iapetus Ocean and the collision of Baltica and Laurentia. The onset of the Caledonian deformation took place in the Late Ordovician and the orogeny reached several peaks of compression until the Early Devonian (Anderson et al. 1992; Roberts 2003). Four compression stages have, so far, been identified: Finnmarkian (Late Cambrian), Trondheim (Early Ordovician), Taconian (Mid-Late Ordovician) and Scandian (Mid Silurian-Early Devonian). The tectonostratigraphy is generally divided into Lower, Middle, Upper and Uppermost Allochthons. According to the classification of Anderson et al. (1992) for northwestern Troms, the Middle Allochthon corresponds to the Målselv Nappe. The Upper Allochthon is composed of the Vaddas, Kåfjord and Nordmannvik Nappes, but also of the Lyngen Nappes Complex (Andresen 1988; Indrevær 2011). Finally, the Tromsø Nappe Complex, which gathers the Tromsø and Nakkedal Nappes (Indrevær 2011), has been inferred as the Uppermost Allochthon (Fig. 5). The Lower Allochthon (c.f. Kalak Nappe on fig. 5) has not been recognized in the surrounding of the basement rocks and will then not be discussed here.

The Målselv Nappe has been described as a mix of Mesoproterozoic dolomite and quartzite, and of Precambrian basement rocks, possibly amphibolite and hornblende-schist,

that have been reworked during the Caledonides formation (Knutsen 2012). Dallmeyer (1988) reported mylonitic metapsammites and metapelites directly at the contact with the basement rocks of the Mauken Window. These rocks are thought to have only undergone low-grade metamorphism (Anderson et al. 1992; Zwaan et al. 1998).

Zwaan et al. (1998) observed a majority of marbles, metagreywackes and micaschists in the Vaddas Nappe, at the base of the Upper Allochthon (Fig. 5). These rocks directly lie over the Målselv Nappe and display amphibolitic metamorphic facies (Indrevær 2011). A granitic gneiss has been given an age of 602 ± 5 Ma by Corfu et al. (2007). The Vaddas Nappe is overlain by a pretty similar unit, the Kåfjord Nappe. This nappe mainly consists of metagranites and pegmatites. A certain amount of metasediments such as marbles, micaschists and quartzites, all showing amphibolitic facies metamorphism, has also been identified (Andresen 1988; Dallmeyer 1988; Zwaan et al. 1998). On top of the Kåfjord Nappe lies the Nordmannvik Nappe. This nappe differs from the other units by the granulite metamorphic facies it displays, and it is dominantly made of marbles, micaschist and gneisses. An estimation of 492 ± 5 Ma for the age of the Nordmannvik Nappe has been provided by Lindstrøm & Andresen (1992).

The last lithological unit of the Upper Allochthon is the Lyngen Nappe Complex (Fig. 5). This nappe complex is actually made of two sub-units: the Lyngen Magmatic Complex and the Balsfjord Group (Andresen 1988; Andresen & Steltenpohl 1994; Selbekk et al. 2000; Corfu et al. 2003b; Indrevær 2011). The Lyngen Magmatic Complex comprises metasediments (phyllites) and metavolcanics at the base of a major ophiolitic body: the Lyngen Gabbros, which has undergone greenschist to low-amphibolite metamorphism, and is crosscut by the N-S striking, ductile Rypedal shear zone (Dallmeyer 1988; Andresen & Steltenpohl 1994; Indrevær 2011). A minimum U-Pb age of 469 ± 5 Ma has been obtained on a zircon by Oliver & Krogh (1995). The Balsfjord Group overlies the ophiolitic body, and is dominated by psammite-schists and a minor carbonate unit (Andresen 1988; Dallmeyer 1988; Andresen & Steltenpohl 1994; Corfu et al. 2003b). The unconformity separating these two sub-units has been constrained by Late Ordovician-Early Silurian fossils found in the Balsfjord Group (Bjørlykke & Olaussen 1981).

The Tromsø Nappe Complex forms the Uppermost Allochthon of the Caledonides. It has been split up in the Nakkedal Nappe Complex and the overlying Tromsø Nappe (Andresen 1988; Andresen & Steltenpohl 1994; Zwaan et al. 1998). The Nakkedal Nappe Complex is made of quartzo-feldspathic gneisses in the lower part, and amphibolitic rocks intersected by numerous dykes that make up the Skattøra Migmatite Complex in the upper part (Selbekk et al. 2000). On the other hand, the Tromsø Nappe is dominated by ultramafic peridotitic rocks, metasediments (mica-schists and calc-silicates), and high-grade (amphibolite to eclogite) lenses of mafic rocks (Andresen 1988; Krogh et al. 1990; Anderson et al. 1992; Indrevær 2011). Krogh et al. (1990) dated the Tromsø Nappe to 433 ± 12 Ma using the Rb-Sr dating method. Fabric overprints include two foliations, a crenulation cleavage, and isoclinal and open folds (Corfu et al. 2003b). The limit between the Tromsø Nappe and the Nakkedal Nappe Complex is strongly mylonitized and corresponds with a major thrust (Zwaan et al. 1998; Selbekk et al. 2000)

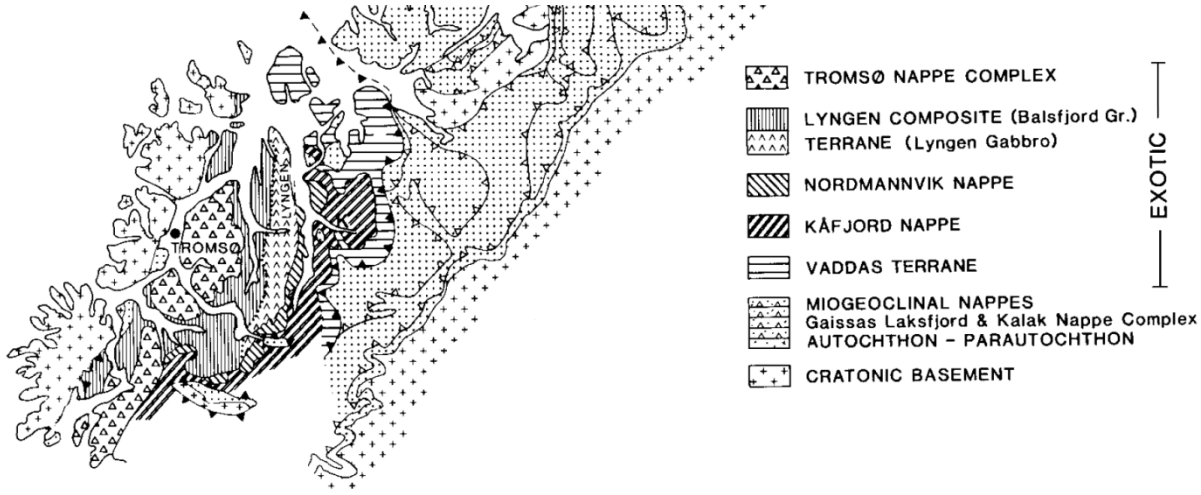

Figure 5: Geological map of the main Caledonian units in Troms. Modified after Andresen (1988).

On the one hand, Roberts (2003) argued that the Middle Allochthon and the base of the Upper Allochthon were formed by accumulation of Neoproterozoic sediments on a passive margin, but on the other hand, Roberts et al. (2007) proposed that the upper part of the succession (Lyngen Magmatic Complex and Uppermost Allochthon) was detached from Laurentia since they identified NW-vergent thrusts that are typical from the Appalachians. The first stage of the Caledonian orogeny (Finnmarkian) took place in the Late Cambrian and is the result of the collision of Baltica with a magmatic arc above a subduction zone. Then from the Early Ordovician to the Mid-Late Ordovician, a major phase of deformation

occurred when ophiolites were obducted (c.f. the Lyngen Magmatic Complex). This is referred as the Trondheim event. An accretionary wedge and a sedimentary basin (c.f. Balsfjord Group) developed during the Taconian orogeny in the Mid-Late Ordovician to the Mid-Silurian (Andresen & Steltenpohl 1994). The margin got intruded by arc-related plutons while some rocks reached eclogite facies conditions (eclogite lenses in the Tromsø Nappe). This is potentially due to dragging into the subduction complex and rapid exhumation (Anderson et al. 1992; Roberts 2003). Finally, during the Scandian phase occurred the collision and the subduction of Baltica under Laurentia. The major allochthonous nappes were emplaced on top of each other from the Mid-Silurian to the Early Devonian. This last orogeny is thought to be the main deformation event in the Caledonides history because it overprinted all the previous fabrics of the Allochthons with SE-vergent folds and thrusts (Roberts 2003).

Even though convergence was still dominant at lower levels in the crust, a post-orogenic extensional phase started to reactivate low-angle ductile detachments that were involved in W/SW shearing, and sedimentary basins progressively developed in the Early Devonian (Roberts 2003). Although not yet identified in Troms, this extensional episode was recognized in Lofoten and Vesterålen by Eig et al. (2008b) and Steltenpohl et al. (2011) that both documented uplift of metamorphic core complex (Osmundsen et al. 2005) during this period. The Caledonian nappes were then down-faulted to the South-East during successive rifting events, by fault segments that are believed to belong to the Vestfjorden-Vanna fault complex (Forslund 1988; Olesen et al. 1997; Roberts & Lippard 2005).

1.4.4 Post-Caledonian faulting: rifting extension and passive margin formation

Post-Caledonian sedimentary rocks are not preserved onshore in Troms, but in the island of Andøya just west of Senja (Fig. 6), Jurassic-Cretaceous strata crop out in a local basin (Dalland 1981; Fürsich & Thomsen 2005; Bøe et al. 2010) that seem to be linked to the fjord and the offshore sedimentary successions (Davidsen et al. 2001). Still other near-shore strata are considered to be present elsewhere in the fjord of Vesterålen (Dalland 1981; Davidsen et al. 2001). The series is composed of Paleozoic granites underlying Jurassic and Cretaceous sequences. The Paleozoic granites apparently experienced weathering and are unconformably covered by sandy limestones of potentially Carboniferous age. On top of the

limestones lies the Jurassic sequence made of coarse-grained fluvial sandstones and bituminous shales that are fining towards the top of the series. They have likely been deposited from Bajocian to Berriasian times and are separated from the Paleozoic rocks by another unconformity (Dalland 1981; Fürsich & Thomsen 2005; Bøe et al. 2010). N-S trending faults individualize tilted blocks that define a graben geometry (Dalland 1981; Bøe et al. 2010). The Cretaceous (Valanginian to Aptian) sediment package also fines upwards, correlating well with the contemporaneous eustatic variations. The marine silty sandstones overlying the Jurassic strata progressively turn into shales interbedded with fine turbiditic layers and embedding basement blocks. Although less obvious than for the Jurassic sequence, extensional faulting can be inferred from the turbidites layers and the basement blocks (potential olistostrome deposits). As noticed by Dalland (1981) several, more or less clear, erosional discontinuities seem to appear in the Mesozoic sediment pile in Andøya, and this may indicate different phases of uplift and rifting from the Mid-Jurassic to the Early Cretaceous.

Post-Caledonian brittle faulting in the West Troms Basement Complex has a complex history and involved Late-Paleozoic (Permian) to Cenozoic, mainly extensional brittle deformation during the rifting and opening stages of the North-Atlantic Ocean (Olesen et al. 1997; Davids et al. 2010, 2012b; Hansen et al. 2011, 2012). In southwestern Kvaløya two dominant brittle fault sets were mapped by Thorstensen (2011), trending N-S to NE-SW and with variable dips to the west and east, and some of them locally including cataclastic fault rocks and slickensided surfaces. The nature, correlation, kinematic significance, timing and evolution-reactivation history is still unknown, but the idea is that they both may be correlated with the Rekvika fault zone. Various tectonic and evolution models have been proposed for the formation of brittle fault sets e.g. in the Lofoten-Vesterålen area, including progressive successions, step-wise and/or synchronous events, e.g. due to shifts in the regional strain fields in Mesozoic-Cenozoic times (cf. Wilson et al. 2006; Bergh et al. 2007a; Davids et al. 2010, 2012b; Eig & Bergh 2011; Hansen et al. 2012; Hansen & Bergh 2012).

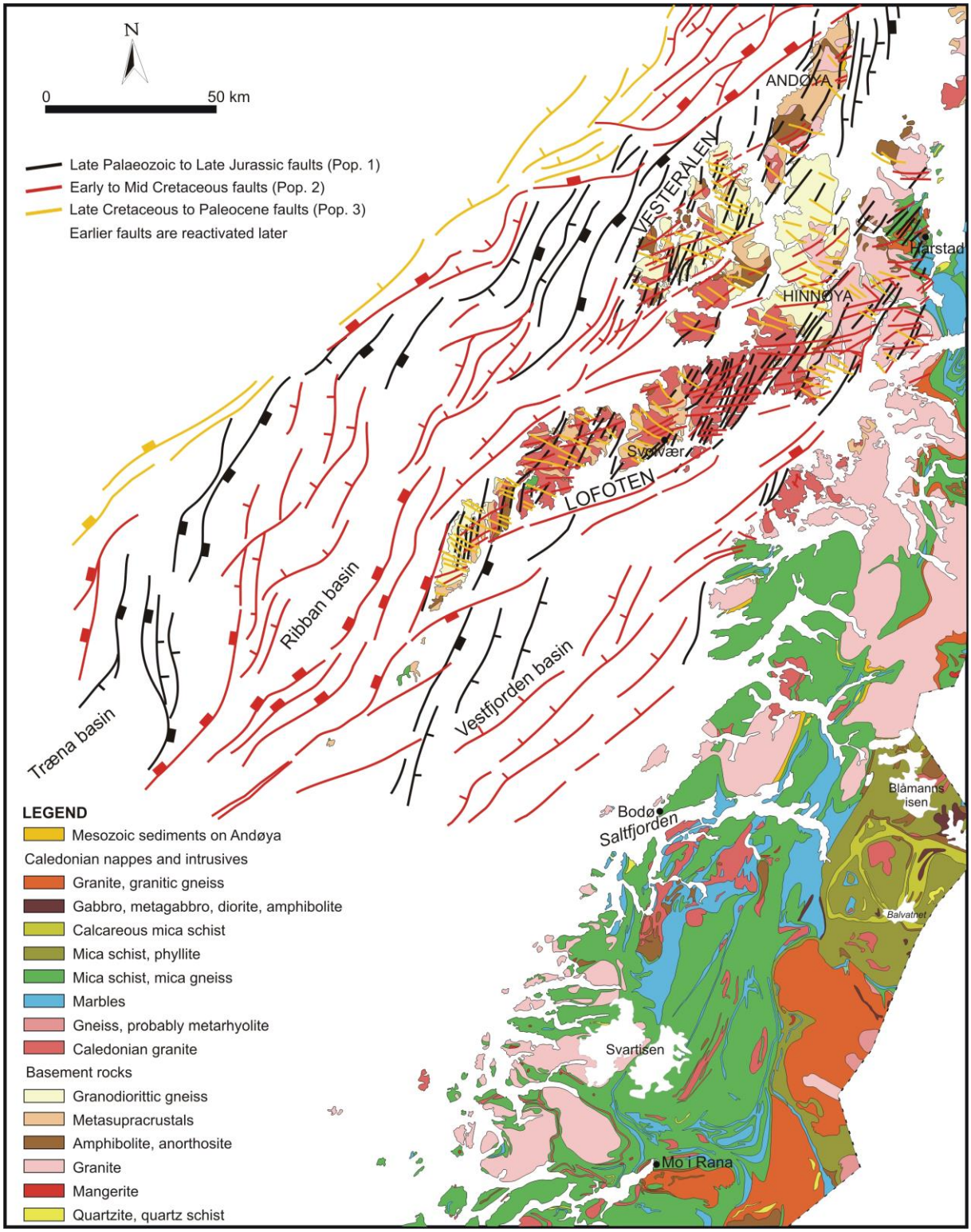

Figure 6: Correlation between onshore lineaments and offshore faults and fractures on the Lofoten-Vesterålen Margin. This map documents tectonic structures using Bergh et al. (2007a) classification; see figure 3 for location. From Eig et al. (2008a).

The network of onshore brittle faults in coastal areas of Troms is yet to be investigated, but local analyses have been carried out (Forslund 1988; Gagama 2005; Antonsdóttir 2006; Thorstensen 2011) and three major sets of linear fractures have been

highlighted, trending N-S, NE-SW, and NW-SE. Post-Caledonian brittle fault systems in Troms have tentatively been linked into a regional framework by Olesen et al. (1997), and more particularly by Antonsdóttir (2006) in northwestern Kvaløya (Rekvika), Thorstensen (2011) in western Kvaløya, Gagama (2005) in western Senja (Sifjorden) and by Forslund (1988) in the south-east of Kvaløya.

The NE-SW trending Rekvika fault zone crops out in the northwestern part of Kvaløya and it potentially accommodated sinistral-oblique displacement (Antonsdóttir 2006). The foliated host-rock displays hydrothermal alteration evidenced by chlorite, epidote and hematite precipitation, and quartz and calcite veins on the fracture surfaces. Antonsdóttir (2006) reported NE-SW-striking greenish (proto)cataclasite, and locally devitrified pseudotachylyte along the core of the Rekvika fault zone. Three fault sets have been identified trending NE-SW, NNW-SSE to N-S and WNW-ESE. The first two were interpreted as dominantly dip-slip faults with evidence for minor strike-slip movements. On the contrary the third set of faults is thought to have experienced major strike-slip and additional dip-slip normal motions.

In western Kvaløya, the Hillesøya and Storsalen fault zones were briefly investigated by Thorstensen (2011). The faults showed (ultra)cataclasite from 10 centimeters to one meter thick, and epidote, chlorite and hematite precipitations on their surfaces. The Hillesøya fault zone has been observed trending NNE-SSW whereas the Storsalen fault zone progressively changes orientation from NE-SW in the south to N-S in the north. The brittle fractures are thought to be localized along a pre-existing weakness in the crust corresponding with a Svecofennian macro-fold, which may explain the changes in brittle fabric strike. Thorstensen (2011) recorded three fault patterns: NNE-SSW, NE-SW and NW-SE trending, and interpreted most of these faults as normal dextral/sinistral faults.

Gagama (2005) has performed a kinematic analysis of brittle structures around the Sifjorden fault zone in Senja. The fracture surfaces were divided into three groups striking N-S, NE-SW to E-W, and NW-SE, and were commonly covered by chlorite and epidote precipitation. The N-S trending fractures have been interpreted as normal faults showing a dextral strike-slip movement component. The NE-SW to E-W trending faults were interpreted as dip-slip normal faults showing a minor strike-slip component, and the NW-SE

structures were described as *en echelon*, strike-slip faults that developed parallel to the basement fabric.

The Straumsbukta-Kvaløysletta fault complex described by Forslund (1988) is actually made of two listric, SE-dipping fault-segments, the Straumsbukta fault trending NNE-SSW and the ENE-WSW trending Kvaløysletta fault segment. Both semi-ductile (phyllonites, mylonites) and brittle deformation (breccias, cataclasite, pseudotachylyte) were observed along the fault zone. On the one hand, the ductile fabric is apparently linked to a low-angle Caledonian thrust that shows similar strike, dip and transport direction (to the SW) as the Straumsbukta-Kvaløysletta fault zone. This could mean that the mylonitic foliation helped localizing brittle faulting. On the other hand, brittle deformation seems to overprint the semi-ductile fabric along a high-angle normal fault that probably accommodated dip-slip and sinistral strike-slip movements. A minimum displacement of 2500-3000 meters has been inferred from the breccias thickness for this fault zone. A possible southward continuation of this fault has been considered in Straumsfjord, south of Kvaløya (Forslund 1988), and in the NE, west of Reinøya where it is thought to link up with the Grøtsundet fault zone (Andresen, unpublished).

It is commonly accepted that the Straumsbukta-Kvaløysletta fault zone belongs to the Vestfjorden-Vanna fault complex that marks the limit between the Precambrian basement and the Caledonian nappes (Andresen & Forslund 1987; Forslund 1988, Roberts & Lippard 2005). This fault complex consists of NNE-SSW and ENE-WSW trending fault segments for which sinistral normal oblique-slip movements are probable (Andresen & Forslund 1987; Forslund 1988; Tveten & Zwaan 1993; Olesen et al. 1993; Roberts & Lippard 2005). To the south-west it seems to link up with the East Lofoten Border Fault, which is a major basin-bounding fault on the Lofoten-Vesterålen Margin (Olesen et al. 1997; Bergh et al. 2007a). Olesen et al. (1993, 1997) identified a shift in polarity at the intersection with the NW-SE striking Bothnian-Senja fault zone, within the Senja Shear Belt. This could imply a reactivation of this structure as a transfer fault during the formation of the Vestfjorden-Vanna fault complex (Olesen et al. 1993, 1997; Zwaan 1995). This structure was named the Lenvik transfer zone (Olesen et al. 1993; Zwaan 1995). Interestingly, the ENE-WSW striking Sifjorden fault zone in Senja (Gagama 2005) trends parallel to the nearby Stonglandseidet fault, that is generally considered as a dominantly strike-slip fault segment of the

Vestfjorden-Vanna fault complex (Tveten & Zwaan 1993; Olesen et al. 1993, 1997). The Rekvika fault zone trends roughly parallel to the Straumsbukta-Kvaløysletta fault zone (Fig. 2) and was also suggested to be part of the Vestfjorden-Vanna fault complex by Antonsdóttir (2006).

Offshore northwestern Kvaløya, bathymetric data from Thorstensen (2011) display similar fault patterns than observed onshore, trending NNE-SSW, NE-SW and NW-SE. Troughs off Hillesøya describe a Z-shape across the Senja Shear Belt, likely related to Svecofennian macrofolding. The apparent steeper dip to the NW of these faults possibly comes from preferential glacial erosion. The NW-SE trending brittle fractures formed parallel to the Precambrian foliation, along ductile shear zones that correspond to the offshore continuation of the Senja Shear Belt. Thorstensen (2011) interpreted the NW-SE trending fractures as normal dextral/sinistral faults. The crosscutting relations indicate that the NNE-SSW trending faults formed first, subsequently followed by the formation of NE-SW fractures. The NW-SE striking faults truncate the previous two sets and are therefore considered to be younger. The NE-SW trending faults were correlated to major structures such as the Troms-Finnmark fault complex described by Gabrielsen et al. (1990) and that trends NE-SW to E-W. The Troms-Finnmark fault complex is made of several fault segments as for example the NE-SW trending Måsøy fault complex that formed in the Late Permian (Aftab 2011). Other major structures off the Barents Sea Margin are the N-S trending Ringvasøy-Loppa fault complex, the NE-SW striking Bjørnerenna fault complex and the E-W Asterias fault complex (Fig. 1) that have been described in more detail by Gabrielsen et al. (1990).

Tectonic models involving two or three discrete stages have been proposed for the development of brittle faults in western Troms. A first phase probably took place from Permian times and through Jurassic (Andresen & Forslund 1987; Forslund 1988; Roberts & Lippard 2005) under WNW-ESE to NW-SE orthogonal extension, with incremental oblique extension. A second stage likely settled during the Early Cretaceous, and Antonsdóttir (2006) proposed a shift in the extension direction from WNW-ESE to a NNE-SSW trend. In Sifjorden, Gagama (2005) argued that N-S trending faults formed first in the Permo-Jurassic, and that NE-SW to E-W striking faults developed later. Antonsdóttir (2006) drew a contradictory conclusion in Rekvika where NE-SW trending faults developed first and NNW-SSE to N-S

trending faults developed later during two distinct faulting events. At last, WNW-ESE to NNW-SSE striking faults are thought to have formed due to NNW-SSE orthogonal and E-W oblique extension (Antonsdóttir 2006). Gagama (2005), however, argued that they could have formed as tensional fractures under NW-SE orthogonal extension. Gagama (2005) and Antonsdóttir (2006), nonetheless, agree on a Late Cretaceous-Tertiary age for these structures. Furthermore, the NNW-SSE to N-S and the NE-SW to E-W trending fault patterns may have been reactivated during Cretaceous rifting and Early Cenozoic ocean opening (Andresen & Forslund 1987; Forslund 1988; Roberts & Lippard 2005; Antonsdóttir 2006). Some workers also argued for tectonic inversion of some extensional fault zones in the latest Cretaceous-Early Cenozoic (Gabrielsen et al. 1990, 1997; Faleide et al. 1993; Knutsen & Larsen 1997; Aftab 2011). New geochronological data from Davids et al. (2010, 2012b) support a single-stage faulting history coupled to a hydrothermal event that would have taken place in the Permian-Triassic, in western Troms. Their Apatite Fission Track data provide evidence for rapid cooling down to 70°C and exhumation in Permian-Early Triassic times with a minimum age constraint for main faulting of ca. 200 Ma. $^{40}Ar/^{39}Ar$ age dating of K-feldspar indicate an age of ca. 280-250 Ma and a temperature of about 350-200°C for the hydrothermal event. No later, major reactivation has yet been evidenced, and this could be linked to a westward shift of extensional faulting.

More detailed studies were conducted on the Lofoten-Vesterålen Margin (Fig. 6) and it seems that the major fracture groups inferred for this area trend very similarly to the major sets described in Troms: N-S to NNE-SSW, ENE-WSW and NW-SE trends (Olesen et al. 1993; Bergh et al. 2007a; Eig et al. 2008a; Hansen et al. 2009, 2012; Hendriks et al. 2010; Eig & Bergh 2011; Hansen & Bergh 2012).

Eig et al. (2008a) carried a detailed analysis of the kinematics of the brittle fractures onshore Lofoten and Vesterålen. They proposed an interpretation as dip-slip normal faults, later reactivated as oblique/strike-slip faults for right-stepping, NNE-SSW striking faults. A ENE-WSW trending fault set is in fact made of two conjugate, Riedel shear, fracture sets trending E-W and NE-SW, reactivated as dip-slip normal to oblique-slip faults that crosscut and sometimes bend the NNE-SSW trending fractures. Finally, NW-SE trending fractures truncate all the other brittle structures and are composed of NNW-SSE and WNW-ESE trending, strike-slip to oblique-slip, Riedel shear fractures later overprinted by a minor dip-

slip normal component (Eig & Bergh 2011). Bergh et al. (2007a) emphasized that many of the fractures they observed run parallel to the fjords and sounds in Lofoten-Vesterålen. Hansen et al. (2009) support the idea that the ENE-WSW and NW-SE trending faults developed along inherited fabric from the basement such as foliation, ductile shear zones (e.g. the NW-SE trending Senja Shear Belt), Caledonian thrusts (onshore continuation of the Love transfer zone), lithological boundaries (ENE-WSW striking faults localized along pegmatite dykes).

The orientations of the offshore faults are quite consistent with the strike of the onshore brittle fractures. Bergh et al. (2007a) and Hansen et al. (2009, 2012) identified NNE-SSW and ENE-WSW trending sets of faults (Fig. 6). The NNE-SSW trending structures have been interpreted as a composition of low-angle detachments, dipping to the ESE and accommodating dip-slip movements, and of antithetic (NW-dipping) *en-echelon*, planar normal faults that experienced additional dextral strike-slip motions. On the other hand, the ENE-WSW trending fault set includes planar and listric normal faults showing northwestern dips (Bergh et al. 2007a). As inferred for the onshore brittle faults, the offshore faults are suspected to follow pre-existing fabrics and to accommodate basement weakness (Hansen et al. 2009).

Eig et al. (2008a) believe these fault patterns formed during three discrete deformation events. The first of them took place in the Permian-Jurassic and is responsible for the development of the right-stepping *en echelon*, NNE-SSW trending faults due to WNW-ESE orthogonal extension. A shift in the extension direction from WNW-ESE to NNW-SSE is supposed to have occurred in the Mid/Late Jurassic-Early Cretaceous, in order to enable the development of the ENE-WSW striking faults. However Hansen & Bergh (2012) argued that such a shift in the extension direction is not necessary to form ENE-WSW trending fractures, and that a simultaneous formation of the ENE-WSW and NNE-SSW trending faults is more likely. The ENE-WSW striking faults potentially acted as sinistral strike-slip soft and hard-linked transfer faults linking up the NNE-SSW striking faults, and resulting in the zigzag pattern described by Bergh et al. (2007a). Olesen et al. (1997) and Tsikalas et al. (2001, 2005, 2008) proposed another set of NW-SE striking transfer zones to explain the change of polarity of onshore faults, as for example the Bivrost Lineament south of Lofoten, the Vesterålen transfer zone, or the Lenvik transfer zone in southwestern Troms. They also stated that the offshore continuation of these NW-SE striking lineaments were

linked to oceanic transforms such as the Bivrost Fracture Zone for the Bivrost Lineament (Blystad et al. 1995; Olesen et al. 1997; Brekke 2000; Tsikalas et al. 2001, 2005). This hypothesis was later rejected by Olesen et al. (2007) who attributed these offshore fracture zones to navigation errors. Finally, NW-SE trending joint fractures formed during a third stage in the Late Cretaceous-Paleocene under NW-SE contraction and NE-SW extension, due to ridge-push forces. Wilson et al. (2006) proposed a completely different model where the margin would be segmented in distinct domains, each domain deforming differently with regard to an extension direction constantly oriented WNW-ESE.

1.5 Methods and data

1.5.1 DEM satellite imaging

3D satellite images (DEM) and photo analysis (e.g. Virtual Globe from www.norgei3d.no) were used to locate structurally controlled lineaments, scarps, depressions, uplifts, terraces and lithological boundaries in the landscape on Kvaløya and Senja islands in conjunction with suitable orientations and shapes of brittle fault-fracture sets.

Fault zone maps were drawn using *Corel Draw X5*. They show the major brittle structures accompanied by their strike, dip and potential kinematics when possible, and the lithological boundaries. Ductile features were also plotted when recorded in the surroundings of the fault zones.

1.5.2 Field work

The following observations and interpretations are the result of field work that has been carried in August and September 2011 and from August to October 2012. It led to the identification of the main lithological boundaries, the mapping and description of ductile features (shear zones, folds) and of major fractures and their associated brittle structures. The lithogical units are from Zwaan et al. (1998).

The mapping of western Kvaløya, with emphasis on the Rekvika fault zone, has been followed by additional field studies, especially in Straumsbukta, Bremneset, Tussøya-Røkneset, Hillesøya and Stonglandseidet (see fig. 4). The resulting maps show the rock type boundaries, structural orientation data (strike and dip), kinematic data (slickensides, sense of shear indicators, offsets, rotation-bending, duplexes, etc.) as well as stereoplot obtain via Orient software. The structures were investigated in traverses and partly along-strike.

The description and analysis of the fault rocks include the characteristics of the fault core (process zone) and the damage zone, and the dominant deformation mechanism: cataclasite (proto, ultra), breccias, gouge, pseudotachylyte, phyllonite (Fig. 7 and table 1).

Relative timing for the different fault patterns has been deduced from the field observations like crosscutting relations or fault rock analysis, and is supposed to end in regional comparison and correlation of the Rekvika fault zone trend with other major faults and lineaments within and/or bounding the Precambrian basement horst of the West Troms Basement Complex and the Lofoten Ridge.

1.5.3 Thin sections analysis

Samples of fault rocks were collected in the field and studied with a Leica DMLP microscope. Critical areas were then selected and photographed using an EOS 650 D camera. A brief description of the mineral composition of the host rock is given with the microstructures analysis, and potential kinematic indicators and deformation processes will be discussed (brittle or/and plastic). Important aims are the correlation between micro and macrostructures and the estimation of the pressure-temperature range of faulting in order to discuss the successive deformation history (single or multiple phases).

1.6 Definitions

The aim of this chapter is to define geological and structural terms used in the thesis and supplementary, to avoid ambiguity on some geological terms that have been defined differently by several authors.

Term	Description
Fault rocks	Commonly formed through strain concentration within a tabular or planar zone that experiences shear stress (Braathen et al. 2004).
Frictional flow	Pressure, subordinate temperature, and fluid-controlled deformation mechanisms which have a brittle style: granulation of grains by intergranular, intragranular, and transgranular microfracturing, and intragranular or intergranular frictional sliding with abrasion of fracture walls and grain margins (e.g. cataclastic flow; Braathen et al. 2004).
Plastic flow	Mainly thermally activated, continuous deformation without rupture, with a ductile style of deformation: dislocation creep and glide, solid state diffusion creep, diffusional mass transfer, and viscous grain boundary sliding (Braathen et al. 2004).
Cemented	Consolidated through mineral precipitation in pores of the matrix (Braathen et al. 2004).
Indurated	Consolidated by compaction due to directed pressure, annealing by recrystallization of grains, or neomineralization (e.g., muscovitization, silicification, albitization, epidotization, saussuritization). The term disregards cementation unless related to general neomineralization (Braathen et al. 2004).
Matrix	Fine-grained material in a fault rock formed by granulation or dynamic recrystallization of grains, filling the interstices between larger clasts of original rock (Braathen et al. 2004).
Breccia	Mainly chaotic, noncohesive fault rock, generated by fractional flow (Braathen et al. 2004).
Cataclastic rock	Mainly chaotic fault rock that developed with cohesion, which is generated by mainly frictional flow (Braathen et al. 2004).
Protocataclasite	Cataclastic rock containing 0-50% of cataclastic matrix (Braathen et al. 2004).
Cataclasite	Cataclastic rock containing 50-90% of cataclastic matrix (Braathen et al. 2004).
Ultracataclasite	Cataclastic rock containing 90-100% of cataclastic matrix (Braathen et al. 2004).
Mylonite	Fault rock with distinct mineral fabric, and dominated by plastic flow (Braathen et al. 2004).
Fault-generated Pseudotachylyte	Glassy, veining material formed by frictional melting in cold dry crystalline rocks during earthquake faulting (Maddock et al. 1987).
Incisement	Successive generations of fractures progressively biting into deeper parts of the lower plate along a bowed detachment (Lister & Davis 1989).
Excisement	Successive generations of fractures progressively biting into shallower parts of the upper plate along a bowed detachment (Lister & Davis 1989).
Horse	In extensional duplexes, fault-bounded block located between low-angle normal faults (Root 1990).
Extensional duplex	Brittle structure developed along a flat/ramp-geometry detachment, by incisement or excisement of the crust in the ramp region, where low-angle normal faults delimit horses and define an upper boundary

	fault called the roof and a lower boundary fault named the floor (Gibbs 1984; Lister & Davis 1989; Root 1990)
Strike-slip duplex	Imbricate fault arrays developed along a sub-vertical, mostly strike-slip major fault defining a straight-bend geometry (Woodcock & Fischer 1986).
Synthetic fault	Minor fault that has a similar orientation and the same displacement sense than a related major fault; also referring to two related faults having the same shear sense (Gibbs 1984).
Antithetic fault	Minor fault that has a similar orientation but an opposite dip to a related major fault; also used to describe two related faults with opposite shear senses (Gibbs 1984).
Accommodation zone	Area of deformation that transfers strain or displacement between two overlapping faults that need not to have been active at the same time (Peacock et al. 2000).
Transfer zone	Area of deformation and bed rotation between two normal faults that overstep in map view and that were active at the same time (Peacock et al. 2000).
Transfer fault	Fault that links, is at a high angle to, and that transfers displacement between two normal faults (Gibbs 1984).
Core zone	Area accommodating most of the displacement in a fault zone (Caine et al. 1996).
Damage zone	Area of fracturing around and mechanically related to a fault (McGrath & Davison 1995).
Slickenside	Polished fault surface that can be used to determine movement direction and shear sense along a fault zone (Passchier & Trouw 2005).
Groove	Scratches or linear markings on a slickenside that indicate slip direction along the slickenside (Passchier & Trouw 2005).
Fiber	fibrous grains along a slickenside, parallel to the fault and usually parallel to the direction of latest movement along the fault (Passchier & Trouw 2005).

Table 1: Definitions of fault rocks, deformation mechanisms and structural terms.

2 Description of brittle structures

2.1 Introduction

The description of the studied brittle fault complexes in western Troms will be organized in a systematic manner, starting with the large-scale outline of the fault trace in map view, followed by a description of the fault in the core and damage zone in map view, including lithologies near the brittle fault zones. Then the geometry of the fault zones (in the core and damage zones) will be described, including orientation (strike and dip) illustrated e.g. by stereo-plots, movement character, kinematic indicators (offsets of marker fabrics, slickensides, microstructures, etc., estimates of displacement/slip, and relative timing constraints shown by e.g. cross-cutting relationships. Next, the fault rocks will be described utilizing meso-scale and micro-scale (thin-section) data and observations, in order to make constraints on the mechanical aspects of faulting, deformation mechanisms, and P-T conditions of faulting in the discussion chapter. A description of pre-existing (ductile) fabrics in the host rocks relative to the fault zone fabrics will also be included in order to discuss the probable controlling effect of basement fabrics. The final subchapter will include preliminary interpretation, and/or tentative evolution of the fault zones. The evolution the fault complexes, will be inferred from the descriptive parameters and thus provide the basis for more comprehensive kinematic and dynamic analyses in chapter 3.

2.2 The Rekvika fault complex

In this thesis the NE-SW trending “Rekvika fault complex” will refer to potentially linked or at least related fault zones exposed on the northwestern part of Kvaløya, in the West Troms Basement Complex, including the Rekvika, Bremneset, Tussøya-Røkneset and Hillesøya fault zones (Fig. 4). These individual fault zones have been interpreted as a common fault complex because they show a similar overall NNE-SSW orientation, comparable geometries and associated structures along strike and especially duplex-like structures and *en echelon* patterns, similar kinematics including dominant dip-slip normal movements, potential relative ages, and comparable fault rocks (cataclasite) and mineral assemblages precipitated on fault surfaces such as quartz, chlorite, epidote, and hematite.

These isolated fault segments are believed to be linked by probable ENE-WSW trending faults.

2.2.1 Rekvika fault zone

2.2.1.1 Large scale field relations and host rock characteristics

The fault zone crops out in Rekvika, in northwestern Kvaløya (Fig. 4) close to the contact between the Ersfjord granite (1.79 Ga) and the presumed Neoarchean gneisses of the Kattfjord complex (Zwaan 1995), defining a NE-SW trending, ca. 50 meter-wide fault zone steeply dipping SE. The fault has been traced several km further to the NE (Antonsdóttir 2006). The host rock southeast of the Rekvika fault, the Ersfjord granite, is a fine-grained, locally medium-grained, massive igneous body that intruded the migmatitic amphibolitic gneisses of the Kattfjord complex (Bergh et al. 2010). The contact between these two lithologies is folded (Fig. 7). The granite body is mainly composed of K-feldspar, quartz, epidote, chlorite and of minor amounts of plagioclase and white mica (Fig. 8a). Along the main trace of the Rekvika fault zone pronounced fracture sets and zones of hydrothermal alteration define a few meters wide core zone made of cataclastic granite truncated by meter-scale quartz veins (Fig. 8b & c). Notably, in distance up to 100 m away from the fault core to the north and southeast, the granite is largely undeformed, but displays a remarkable red coloration. The red-stained granite in the core zone comprises a weak, semi-ductile, NE-SW striking fabric/foliation and numerous thin quartz veins (Fig. 7). On the northwestern side of the fault zone, a relic (Proterozoic) ductile shear zone in migmatitic gneisses of the Kattfjord complex, containing chlorite and quartz as the essential fabric minerals, merges into parallelism with the Rekvika fault zone (Fig. 7 & 8d). This pre-existing ductile shear zone has so far not been found southeast of the Rekvika fault zone, but could potentially be used as a drag-folded, partly offset marker unit for the estimation of shear-sense and amount of displacement along the fault zone.

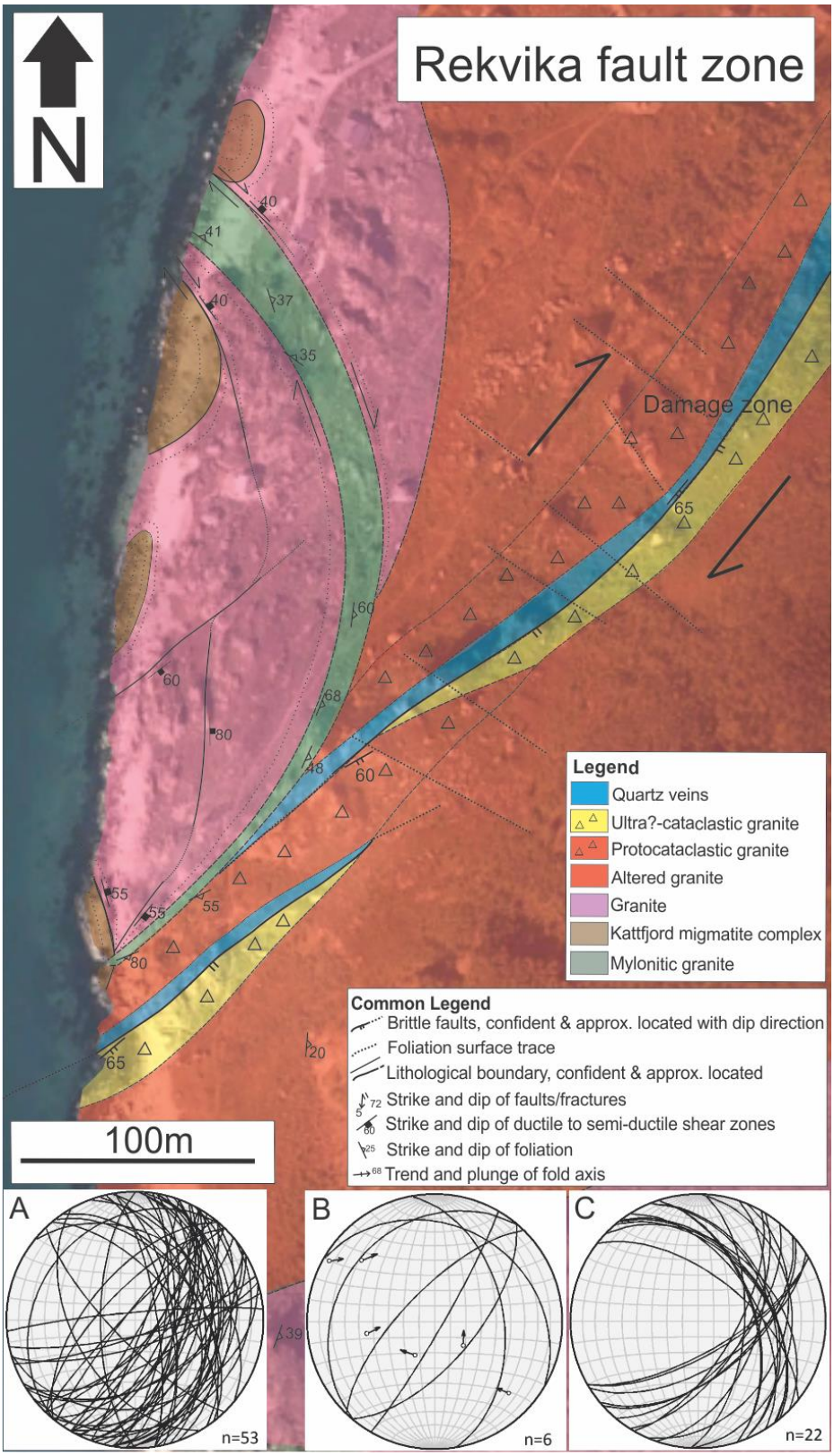

Figure 7: Structural and lithological map of the Rekvika fault zone. The host rock is the Ersfjord granite, which includes a pod of altered granite along the main fault trace, and the Kattfjord complex gneisses that crop out along the shore. The Rekvika fault zone trends NE-SW and is characterized by cataclastic fault rocks and comprehensive quartz veining in the core zone. Note the ductile shear zone in the west of the main fault and the ductile foliation affecting the entire area. (A) Stereonet showing the fracture orientations in Rekvika (B) Stereonet displaying the slickenside data relative to the Rekvika fault zone (C) Stereonet plotting minor shear zones observed in Rekvika.

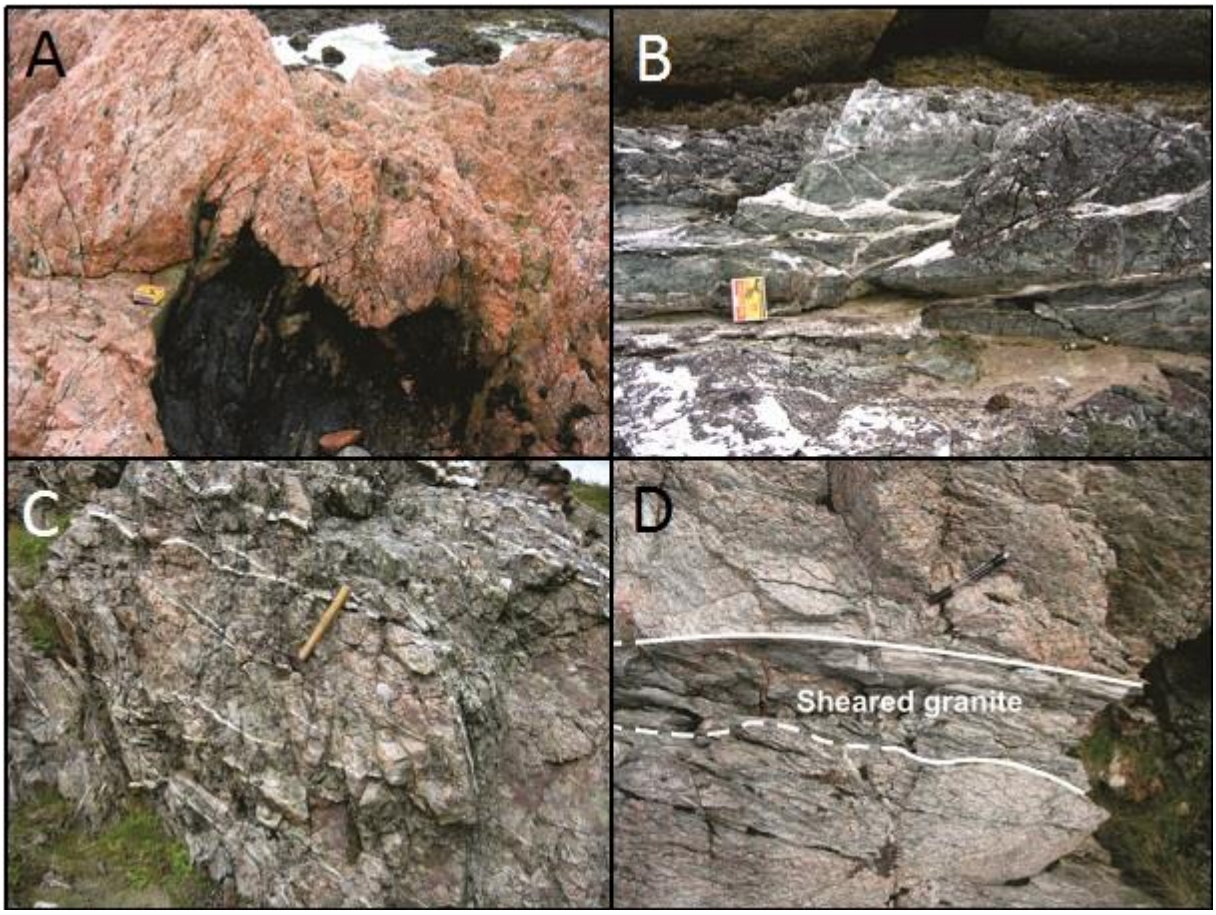

Figure 8: Outcrop photographs of the Rekvika fault zone and associated structures. (A) Ersfjord granite in Rekvika, showing red-staining probably due to hydrothermal alteration, and including a lens of mafic gneisses (B) Greenish matrix cropping out in the core of the Rekvika fault zone. It is thought to correspond to cataclastic fault rock (C) Highly fractured core zone showing mainly quartz veining (D) Mylonitic shear zone in the Ersfjord granite, in the NW of the Rekvika fault zone (cf. fig. 7). Photos from Steffen Bergh.

2.2.1.2 Description of brittle fractures and associated structures in the fault zone

The Rekvika fault zone trends NE-SW and dips steeply to the SE. The main fault is composed of a few meters wide NE-SW oriented, core zone (cf. fig. 7). As also revealed by previous authors (Antonsdóttir 2006) a majority of planar fractures strike NE-SW to NNE-SSW with a steep to gentle southeastern dip, and have a high frequency in the hydrothermal core of the fault zone (Fig. 7a & 8c). Few NNE-SSW to NE-SW trending fractures steeply dip to the NW and they might then correspond to a conjugate set of the SE-dipping fractures. These fractures are commonly filled with quartz and calcite veins up to tens of centimeters wide. Occurrences of chlorite, epidote and more rarely hematite were also noticed along distinct, high-frequency, NNE-SSE to NE-SW trending fracture surfaces in the core zone. A set of NNW-SSE to NW-SE trending fractures dipping steeply to the NE (Fig. 7a) and frequently filled up with quartz seems to crosscut the dominant NNE-SSW to NE-SW trending set of

fractures, confirming a relative time difference between them (cf. Antonsdóttir 2006). From interpreted DEM satellite images this set of fractures looks well-developed in the NE-SW striking main fault trace (Fig. 7). NW-SE striking microfaults apparently truncate NNE-SSW trending microfractures. In general slickensided fracture surfaces are hard to locate in Rekvika. Despite frequent quartz and calcite veins or chlorite, epidote and hematite precipitations, only few grooves were found. Weak apparent foliation and duplex-like structures in highly fractured granite occur in the core zone of the Rekvika fault zone. They are mainly composed of chlorite grains, and minor amounts of epidote and white micas (Fig. 9a). Optionally they may correspond to modified ductile fabrics (see chapter 2.2.1.5 on pre-existing fabrics).

2.2.1.3 Description of kinematic data

The analysis of the scarce slickenside striations found on the fault surfaces in Rekvika showed oblique-normal movements along the faults, indicating strike-slip component on gently dipping normal faults (Fig. 7b). Some slickensides may indicate minor dip-slip reverse movements. Unfortunately most of the studied fractures did not display any evidence of displacement, making the data regarding slickensides insignificant; even the sense of slip of the slickensides included in this study was difficult to assess. However the asymmetric geometry displayed by the pod of altered granite on each side of the Rekvika fault zone, to the north and to the southeast (Fig. 7), may account for some dextral strike-slip displacement. Moreover the dragfolded-looking and likely offset shear, as it has not been found on the southeastern side of the Rekvika fault, would also favor dextral strike-slip movements along the Rekvika fault zone (Fig. 7). On the other hand, the chloritic, epidote and white micas-bearing, S-C, duplex-like fabric may indicate sinistral sense of shear in an extensional context along the main fault (Fig. 9a). Thin-section studies of cataclastic rocks and microscopic offset markers support a dominant normal component of movement on the Rekvika fault zone (Fig. 9b). Both minor sinistral and dextral displacement have been identified along NW-SE microfaults that offset a NNE-SSW microfracture (Fig. 9c & d). The quartz fibers that developed along NW-SE trending microfractures display a NE-SW oriented long axis that suggests a NE-SW directed extension (Fig. 9e; Passchier & Trouw 2005).

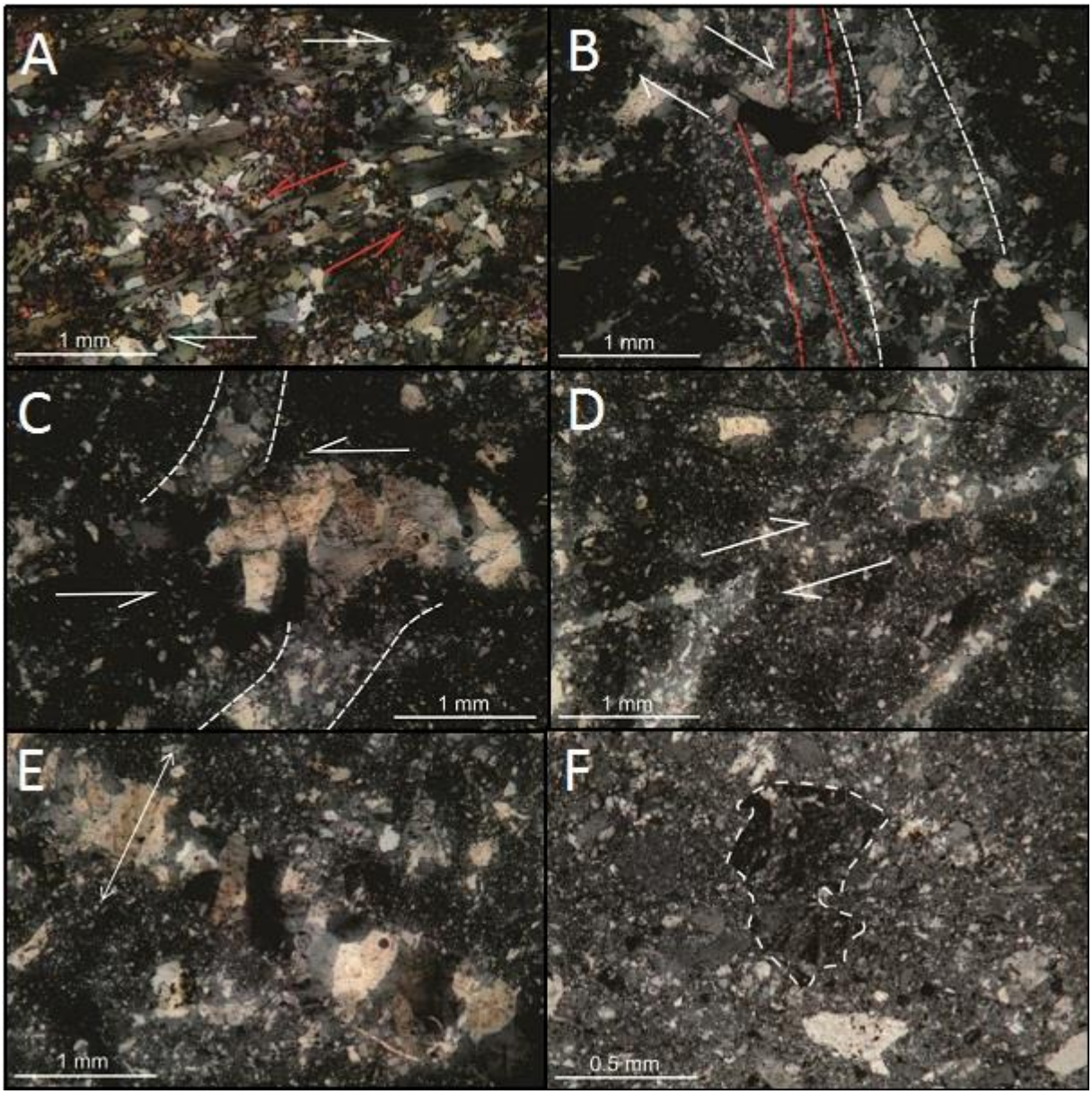

Figure 9: Microphotographs of the Ersfjord granite and cataclastic fault rock along the Rekvika fault zone. (A) Oblique cleavage relations (S-C fabric?) made of chlorite crystals, that could either correspond to healed duplexes indicating normal faulting (red arrows), or to a ductile foliation indicating dextral shearing (white arrows) (B) Cataclasite in the core of the Rekvika fault zone showing two sub-vertical quartz veins (dashed red and white) truncated by a third, oblique, NE-SW trending quartz vein, indicating normal movements (C) Micro-offset along a NW-SE trending quartz vein, indicating sinistral strike-slip displacement (D) Micro-offset along a NW-SE trending quartz vein indicating dextral displacement (E) Elongated quartz grains in a quartz vein suggest a NE-SW extension direction. The white arrow indicates the grain elongated axis (F) Clast of dark cataclasite (dashed white) embedded in a younger quartz and feldspar-rich cataclastic matrix.

2.2.1.4 Description of fault rocks

The epidote and chlorite-rich granite predominating in the damage zone looks highly fractured. The core zone identified in Rekvika (Fig. 7) includes thick meter-scale quartz veins, and a greenish matrix crisscrossed by millimeter to centimeter-thick calcite and quartz veins, which sometimes embeds clasts of unaltered and undeformed granite, (cf. Antonsdóttir

2006; fig. 8b). The damage zone is marked by a protocataclastic granite layer in the footwall that frequently contains angular to sub-angular clasts of plagioclase, and a cataclastic to ultracataclastic granite in the hanging-wall (Fig. 8b). The content of cataclastic matrix in the granite can reach up to 90% of the whole composition along the main fault and is mainly composed of rounded quartz, feldspar and white micas. The remaining clasts floating in the well-sorted, quartz and feldspar-rich matrix comprise quartz, feldspar and occasionally clasts of brownish cataclastic material, potential indicator of an earlier generation of cataclasite (Fig. 9f).

2.2.1.5 Pre-existing fabrics along the fault zone

Older ductile fabrics were observed around the Rekvika fault zone, including an N-S to NNE-SSW striking gneiss foliation trend that seems to prevail in the area (Fig. 7). This foliation appears to be folded parallel to the lithological boundary. The highly fractured granite in the core zone of the main fault displays a slightly different NE-SW trending fabric/foliation that appears as chlorite-rich bands. The microscopic study reveals alignments of stretched chlorite grains forming a well-defined S-C fabric that could indicate dextral strike-slip motions (Fig. 9a). A similar S-C mylonitic fabric dominated by clasts of quartz and feldspar, and alignments of chlorite or/and white mica has been identified on minor steeply dipping shear zones and more particularly in the NW on a probably Proterozoic, NE-dipping, several meter-wide ductile shear zone that cuts through the gneisses of the Kattfjord complex (Fig. 8d). Minor shear zones display two major trends: NE-SW with a southeastern dip, and NW-SE dipping northeastwards, conceivably representing conjugate sets (Fig. 7c), whilst the large shear zone trends NW-SE to N-S defining a trough in the local topography, and bends towards the Rekvika fault zone (Fig. 7). The fabric of the undeformed granite is bent clockwise toward the mylonitic NW-SE to N-S trending shear zone, which suggests dragfolding occurred under dextral shearing. Analogously the trend of the mylonitic fabric varies in the bending ductile sheared arm until its orientation merges into parallelism with the NE-SW foliation trace previously described in the intensely fractured granite of the damage zone. Similar to the observed change in attitude of the granite fabric, the microstructural analysis of σ-shaped clasts and chlorite and white micas alignments in the S-C geometry indicate dextral strike-slip movements in the shear zone.

2.2.1.6 Summary and preliminary interpretations

The Rekvika fault zone trends NE-SW and dips to the SE. A NNE-SSW to NE-SW trending fracture set of high frequency is thought to dominate, especially in the core zone along the main fault trace (Fig. 8c). A second fracture pattern, striking NNW-SSE to NW-SE, crosscuts the entire area, clearly denoting a younger age for these fractures, and likely unrelated to the formation of the Rekvika fault zone. The ca. 50 meter width of the Rekvika fault zone suggests quite localized deformation. A major hydrothermal event has taken place along the Rekvika fault zone, accounting for widespread quartz precipitation along the main fault surface in the core zone (Fig. 8c), quartz and calcite veins and epidote, chlorite and hematite precipitations on the fracture surfaces. The core zone is mainly composed of highly fractured, cataclastic granite truncated by quartz and calcite veins (Fig. 8b). The presence of epidote and chlorite in the cataclasites indicates a depth of about 5 to 10 kilometers, i.e. a pressure range from 0.2 to 0.3 GPa, and temperatures of ca. 350-500°C, i.e. greenschist metamorphic conditions (cf. Bucher & Grapes 2011). The kinematic indicators suggest predominant dextral-oblique normal movements along the main, NE-SW trending fault surfaces and the minor faults, whereas the NW-SE trending faults show strike-slip motions. This is supported by the dextral offset of the altered pod of granite and mostly dip-slip normal motions for the NNE-SSW to NE-SW microfaults in cataclastic fault rocks, and by dextral/sinistral displacement along NW-SE striking microfaults. Elongated quartz fibers along NW-SE microfractures suggest a NE-SW local extension for the Rekvika fault zone during the development of these fractures (Passchier & Trouw 2005). The presence of clasts of brownish cataclasite embedded in a potentially second-generation, quartz and feldspar-rich cataclastic matrix in the core zone indicates that the Rekvika fault zone may have been reworked/reactivated in steps after its main movement. The bending of the NW-SE to N-S trending ductile shear zone into the Rekvika fault zone is not associated with any brittle structures and might therefore be the result of Precambrian drag-folding into a steep, NE-SW trending, Svecofennian shear zone that trends parallel to the Rekvika fault zone. This is suggested by the remnant, NE-SW trending, S-C foliation along the Rekvika fault zone (Fig. 7c). In this respect, such a Precambrian ductile shear zone would have constituted a zone of preferential weakness for the development of the Rekvika fault zone (see chapter 3.4 for discussion).

2.2.2 Bremneset fault zone

2.2.2.1 Large scale field relations and host rock characteristics

The Bremneset fault zone lies in the south-west of Rekvika on Kvaløya island (Fig. 4), within the Kattfjord complex gneisses, and away from the boundary with the Ersfjord granite (Fig. 10). The local lithology is dominated by Neoarchean migmatitic gneisses of the Kattfjord complex that commonly incorporate lenticular granitic bodies that are 0.5 meter to few meters large. These granites occur in lenses and/or as fine-grained folded felsic dykes, typically tens of centimeter wide (Fig. 11a), and veins of granitic material seem to be injected into the gneisses. The mineral composition and alteration character adjacent to the main fault zone resemble the red-colored altered Ersfjord granite that crops out in Rekvika, and therefore, the granites may be related to the Ersfjord granite of the region. The granite lenses mineral composition is dominated by quartz, K-feldspar, epidote, white micas, few chlorite and occasionally highly altered plagioclase. The Bremneset fault zone shows a length of ca. 1 km and dips to the SE. The trend of the Bremneset fault zone varies slightly along strike, but mostly is NNE-SSW, partly oblique to the foliation of the Kattfjord complex gneisses, which is NW-SE trending, and consists of an approximately 50 meters wide damage zone and of a narrow (ca. 0-3m thick) core zone of highly fractured, epidote-rich granite and gneisses (Fig. 11b). A weak ductile fabric, likely gneiss foliation, seems to strike oblique to the main NNE-SSW to NE-SW Bremneset fault zone, but appears to be parallel to a minor, NW-SE trending, fracture set.

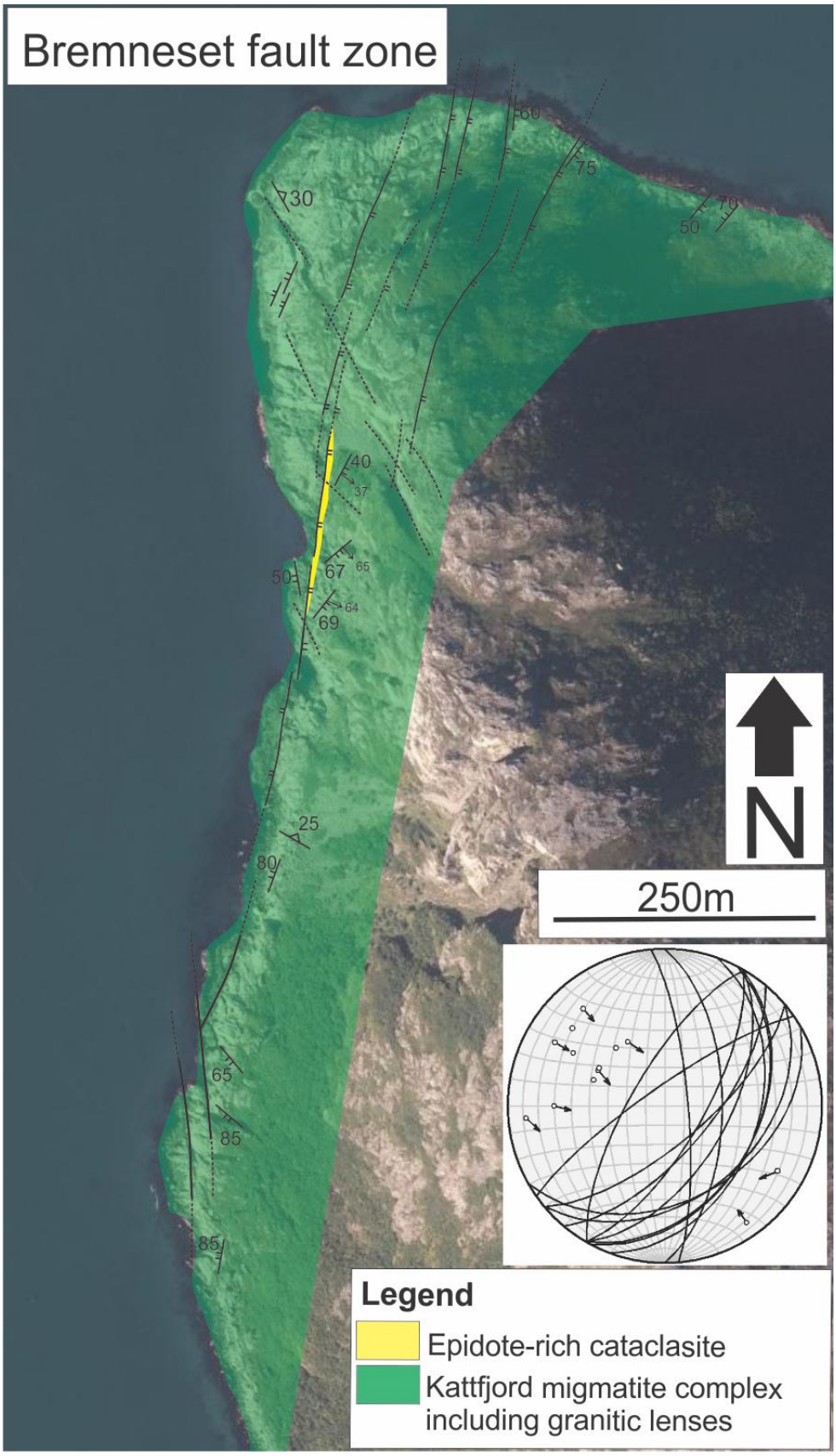

Figure 10: Structural and lithological map of the Bremneset fault zone, in northwestern Kvaløya. The Kattfjord complex gneisses dominate the lithology and are affected by a NW-SE trending ductile foliation, and truncated by major, NNE-SSW to NE-SW and NW-SE trending lineaments. Note the stereoplot showing the slickenside data of the Bremneset fault zone. For structural legend see "common legend" in fig. 7.

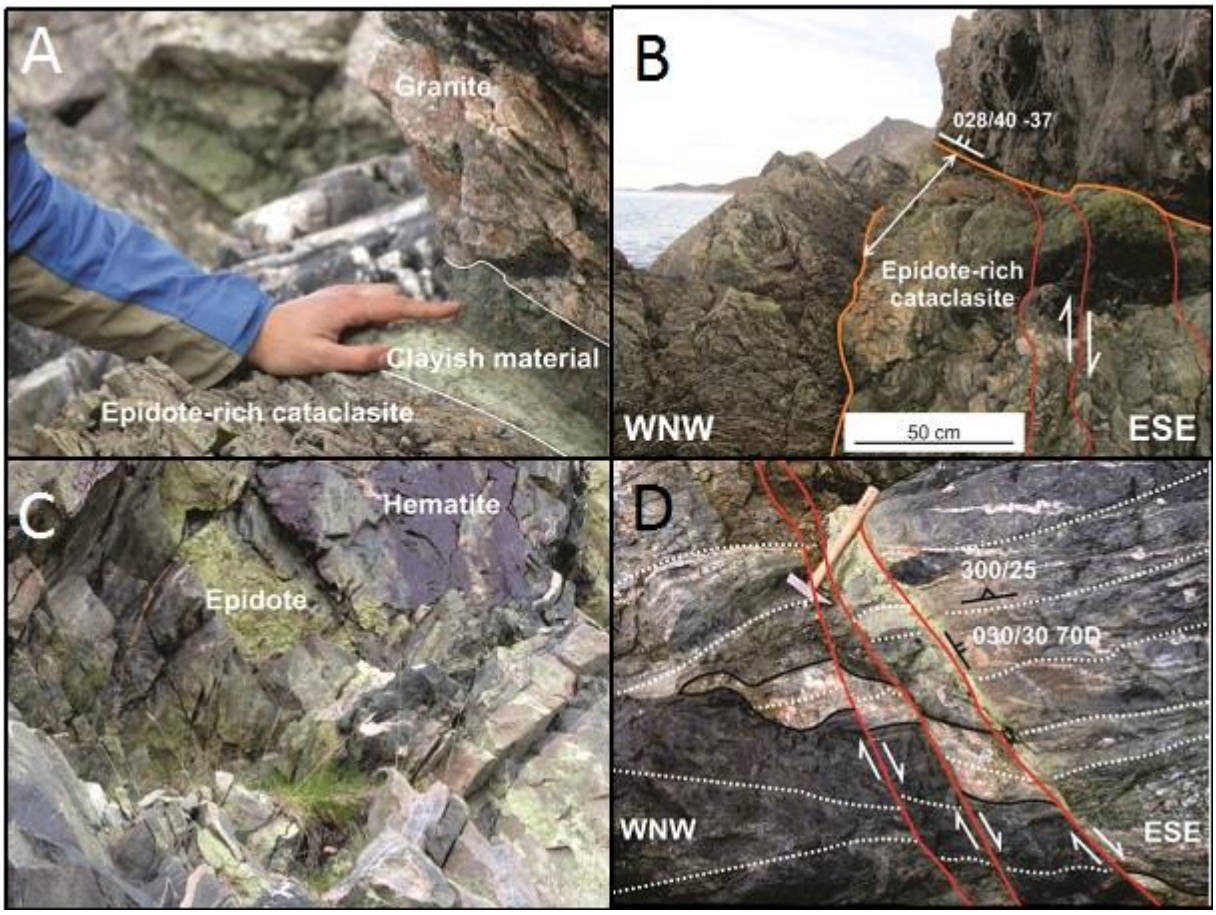

Figure 11: Outcrop photographs of the Bremneset fault zone and associated structures. (A) Fine-grained granite underlain by clayish and epidote-rich cataclastic material defining the core of the Bremneset fault zone (B) Highly fractured, epidote-rich cataclastic core zone showing major NNE-SSW striking faults (orange) bending high-frequency, NE-SW trending fractures (red), and delineating a duplex-like structure that may indicate dip-slip normal movements (C) Epidote and hematite precipitations on fracture surfaces in the damage zone of the Bremneset fault zone (D) Pegmatite dyke (black) showing down to the SE, normal offsets along localized mesoscale faults (red). Note the foliation (dotted white) that affects both the gneisses and the pegmatite.

2.2.2.2 Description of brittle fractures and associated structures in the fault zone

The Bremneset fault zone trends NNE-SSW and shows a moderate southeastern dip (Fig. 10). The fault zone localizes into a narrow zone in the south (less than 50 meters wide) and suddenly splits up into several fault segments in the north, where mainly synthetic, rectilinear, planar faults and fractures are recorded (Fig. 12). The width of these individual fractures rarely exceeds few centimeters albeit some of them occasionally reach few meters (Fig. 11b). The bulk of fractures show a NNE-SSW to NE-SW trend and steep dips to the SE, although more gently dipping fractures and faults (with slickensides) are not uncommon (Fig. 12). The most prominent fault surface strikes NNE-SSW and dips moderately to the SE. It shows a discontinuous surface composed of fine grained greenish epidote, which is linked to multiple fracture sets that resemble a brittle duplex (Fig. 11b). This duplex-shaped fabric is

made up of epidote-filled, high-frequency NE-SW trending fractures that have been crosscut by and show anticlockwise sigmoidal bending towards major NNE-SSW trending fault surfaces. Alternatively the NE-SW trending, bent fractures appear to splay out from the NNE-SSW striking faults as horse-tail fans (Fig. 11b & 12). Recurrent epidote and younger hematite (Fig. 11c) were found on NNE-SSW and NE-SW trending fracture surfaces. These secondary mineral precipitations often define fibrous striations on the fracture surfaces and suggest a synchronous development of these two sets of fractures. A secondary fracture pattern trending NW-SE, mostly evidenced with DEM satellite images, seems to truncate the NNE-SSW to NE-SW trending fractures that sometimes even die out at the intersection with NW-SE oriented fractures (Fig. 10).

2.2.2.3 Description of kinematic data

Slickenside striations are numerous on most of the fracture surfaces observed in the Bremneset fault zone (Fig. 12). Most of the slickensides recorded in the field define fibrous epidote on fault surfaces close to the fault core and mainly indicate dominant dip-slip normal, down to the SE movements, as well as dextral strike-slip components along the faults in Bremneset (Fig. 10). Notwithstanding, few centimeters up to tens of centimeters offsets of pegmatite dykes in the gneisses indicate normal motion, localized along several minor faults, as shown by fig. 11d. Furthermore, anticlockwise sigmoidal curving of merged, *en echelon*, NE-SW trending, gash fractures towards NNE-SSW trending border faults would tend to favor normal movements along the continuous extensional duplex-shaped system (Eig & Bergh 2011) exposed on the main epidote-rich fault surface (Fig. 11b & 12). The microstructural analysis has largely confirmed dip-slip normal movement, but shows as well offsets that indicate probable dip-slip reverse motion along some microfaults (Fig. 13a & b). The microstructural analysis also evidenced minor sinistral offsets of quartz grains along cataclastic veins, thus addressing a strike-slip component to the Bremneset fault zone (Fig. 13c).

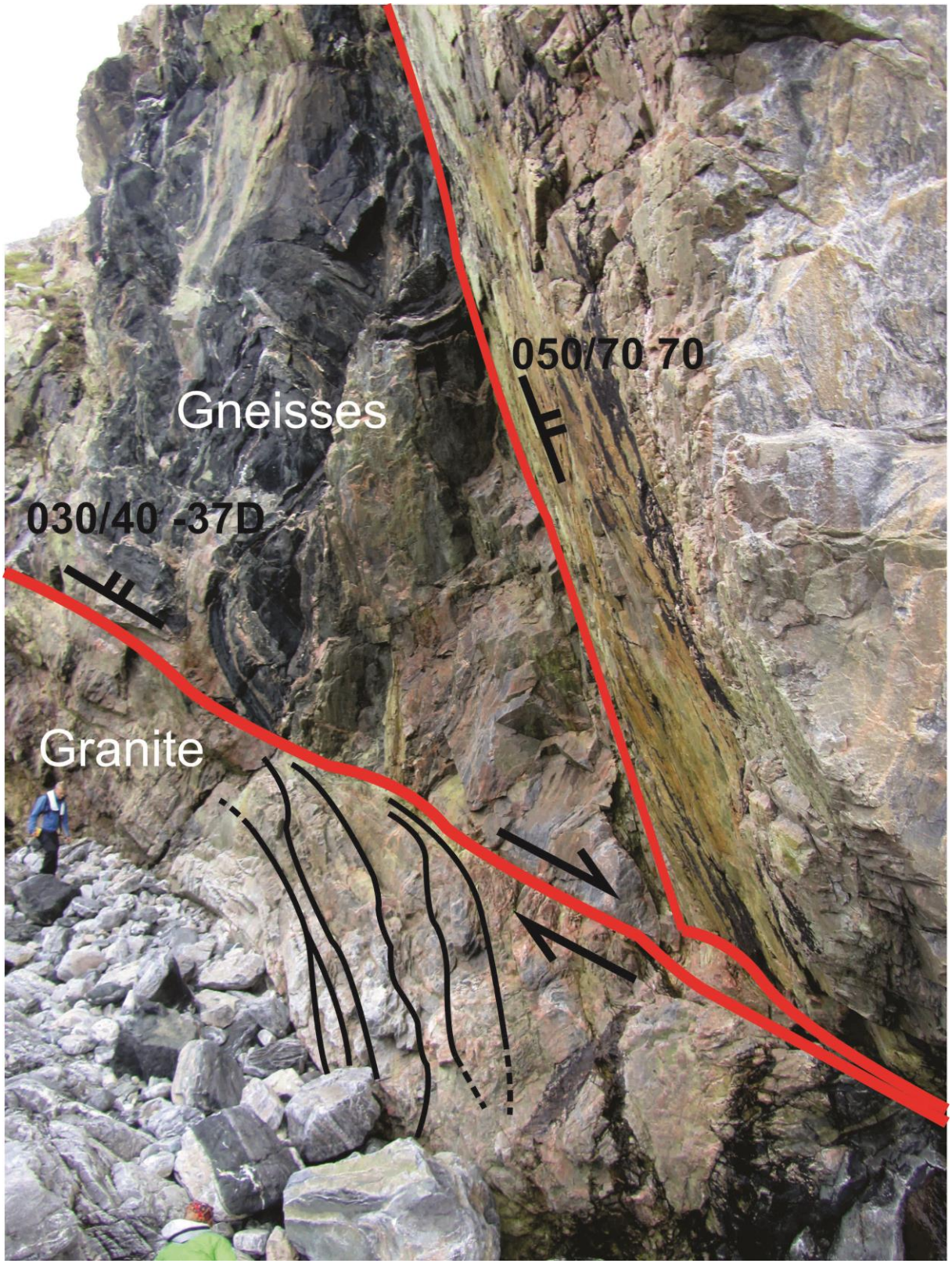

Figure 12: **Major epidote-rich cataclastic zone showing duplex-like geometry, and anticlockwise bending of NE-SW trending fractures (black) towards a low-angle, NNE-SSW trending fault (red), that might indicate normal motions along a probable extensional duplex. The major border faults (red) display both steep and gentle dips to the SE, and planar geometries.**

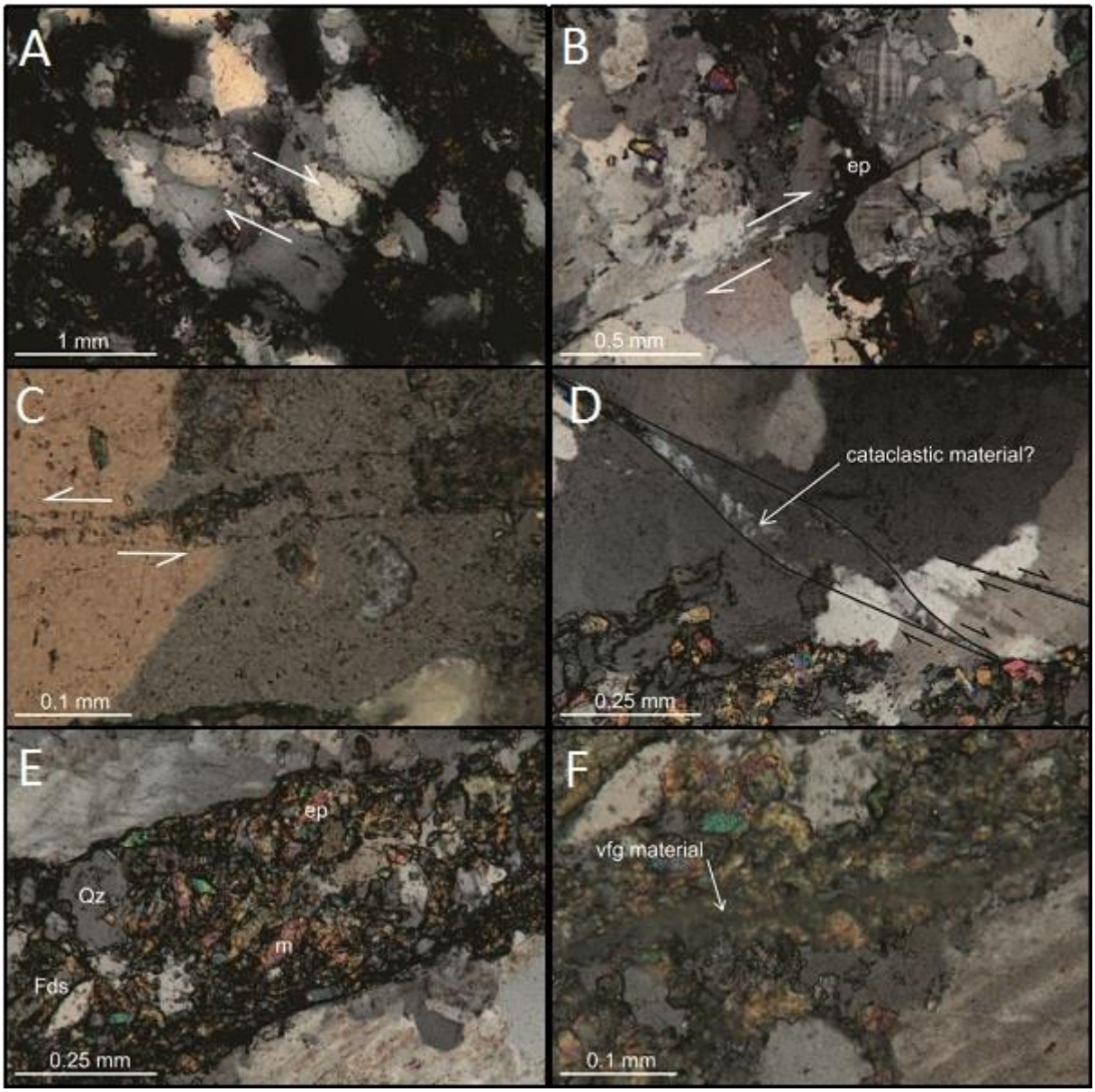

Figure 13: Microphotographs of host rocks and cataclasites along the Bremneset fault zone. (A) Micro-offset of a block of host rock indicating normal displacement (B) Microfault offsetting an epidote vein (ep), indicative of dip-slip reverse movement (C) Micro-offset of a quartz grain showing minor sinistral displacement along an almost healed fracture (D) Microfractures (black) that seem to incorporate recrystallized cataclastic material along strike, displaying micro-offsets indicative of normal displacement (E) Coarse-grained cataclastic matrix containing mostly quartz (Qz), feldspar (Fds), epidote (ep) and white mica (m) (F) Very-fine grained (vfg) to microscopic brownish cataclastic vein.

2.2.2.4 Description of fault rocks

Cataclastic fault rocks occur all along the trace of the main NNE-SSW trending Bremneset fault zone and correspond to a highly cracked greenish to yellowish epidote-rich cataclasite that ranges from centimeter up to few meter in width. The fault rocks typically include a thin layer of clayish material (Fig. 10 & 11a). On a microscopic scale, fractures infrequently incorporate fine-grained material, especially quartz, along the fracture and fault

surfaces (Fig. 13d). The thin sections show a predominance of epidote-rich cataclasite that appears as tenth of millimeter to millimeter thick layers and veins. The matrix is coarse to fine-grained and mostly composed of epidote, quartz, feldspar and white mica, including quartz and feldspar clasts sometimes of millimetric size (Fig. 13e). This cataclasite is crisscrossed by thin veins of very fine-grained to microscopic brownish matrix (Fig. 13f). The highly fractured host rock, which is red-stained granite, forms large blocks surrounded by cataclastic veins. These blocks are composed of quartz, K-feldspar, altered plagioclase, minor chlorite and accessory epidote-rich cataclastic material.

2.2.2.5 Pre-existing fabrics along the fault zone

This area differs from the Rekvika fault zone since no ductile shear zones have been observed in the host rock gneisses. However a ductile gneiss foliation striking NW-SE to WNW-ESE has been mapped in the area, trending approximately parallel to the NW-SE trending fractures (Fig. 10). This ductile fabric affects the mafic gneisses and the pegmatite dykes (Fig. 11d) but the granite lenses look undisturbed (Fig. 11a). South of the studied area, the NW-SE to WNW-ESE trend of the foliation turns into a more N-S trend, potentially indicating macroscale folding (cf. chapter 3.4).

2.2.2.6 Summary and preliminary interpretations

The Bremneset fault zone trends NNE-SSW and dips moderately SE. It has been traced for ca. 1000m and displays a 0-2 m wide core zone. This core zone is composed of high-frequency, planar, NNE-SSW to NE-SW trending faults and fractures (Fig. 10). Eventually a set of NW-SE striking fractures truncates the NNE-SSW to NE-SW trending faults and these structures were then inferred to have formed later, probably not related to the Bremneset fault zone. The epidote and chlorite contained in cataclastic fault rocks, and the epidote coatings found on different fracture surfaces (Fig. 11c) clearly indicate a depth of about 5 to 10 kilometers, i.e. a pressure range from 0.2 to 0.3 GPa, and temperature of 350-500°C indicative of greenschist metamorphic conditions (Bucher & Grapes 2011). A synchronous development seems likely for the NNE-SSW and the NE-SW trending faults and fractures since they display similar epidote and younger hematite precipitations on their surfaces (Fig. 11b). The kinematic and microstructures analyses of fault rocks and brittle fracture surfaces arranged in duplex-like features reveal dominant dip-slip normal movement along the main

fault zone (Fig. 10, 11b, 11d, 12 & 13a). Dextral strike-slip motions were indeed inferred from the slickensides analysis (Fig. 10) and a minor sinistral component from the microstructural analysis (Fig. 13c). On top of that, reverse offsets were found along microfaults, which might suggest several stages of faulting (Fig. 13b). This is also suggested by the crosscutting relationships of different kinds of cataclastic veins, evidenced in the discontinuous layer of epidote-rich cataclasite in the core of the Bremneset fault zone (Fig. 13f). The main, NNE-SSW trending Bremneset fault zone seems to have developed along potential zones of weakness, such as the lithological boundary between the gneisses and lenses of granite, but mostly truncates the gneiss fabric (Fig. 12). The potentially younger, NW-SE trending set of fractures runs parallel to the pre-existing NW-SE striking foliation (Fig. 10). It is therefore suggested that this foliation influenced the development of the NW-SE trending fractures.

2.2.3 Tussøya-Røkneset fault zone

2.2.3.1 Large scale field relations and host rock characteristics

The Tussøya-Røkneset fault zone is exposed on an island lying south-west of Bremneset and Rekvika (Fig. 4). Fine-grained, unaltered and relatively undeformed granite crops out in the west of the island, and this granite resembles the undeformed Ersfjord granite in Rekvika (Fig. 14). It is progressively replaced by a heavily fractured, altered, red-stained, and fine to medium-grained granite when approaching the main fault zone from the east that defines the lithological boundary with banded gneisses (Fig. 14, 15, 16a). Intercalations of granite, typically 1 meter large, were found in the vicinity of the fault zone, in gneisses that probably belong to the Neoarchean Kattfjord complex. The mineral composition of the altered granite is dominantly made of quartz, K-feldspar and plagioclase, and of fewer amounts of chlorite, epidote, white-micas, iron oxide and pumpellyite (Fig. 17a). The Tussøya-Røkneset fault zone is ca. 300 meters long and shows a 50 meters wide damage zone. It strikes NNE-SSW and gently dips to the SE. Most of the brittle deformation and the main fault zone seem localized along the boundary between the hydrothermally altered and highly deformed granite and the amphibolitic gneisses, defining a few meters wide core zone composed of high-frequency, *en-echelon* fractures and possibly containing

cataclasite (Fig. 16a). These fractures apparently trend oblique to the dominant, ENE-WSW to NE-SW trending ductile fabric in the gneisses (Fig. 16b).

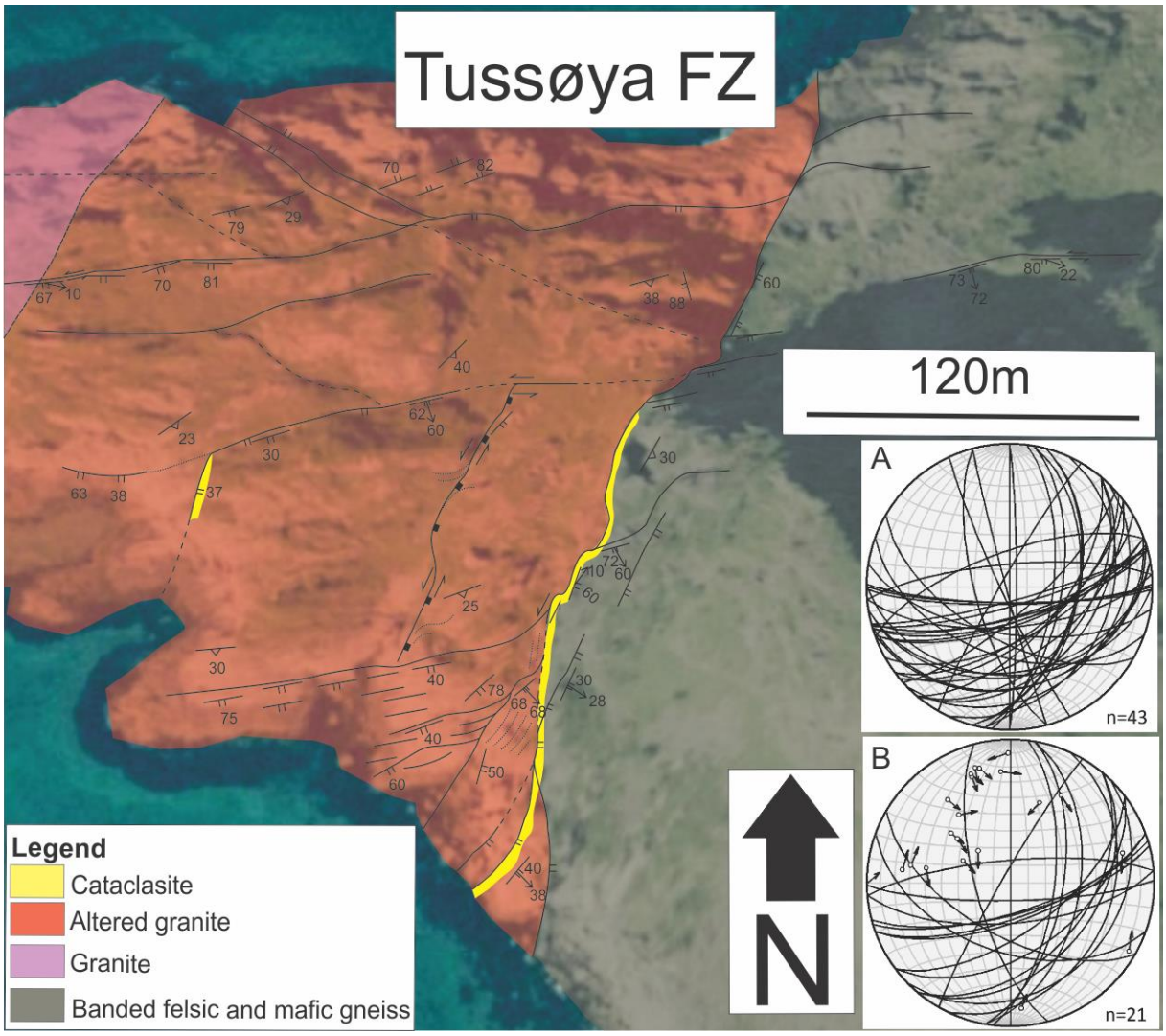

Figure 14: Structural and lithological map of the Tussøya-Røkneset fault zone in northwestern Kvaløya. The main fault zone runs along the contact between the red-colored granite and the Kattfjord complex gneisses, showing a NNE-SSW trend. NNE-SSW and ENE-WSW trending fractures form two major sets of brittle structures. The ductile fabric shows a relatively consistent NE-SW to ENE-WSW orientation around the whole area. (A) Stereonet displaying the strikes of the fractures observed in Tussøya (B) Stereonet showing the slickenside data along the Tussøya-Røkneset fault zone. For structural legend see "common legend" in fig. 7.

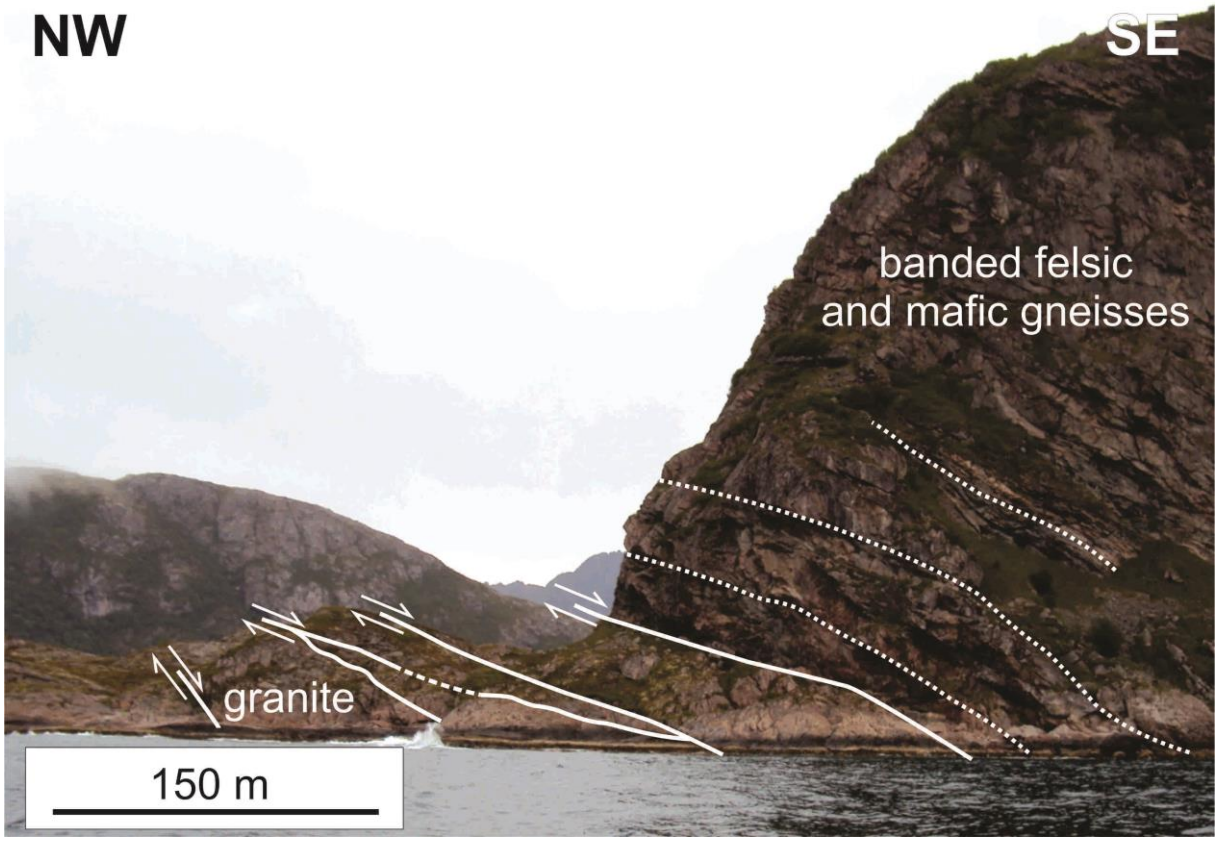

Figure 15: Photograph displaying an overview of the Tussøya-Røkneset fault zone, and showing the lithological contact between the granite and banded felsic and mafic gneisses. The gneiss foliation (dotted white) trends parallel to the lithological contact and the Tussøya-Røkneset fault zone.

2.2.3.2 Description of brittle fractures and associated structures in the fault zone

In Tussøya, the fault zone has a main NNE-SSW strike and dips moderately to the SE. It shows a narrow damage zone (ca. 50m thick) to the north that appears wider in the south where it may reach a width of approximately 80 meters (Fig. 14). The major fault zone is surrounded by anastomosing, oblique splay faults and fractures trending ENE-WSW to E-W (Fig. 16c), that clearly interact with NNE-SSW oriented fractures. Together they outline a relay-ramp geometry both in map view (Fig. 14) and in cross-section view (Fig. 16d), along the main fault surface. The steeply-dipping, ENE-WSW trending fractures merge into the right-stepping *en-echelon*, planar, NNE-SSW trending fractures, likely defining duplex-shaped structures where splays of subsidiary, ENE-WSW trending fractures seem to link major bounding NNE-SSW striking fractures. Alternatively in map view, the NNE-SSW striking fractures also appear to merge with the ENE-WSW trending fractures (Fig. 14). Less prominent NW-SE striking lineaments become more common toward the west of the island, away from the Tussøya-Røkneset fault zone, and they appear to bend perceptibly at the

intersection with ENE-WSW to E-W trending fractures (Fig. 14). The fracture surfaces commonly display epidote, pronounced copper/malachite coatings and hematite mineral precipitations along strike (Fig. 16d). More particularly the epidote-coated fracture surfaces often show fibrous slickensides (Fig. 16e).

2.2.3.3 Description of kinematic data

The kinematics of the Tussøya-Røkneset fault zone has been assessed mostly thanks to fibrous slickensides found on fault surfaces covered by epidote precipitations (Fig. 16e). These structures indicate mainly down to the ESE, dip-slip normal motions along the NNE-SSW trending faults, and especially along the main fault zone. On the other hand, the epidote fibers observed on ENE-WSW trending fault surfaces generally indicate sinistral strike-slip movements, particularly away from the core of the Tussøya-Røkneset fault zone (Fig. 14 & 16e). Similarly, anticlockwise bending of NW-SE striking fractures towards ENE-WSW trending fractures indicates a sinistral strike-slip sense of shear for the latter set of faults (Fig. 14). Anticlockwise curving of the ENE-WSW trending fractures toward NNE-SSW faults forming duplex-shaped structures suggests dip-slip normal movements in cross-section, whereas it indicates sinistral displacement in map view (Fig. 14 & 16d). Bending of NNE-SSW trending fractures toward ENE-WSW striking fractures in map view might however indicate dextral strike-slip motions along the ENE-WSW trending fractures (Fig. 14; see chapter 3.1.1). NNE-SSW to NE-SW trending microfaults, sometimes merging into duplex-like structures, show micro-offsets along cataclastic veins and layers that indicate dip-slip normal displacement (Fig. 17b & 17c). The microstructural analysis also shows minor offsets of quartz, feldspar and plagioclase grains along NNE-SSW trending microfaults that indicate dextral displacement (Fig. 17d).

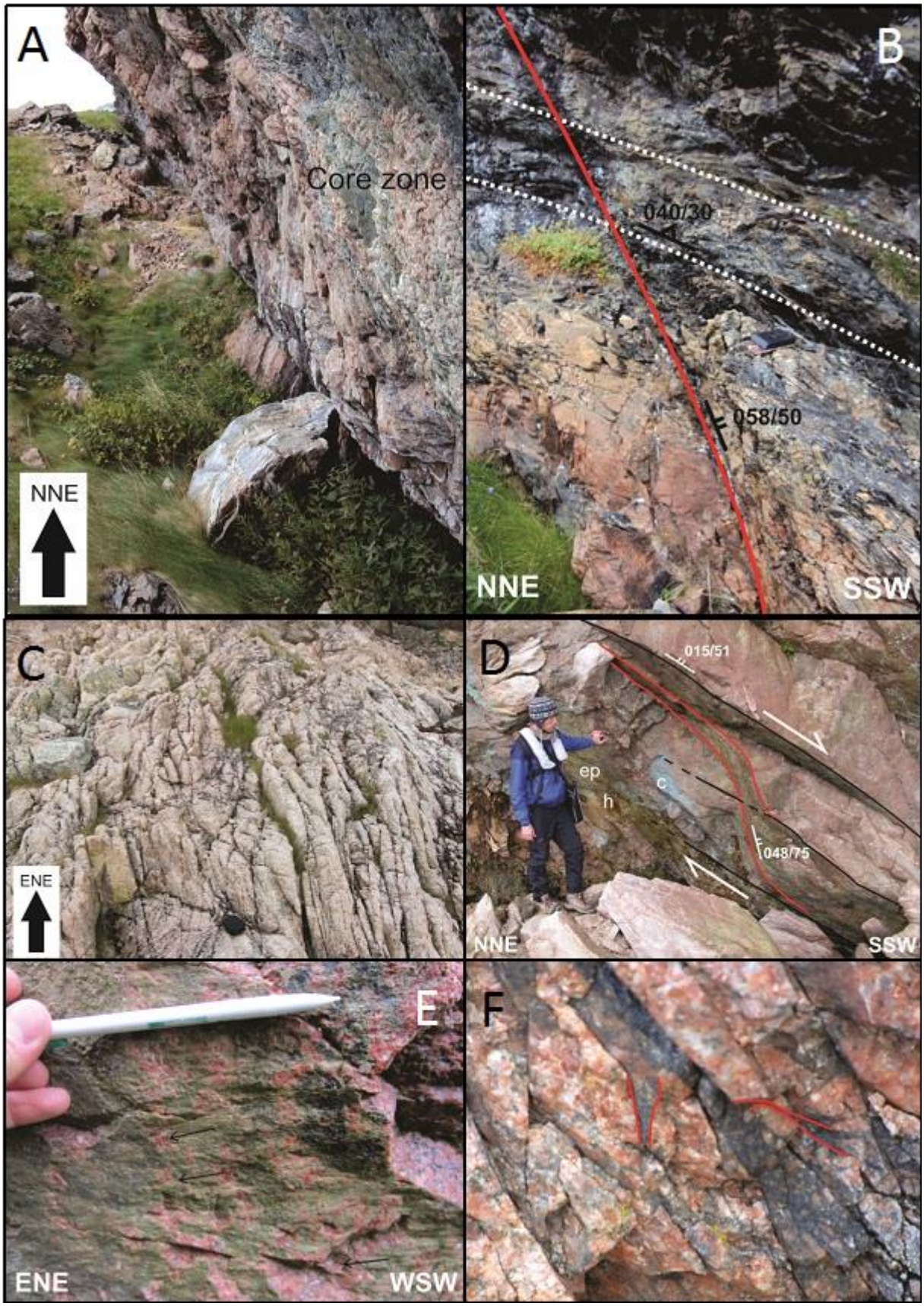
A
Core zone
NNE
B
040/30
058/50
NNE
SSW
C
ENE
D
015/51
ep
h
c
048/75
NNE
SSW
E
ENE
WSW
F

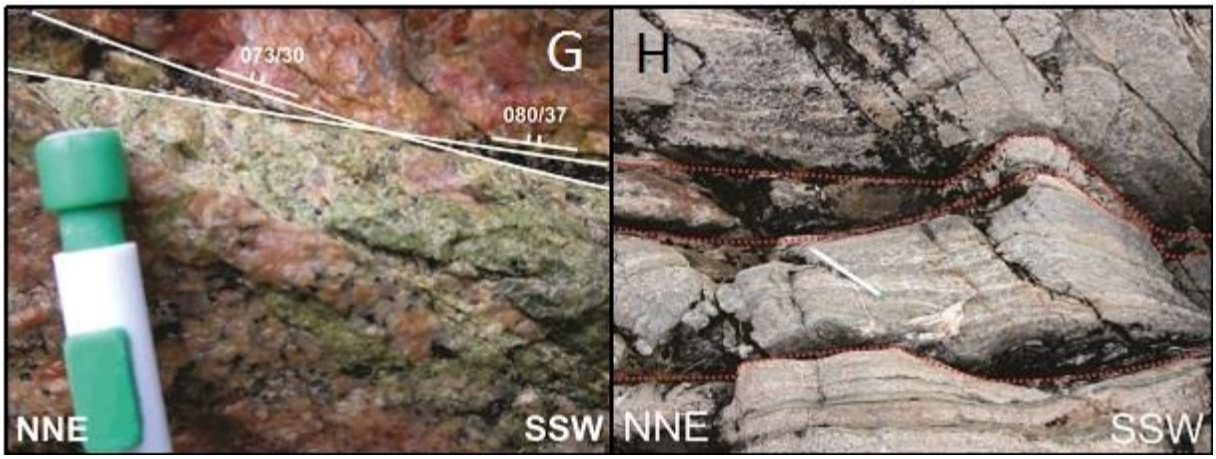

Figure 16: Outcrop photographs of the Tussøya-Røkneset fault zone and associated structures. (A) Highly cracked zone along the lithological boundary between the granite and the gneisses. This represents the core of the Tussøya-Røkneset fault zone, which probably contains cataclastic material (B) ENE-WSW trending fracture (red) running oblique to the main, NE-SW trending foliation trace (dotted white) (C) Major fracture surfaces showing hematite (h), epidote (ep) and malachite/copper (c) precipitations along strike. ENE-WSW striking fractures (red) display an apparent anticlockwise curving towards NNE-SSW trending faults (black), forming duplex-like structures that possibly imply dip-slip normal movements (D) Granite truncated by anastomosing, ENE-WSW striking splay fractures (E) Epidote-rich fault surface trending ENE-WSW and showing fibrous slickensides on the hanging-wall that indicate major sinistral strike-slip movement; the arrows indicate the relative movement of the hanging wall block, i.e. of the block showed on the picture (F) Fine-grained, dark veins, thought to be pseudotachylyte, but containing cataclastic material and clasts of granite. This dark material seems injected into the surrounding granitic host-rock (red) (G) Epidote-rich cataclasite, containing clasts of granite along a major ENE-WSW striking fault (H) Cm-thick ductile shear zones (dotted red) within a major NNE-SSW shear zone, trending parallel to the lithological boundary, and obliquely crosscut by ENE-WSW fractures.

2.2.3.4 Description of fault rocks

The fault rocks in the Tussøya-Røkneset fault zone comprise centimeter-thick veins of very fine-grained, dark material, potentially injected pseudotachylyte along brittle fractures in the altered granite (Fig. 16f), and more locally, greenish, few centimeter-thick, epidote-rich cataclasite, especially on a subsidiary fault surface to the west (Fig. 16g). If epidote precipitations along the fracture surfaces are quite widespread over the fault zone, hematite and malachite/copper sulphide seem localized along the core zone. On a microscopic scale, the potential pseudotachylyte showed on fig. 16f turns out to be a fine-grained, dark, ultracataclastic matrix that shows a mineralogical composition very similar to the granitic host-rock: quartz, K-feldspar and fewer amounts of epidote, chlorite, white mica, plagioclase and calcite. The microscopic study highlighted coarse-grained proto-cataclastic to very fine-grained ultracataclastic veins (Fig. 17b & e). Cataclastic blocks of darker, epidote-rich content seem embedded into a lighter cataclastic matrix, suggesting two generations of cataclasite

(Fig. 17f). Several grains belonging to the dark cataclastic blocks show healed cracks that would indicate a rather older age for the dark cataclasite (cf. chapter 3.2.1 for discussion).

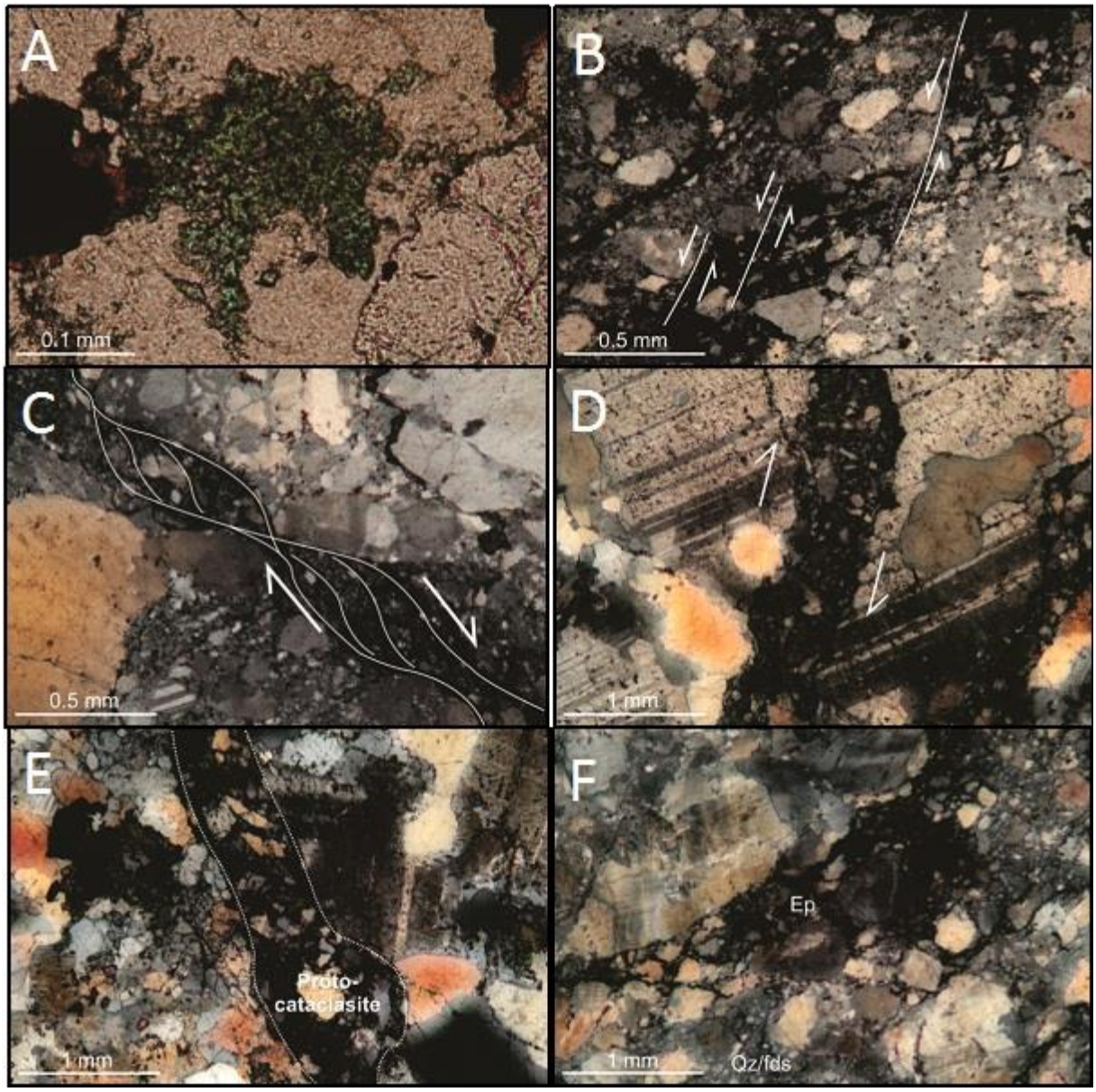

Figure 17: Microphotographs of granitic host rock and cataclasite along the Tussøya-Røkneset fault zone. (A) Pumpellyite in altered granite (B) Micro-offsets of a dark ultracataclasite layer that is overlain by a lighter, grayish cataclasite, indicating dip-slip normal displacement (C) Merged microfaults forming duplex-shaped microstructures and indicating dip-slip normal motion (D) Micro-offset of a plagioclase grain along a NNE-SSW trending microfault, indicating dextral movement (E) Protocataclastic vein showing a coarse-grained matrix (F) Block of epidote-rich, dark cataclasite (Ep) embedded in quartz and feldspar-rich cataclasite (Qz/fds).

2.2.3.5 Pre-existing fabrics along the fault zone

A NE-SW to ENE-WSW trending, SE-dipping gneiss fabric/foliation is truncated by high-angle ENE-WSW trending fractures across the Tussøya-Røkneset fault zone (Fig. 16b), but apparently trends parallel to the high-frequency NNE-SSW striking fractures composing

the core zone. Further west, the ENE-WSW trending fractures strike approximately parallel to the foliation that shows a gentle dip. In the south of the island, the gneiss foliation visibly bends anticlockwise (in map view) towards the main NNE-SSW trending Tussøya-Røkneset fault zone (Fig. 14). In the west, a NNE-SSW trending sinistral shear zone, composed of localized cm-thick shears (Fig. 16h), trends parallel to the main fault zone and is obliquely crosscut by anastomosing splays of ENE-WSW trending fractures. The anticlockwise bending of the foliation towards the Tussøya-Røkneset fault zone, together with the NNE-SSW trending shear zone may indicate the presence of an earlier, NNE-SSW striking, sinistral, ductile shear zone along the Tussøya-Røkneset fault zone.

2.2.3.6 Summary and preliminary interpretations

The Tussøya-Røkneset fault zone displays a general NNE-SSW trend and a southeastward dip (Fig. 14). It can be traced for about 300 meters, and shows a few-meter wide core zone that is composed of high-frequency, right-stepping *en echelon*, NNE-SSW trending fractures. In addition subsidiary, anastomosing, ENE-WSW trending fractures with steeper dip and oblique-truncating characteristics relative to the main fault surfaces are also well developed. The hydrothermally altered core of the Tussøya-Røkneset fault zone exhibits centimeter-thick ultracataclastic veins of dark, fine-grained material and epidote-rich cataclasite in the west (Fig. 16f & g). Mineral precipitation and reaction parageneses of the cataclastic fault rocks reveal upper prehnite-pumpellyite to lower greenschist metamorphic conditions in the cataclastic fault rocks (Fig. 17a), indicating a temperature range between 250 and 350°C and pressure of 0.2-0.3 GPa, i.e. depth of 5-10km for the formation of the cataclastic fault rocks (cf. Bucher & Grapes 2011). The ENE-WSW trending fractures commonly show anticlockwise bending towards NNE-SSW trending fractures, forming sigmoidal or duplex-like structures where the NNE-SSW trending, gently dipping faults seem linked by ramps of ENE-WSW striking splay fractures (Fig. 16d). These structures have been interpreted either as extensional gash fractures developed in extensional duplexes (Eig & Bergh 2011), or sigmoidal fractures formed in an extensional (down-to-the SE) major fault zone. These interpretatione are supported by the slickensides and the microstructural analysis, revealing dominantly dip-slip normal and additional dextral strike-slip movements along the NNE-SSW trending faults and microfaults. NW-SE trending fractures in the area delineate anticlockwise curving against ENE-WSW striking faults, which may indicate sinistral

displacement (Fig. 14). The ENE-WSW trending slickensided fault surfaces similarly suggest a dominant sinistral sense of shear for the ENE-WSW trending fractures. At least two generations of cataclasite may be inferred on a microscopic scale. Blocks with a darker matrix content show healed cracks and apparently look embedded into a lighter, fine-grained cataclastic matrix (Fig. 17f), and this may imply two faulting events. In the west, away from the core of the fault, the ENE-WSW trending brittle fractures clearly trend parallel to the NE-SW to ENE-WSW trending, ductile gneiss foliation of the host rock (Fig. 14). In the east, the ductile foliation bends anticlockwise (in map view) into parallelism with the Tussøya-Røkneset brittle fault zone, where the ENE-WSW striking fractures obliquely truncate it (Fig. 16b). This suggests that the Tussøya-Røkneset fault zone initiated along a pre-existing, NNE-SSW trending, sinistral, ductile shear zone, probably running along the lithological contact between the red-stained, heavily fractured granite and the banded gneisses of the Kattfjord complex (cf. chapter 2.2.3.5).

2.2.4 Hillesøya fault zone

2.2.4.1 Large scale field relations and host rock characteristics

The Hillesøya fault zone is thought to be the south-westernmost segment of the Rekvika fault complex and is exposed on the western edge of the island of Hillesøya (Fig. 4). In this locality, brittle deformation has been accommodated by four, narrow (few meters wide), fault segments that can be traced ca. 500 to 1000m. These segments variably trend NE-SW to NNW-SSE and show western to northwestern dips, locally eastern dips (Fig. 18). Two of them crop out in a wide N-S trending gully, in the eastern part of the map (Fig. 18), where a massive red-stained granitic intrusion comprising lenses of mafic gneisses and pegmatite dykes dominates the host rock lithology. The granitic gneisses display a ductile fabric/foliation that also shows variability in trend and dip: from NE-SW to ENE-WSW trending, and SE and NW-dipping (Fig. 18). The granitic gneisses appear highly fractured, especially in the few meters wide core zone observed on the eastern edge of the gully (Fig. 19). The core zone is 1.5-2m wide, trends NNW-SSE, dips toward the east and is composed of lenses of cataclastic to brecciated fault rocks (Fig. 20).

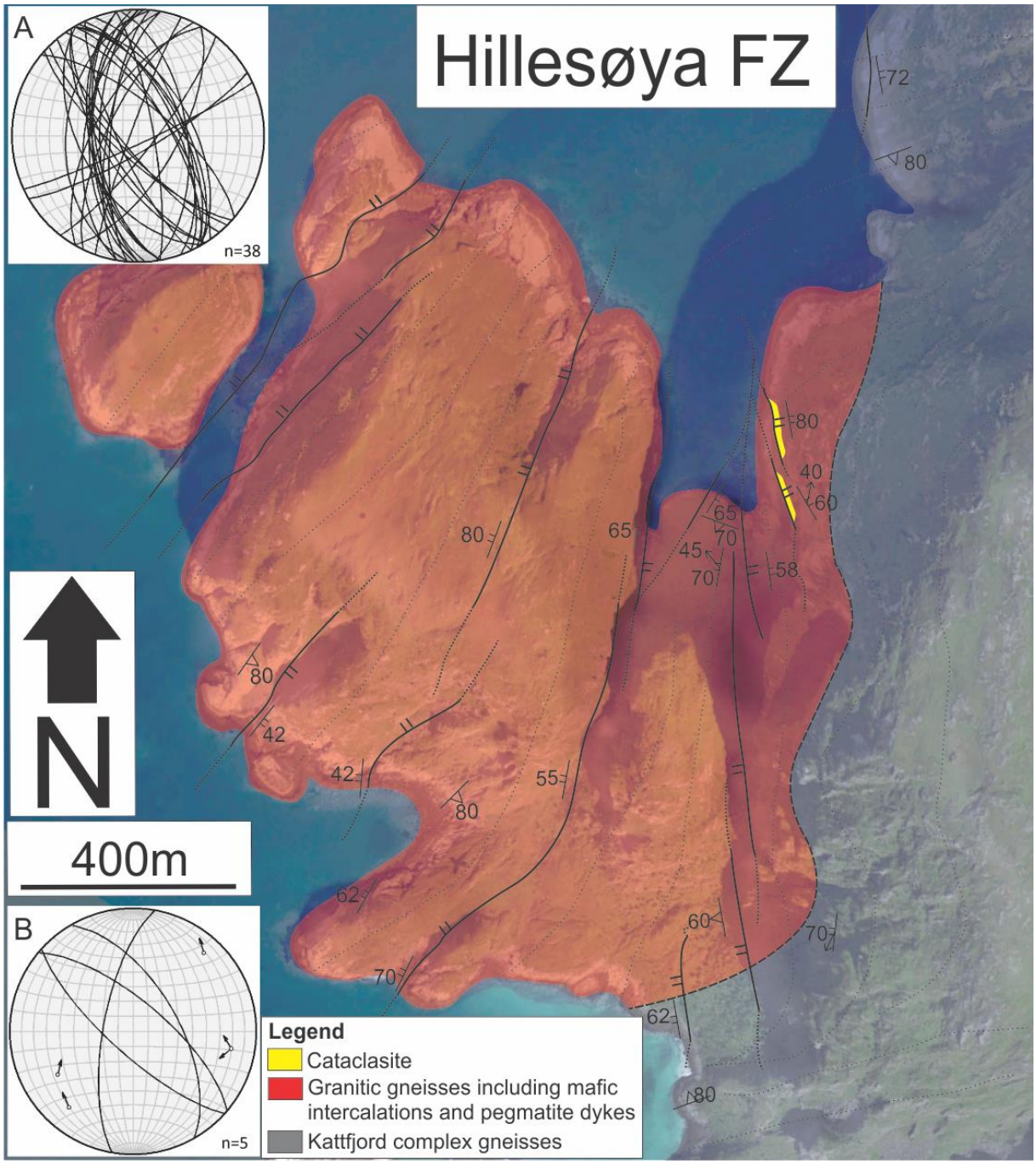

Figure 18: Structural and lithological map of the Hillesøya fault zone in western Kvaløya. The Kattfjord complex gneisses seem intruded by a major body of granitic gneisses. The major lineaments display a variation in trend from NNW-SSE in the east to a NE-SW trend in the west. The ductile foliation generally strikes NE-SW, i.e. parallel to the brittle structures in the west, but it shows a ENE-WSW strike in the NE and the SE. (A) Stereonet showing the trend and dip of the brittle fractures observed in Hillesøya (B) Stereonet displaying the slickenside data of the Hillesøya fault zone. For structural legend see "common legend" in fig. 7.

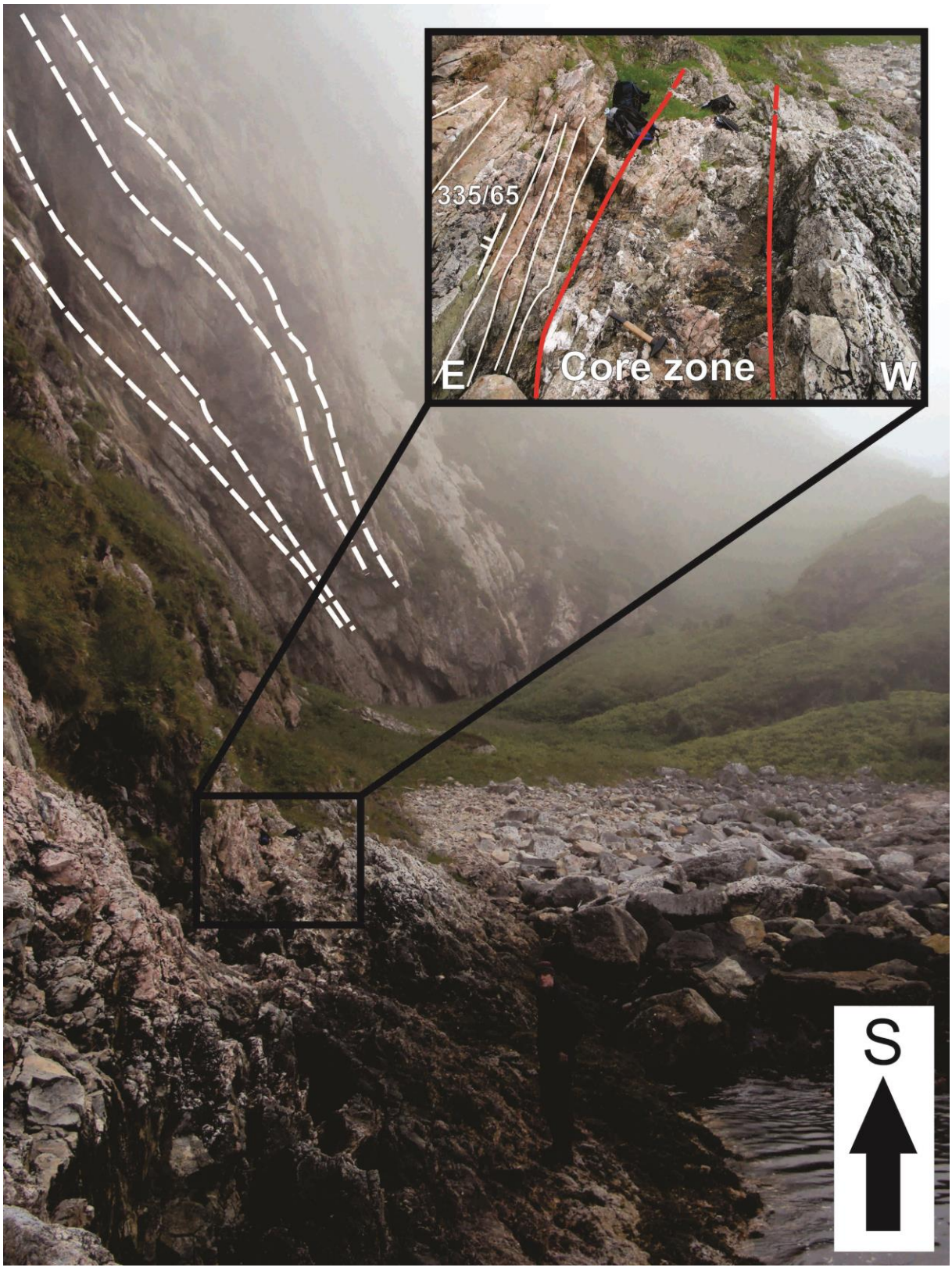

<u>Figure 19:</u> Outcrop photographs of the easternmost, NNW-SSE trending segment of the Hillesøya fault zone, showing the dominant western dip that characterizes the Hillesøya fault zone (dashed white). Locally, the fault surfaces display cataclastic fault rocks along strike and an opposite eastern dip (white, in the frame in the upper right corner). Highly fractured gneisses define the core of the fault zone (red). The fractures show an increased frequency towards the core zone (white, in the frame in the upper right corner).

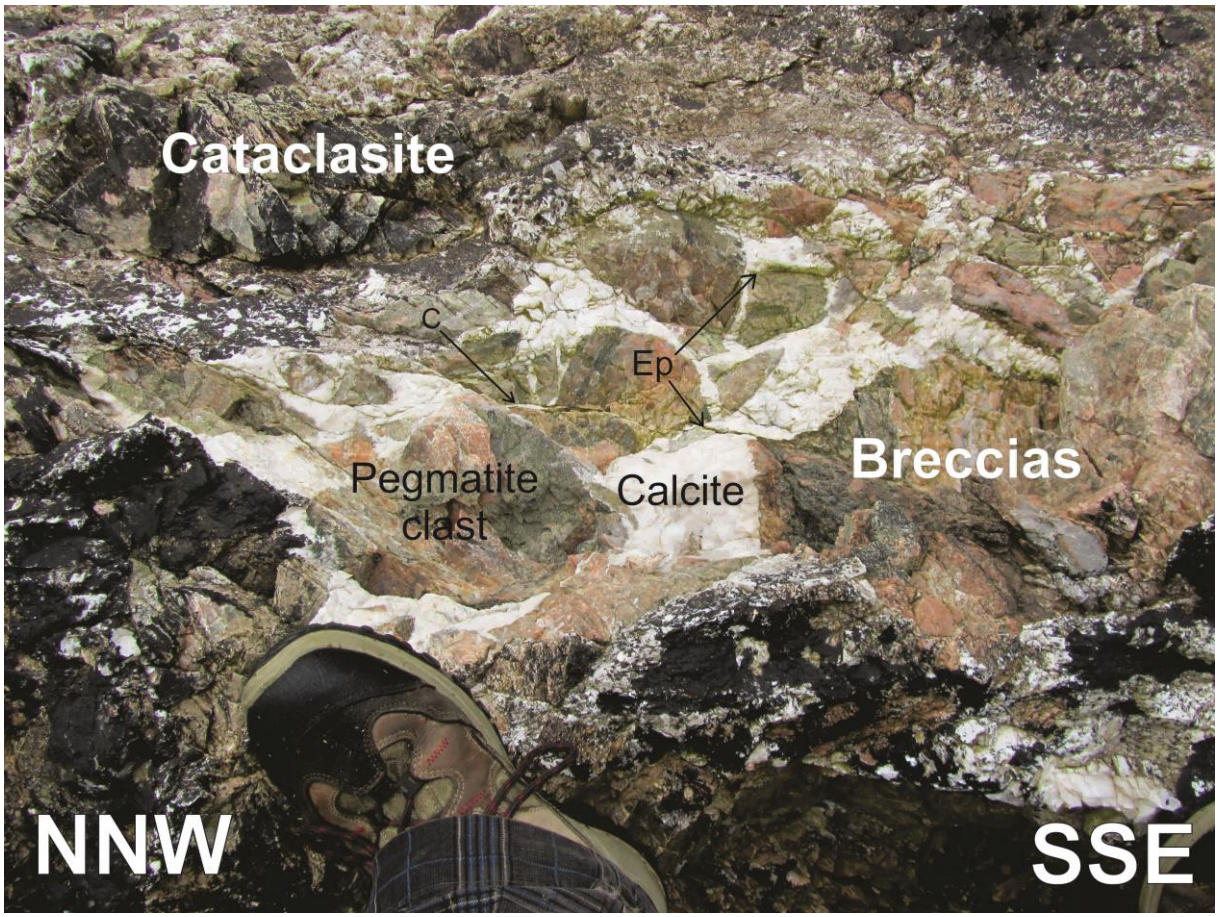

Figure 20: Outcrop photograph of a meter-wide core zone in showing brecciated pegmatite cemented by calcite cement, and calcite-rich cataclastic fault rocks. Epidote-filled fractures (Ep) crosscut the calcitic cement and the pegmatite clasts, and occasionally get engulfed by calcite (c).

2.2.4.2 Description of brittle fractures and associated structures in the fault zone

The brittle fractures observed along the Hillesøya fault zone show a variable strike across the fault zone, i.e. NNW-SSE in the east to NE-SW in the west. They dominantly dip to the west but a minor antithetic set of fractures is dipping towards the east, particularly in the eastern part of the area where e.g. E-dipping faults are characterized by a meter-wide core zone (Fig. 18). In the north of the gully, the major fractures trend NNW-SSE to N-S and exhibit a prominent eastern dip, even though the main fault zone dips to the west (Fig. 18a & 19). In map view, the main brittle fractures display a right-stepping *en echelon* pattern. These fractures show an increased frequency approaching the core of the faults (Fig. 19). The fractures are often filled with epidote veins that crosscut the fault rocks, and that get occasionally engulfed by calcite (Fig. 20). Some NNE-SSW striking fractures visibly bend towards lenses of fault rocks that are exposed along major NNW-SSE to N-S trending faults. The former fractures are also truncated by calcite veins that trend parallel to the major,

NNW-SSE trending fracture surfaces showed on fig. 19. The latter, NNW-SSE trending fracture surfaces often exhibit slickensides that rarely lead to the identification of the sense of shear (Fig. 18b).

2.2.4.3 Description of kinematic data

Although slickensided surfaces were commonly observed in the north of the gully, in the eastern part of Hillesøya (Fig. 18), only few of these structures led to a kinematic interpretation of the faults sense of shear. They mainly indicate oblique-slip motions, generally involving dip-slip normal movements and a sinistral strike-slip component along N-S to NNW-SSE faults (Fig. 18b), and occasionally minor dip-slip reverse and a component of dextral strike-slip movement. Anticlockwise bending (in map view) of NNE-SSW trending fractures toward major N-S to NNW-SSW striking faults that show cataclastic lenses of host granitic gneisses on their fault surfaces, would indicate a sinistral strike-slip sense of shear along these major structures. On a microscale, the fractures identified within the fault rocks do not show any displacement or offset along strike (Fig. 21a).

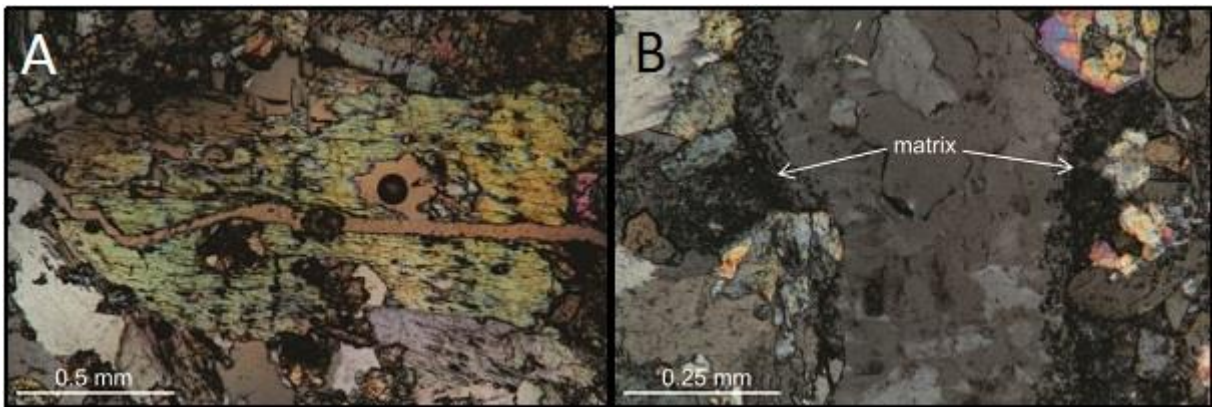

Figure 21: Microphotographs of thin-sections of host rocks along the Hillesøya fault zone, more specifically from the northern part of the gully. (A) Crack showing no apparent offset (B) Microscopic cataclastic matrix surrounding a minor quartz vein.

2.2.4.4 Description of fault rocks

The core zone of NNW-SSE trending faults is exposed over a length of ca. 20 meters along strike, showing ca. 1 to 2 meters wide layer of cataclastic and brecciated fault rocks (Fig. 19). The cataclasite is composed of pegmatite clasts and of a calcite-filled matrix. The breccias generally incorporate angular to subangular clasts of the granitic host rock that range from 1 meter diameter to 5 centimeters, typically 20 centimeters, and show centimeter-thick calcite veins. These breccias contain approximately 25% of matrix, mostly

calcite (Fig. 20). The granite clasts and the calcite cement are truncated by epidote-filled veins and more sparsely by thin quartz-filled fractures. Some of the epidote-filled fractures seem engulfed by calcite infill (Fig. 20) and the microscale quartz veins are surrounded by minor amount of a microcrystalline matrix (Fig. 21b).

2.2.4.5 Pre-existing fabrics along the fault zone

The attitude of the main ductile foliation in the host rock granitic gneisses and the pegmatite dykes in the area varies significantly due to macro-scale folding. This macro-folding is outlined by changes in strike and dip of the foliation, from NE-SW trending and SE-dipping in the west of Hillesøya, to ENE-WSW striking and NW-dipping in the SE (Fig. 18). The macro-fold has a steep/vertical fold axis and steep, NW-SE trending axial surface (Thorstensen 2011; cf. chapter 3.4). In this context, the brittle Hillesøya fault zone is developed on the northwestern limb of the macrofold, i.e. the only location where the dominant, NE-SW trending ductile foliation is parallel to some of the fault segments of the Hillesøya fault zone. Otherwise in the southeast of the area, the foliation trends ENE-WSW and dips NW, i.e. at a high angle to the segments of the Hillesøya fault zone that trend N-S to NNW-SSE in the east of the gully (Fig. 18).

2.2.4.6 Summary and preliminary interpretations

The Hillesøya fault zone comprises at least four individual fault segments in the northwestern part of Hillesøya that can be traced for about 500-1000m each, and trend from NNW-SSE in the east to NE-SW in the west. These fault segments generally show a predominant dip to the NW/W, but a minor set of antithetic fractures dips toward the east, especially in the N-S striking gully (Fig. 18). In map view, the major brittle fractures show a right-stepping *en echelon* pattern. Mesoscale fractures show a locally increased frequency when approaching the core zone, e.g. in the east, which may imply localized deformation (Fig. 19). The core zone comprises thin (0.5-2 m wide) lenses of highly fractured cataclastic, and more locally brecciated fault rocks, including fractured granite clasts and a calcite cement (Fig. 20). Epidote, calcite and more rarely quartz veins fill the fracture surfaces. The epidote veins that truncate the gneissic host rock and the cataclastic fault rocks imply greenschist metamorphic conditions, i.e. a temperature range of 350-500°C, and depth about 5-10 kilometers (i.e. pressure about 0.2-0.3 GPa; Bucher & Grapes 2011). The quartz

veins probably are youngest since they truncate the epidote veins. Slickensided fracture surfaces indicate mostly normal sinistral oblique-slip movements along the Hillesøya fault zone. The mineral-filled fractures, however, do not show any evidence for displacement on a microscopic scale. Reverse dextral slickensides may imply a later, minor tectonic overprint. The variations of attitude, notably in trend and dip, of the individual fault segments composing the Hillesøya fault zone may be explained by attitude variations of the foliation in the northwestern limb of a macro-fold in the area (Thorstensen 2011) that might have acted as a pre-existing zone of weakness for the localization of the brittle fault segments in Hillesøya (cf. chapter 3.4).

2.3 The Vestfjorden-Vanna fault complex

The Vestfjorden-Vanna fault complex includes the Straumsbukta-Kvaløysletta and the Stonglandseidet fault zones that are located on the southeastern edge of the West Troms Basement Complex basement horst. Both of them appear to separate the Precambrian basement rocks from the eastward-lying Caledonian nappes. These fault zones also show comparable sizes (length and width) and amounts of displacement (cf. chapter 3.1.2), similar kinematics, probable relative ages and similar fault rocks (cataclasite), and because of these similarities they are thought to belong to the Vestfjorden-Vanna fault complex that runs from the Lofoten-Vesterålen Margin to the island of Vanna in the north of Troms (Olesen et al. 1997 and this study).

2.3.1 Straumsbukta-Kvaløysletta fault zone

2.3.1.1 Large scale field relations and host rock characteristics

The Straumsbukta-Kvaløysletta fault zone has previously been studied by Forslund (1988) and crops out in several localities in southwestern Kvaløya and appears to be 10's of km long (Fig. 4). Just west of Straumsbukta, the damage zone of the Straumsbukta-Kvaløysletta fault zone is exposed within the footwall block, made up of Precambrian host rocks of the West Troms Basement Complex (Fig. 22). The lithology is predominantly composed of red-colored, altered tonalitic gneisses in the west that is principally made of quartz, K-feldspar, plagioclase, chlorite, epidote and few white mica (Fig. 23a), and

amphibolitic gneisses towards the east that look similar to the gneisses of the Kattfjord complex mapped in Rekvika (Fig. 22 & 24). The tonalitic gneisses contain regular, few meters to 10 meters wide lenses of amphibolitic gneisses, and few meters wide lenses of tonalitic gneisses were found in the amphibolitic gneisses. The host rocks and their ductile fabrics become progressively more deformed towards the east. Moreover the amount of quartz veins together with the cataclastic content in the rocks, show an increasing frequency toward the east (Fig. 23b & 25), suggesting that the core zone of the fault is approaching in this direction (Fig. 22). Cataclastic fault rocks are widespread in conjunction with NNE-SSW, NNW-SSE, and mostly N-S trending, E-dipping fractures. As long as the outcrop abruptly stops it is hard to define a core zone, but the damage zone shows a thickness of at least 100 meters (Fig. 22). The tonalitic gneisses display a foliation striking N-S and dipping gently to the east, which is parallel to lithological contacts (Fig. 22).

2.3.1.2 Description of brittle fractures and associated structures in the fault zone

Numerous brittle fractures and veins occur in the studied section of the fault zone. An N-S trend and moderate to steep easterly dip dominate amongst the brittle fractures that strike from NNE-SSW to NNW-SSE, locally NE-SW (see fig. 22a), roughly parallel to the lithological contacts (Fig. 22). In cross-sections, the brittle fractures display both planar and listric geometries (Fig. 25). Moreover in map view, right-stepping *en echelon* patterns and anastomosing, or at least bending fault arrays, have been observed on few-centimeters wide and tens of meters long fractures (Fig. 22 & 24). The brittle fractures often show distributed, millimeter to 0.5 meter-thick quartz veins and millimeter-thick chlorite veins on their surfaces. These veins crosscut each other without showing any timing difference (Fig. 25 & 26a). Hematite veins are also quite common, but rarely crop out at the same location with chlorite and quartz veins. The hematite veins seem to crosscut all the other fractures except for some thicker major quartz veins (Fig. 26b & c), suggesting they are youngest together with these quartz veins. The epidote and hematite-coated fracture surfaces often display fibrous slickensides that provided substantial information regarding the kinematics of these faults.

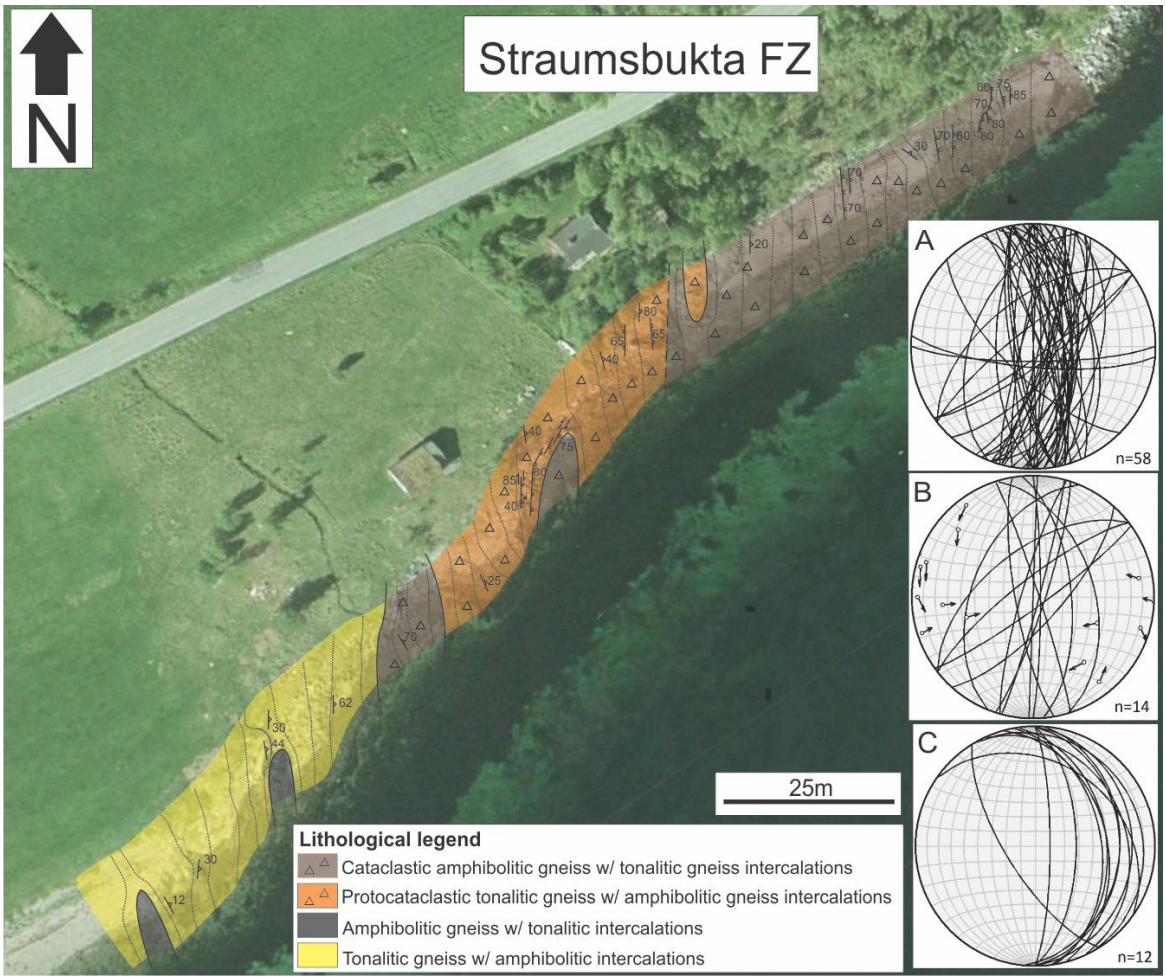

Figure 22: Structural and lithological map of the Straumsbukta-Kvaløysletta fault zone, in the area west of Straumsbukta, in southern Kvaløya. The tonalitic gneisses are progressively more fractured towards the east approaching the contact with cataclastic, amphibolitic gneisses. Most of the brittle fractures trend N-S, ca. parallel to the lithological boundaries and the ductile foliation. (A) Stereonet displaying the fracture orientations in Straumsbukta (B) Stereonet showing the slickenside data related to the Straumsbukta-Kvaløysletta fault zone (C) Stereonet displaying the foliation trends in Straumsbukta. For structural legend see "common legend" in fig. 7.

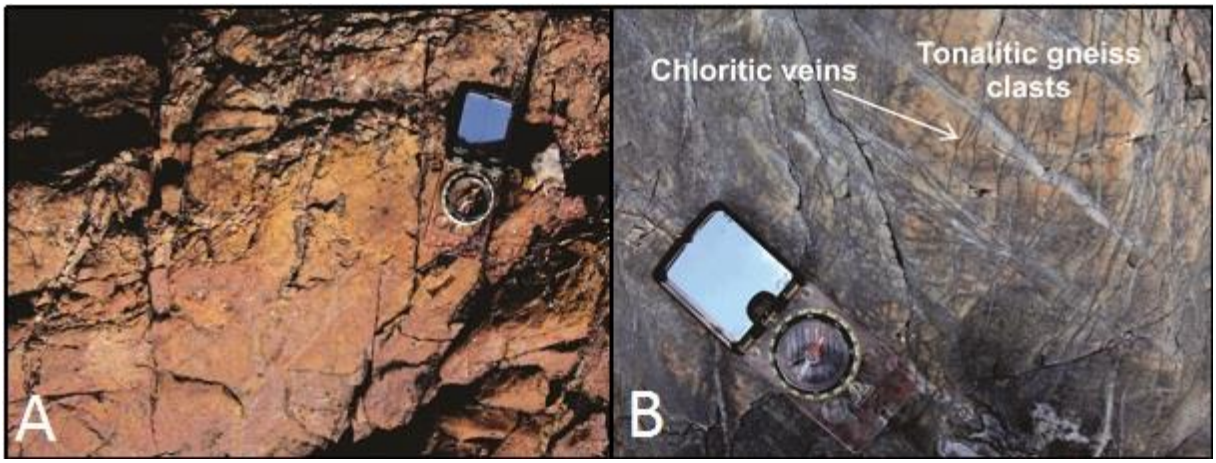

Figure 23: Outcrop photographs of host rocks adjacent to the Straumsbukta-Kvaløysletta fault zone. (A) Tonalitic gneisses cropping out in the west of the Straumsbukta-Kvaløysletta fault zone and showing a red-coloration (B) Centimeter-scale blocks of tonalitic gneiss intercalated in amphibolitic gneisses, and crisscrossed by millimeter thick chlorite veins.

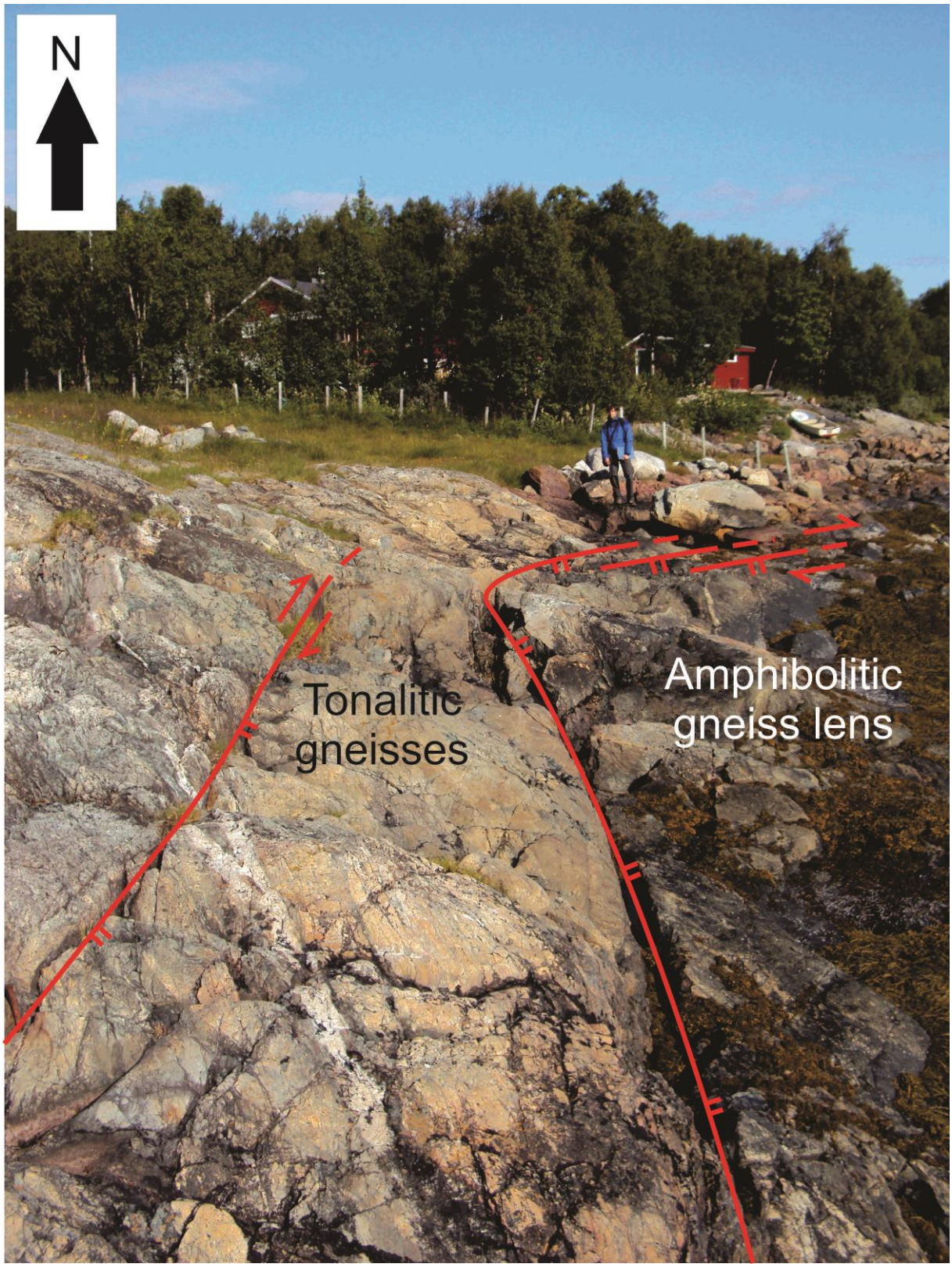

Figure 24: Outcrop photograph of tens of meters long, N-S trending brittle fractures showing curving, right-stepping *en echelon* geometry, and trending parallel to the lithological boundary between tonalitic gneisses and an intercalated lens of amphibolitic gneisses.

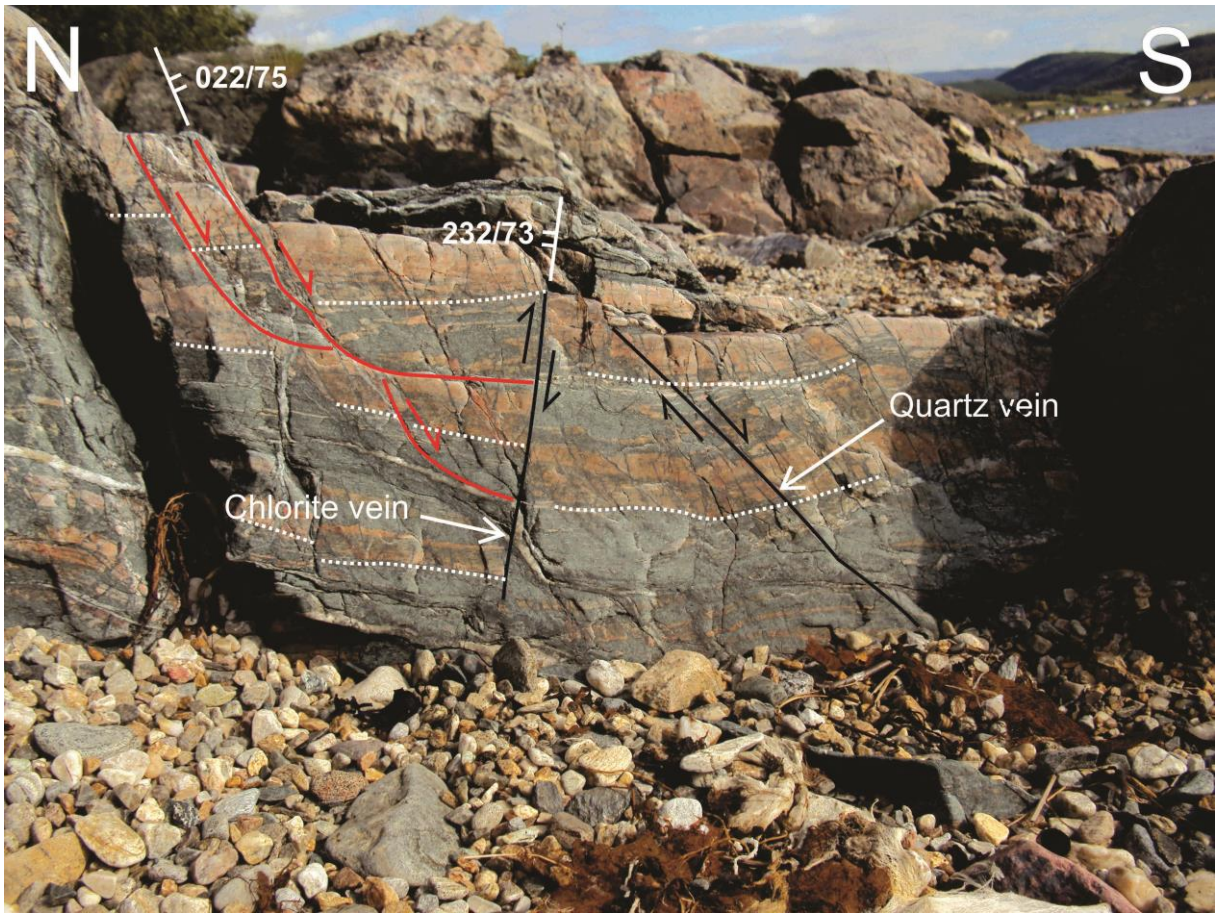

Figure 25: Altered tonalitic gneisses (red-stained) showing a gently east-dipping foliation (dotted white) crosscut by brittle faults that display planar (black) and listric (red) geometries. These faults offset the ductile foliation and dominantly document dip-slip normal movements, even though reverse offsets occur locally. The arrows show the relative motion of the faulted blocks. Note the quartz and chlorite precipitations along the fracture surfaces.

2.3.1.3 Description of kinematic data

Slickenside mineral fibers have been observed on a number of N-S trending fractures, in particular on epidote and hematite-coated fractures. Slickensides on fracture surfaces usually trend E-W and plunge at an angle similar to the dip of the fracture surface, indicating mostly pure dip-slip normal and subsidiary oblique-dextral movement component (Fig. 22b), and show as well little evidence of dip-slip reverse motions. Micro-offsets along quartz/chlorite-filled microfaults confirm the dominance of dip-slip normal motions and of an additional dextral component (Fig. 26d & e). However occasional micro-offsets showing dip-slip reverse displacement may indicate a second faulting event (Fig. 26f). Micro-offsets along quartz veins also provide indications of sinistral strike-slip displacement along the Straumsbukta-Kvaløysletta fault zone (Fig. 26g). Finally, elongated quartz grains that grew as fibers in N-S trending veins finally support an E-W extension (Passchier & Trouw 2005),

perpendicular to the main orientation of the fractures and the lithological contacts in Straumsbukta (Fig. 26h).

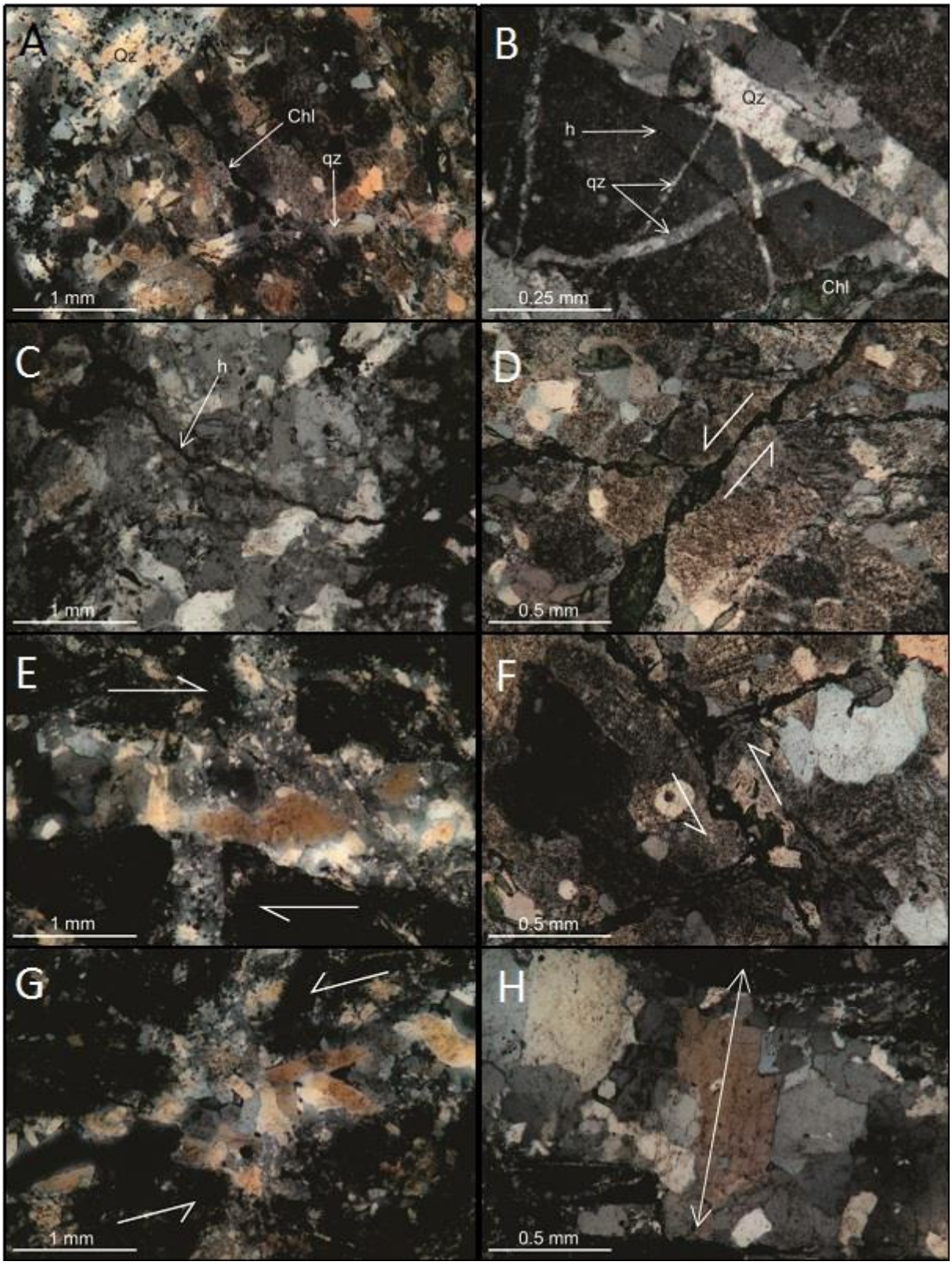

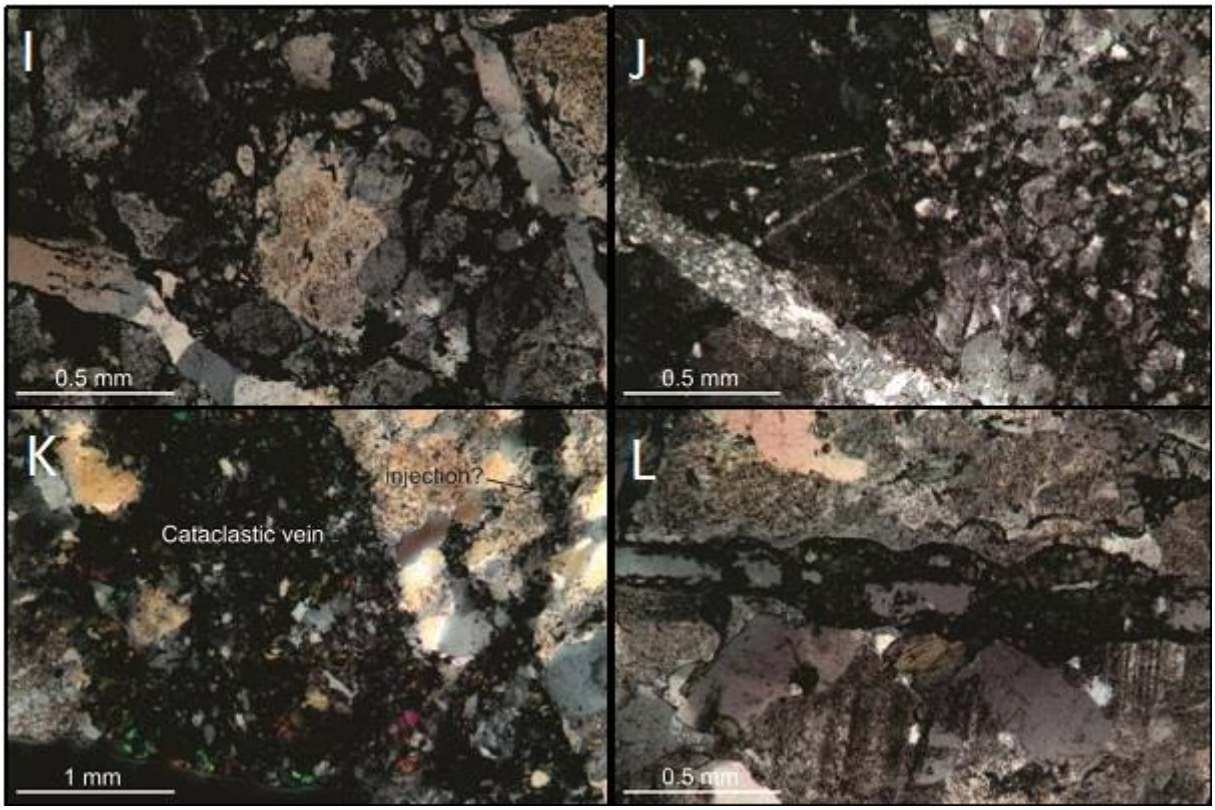

Figure 26: Microphotographs of host rocks and cataclasites from the Straumsbukta-Kvaløysletta fault zone. (A) Chlorite vein (Chl) crosscutting a minor quartz vein (qz), and truncated by a major quartz vein (Qz) (B) Hematite vein (h) cutting through minor quartz veins (qz) and chlorite (Chl), but truncated by a major quartz vein (Qz) (C) Hematite vein (h) crosscutting a major quartz vein (D) Micro-offset along a chlorite vein, indicating dip-slip normal motion (E) Minor quartz vein showing a micro-offset along a major horizontal quartz vein, indicating dextral displacement (F) Subvertical chlorite vein that offsets a sub-horizontal vein, indicating reverse displacement (G) Sub-horizontal quartz vein showing a micro-offset indicative of sinistral strike-slip movement (H) Quartz fibers showing an elongated axis (white arrow), indicating an E-W directed extension (I) Protocataclasite comprising a fine-grained matrix (J) Ultracataclasite including a medium-grained (on the right) to microscopic (on the left) matrix (K) Millimeter-thick ultracataclastic vein mostly composed of a medium-grained matrix, and that shows potential traces of injection (L) Quartz vein progressively replaced by chlorite.

2.3.1.4 Description of fault rocks

As previously mentioned, the footwall host rock gneisses are getting more brittely deformed, and cataclastic fault rocks increase in abundance towards the east (Fig. 22). The tonalitic gneisses change progressively from a relatively undeformed state in the west, to protocataclastic towards the east. In the east, the cataclastic amphibolitic gneisses contain centimeter-thick clasts of feldspar and tonalitic gneiss (Fig. 23b). On a microscopic scale, the fault rocks range from protocataclasite containing fine-grained matrix, in tonalitic gneisses in the west, to ultracataclastic amphibolitic gneisses in the east showing medium-grained to microscopic matrix (Fig. 26i & j). The microscopic study also shows that many cataclastic veins comprise medium to fine grained, ultracataclastic, quartz content that can reach a

thickness of few millimeters and sometimes shows traces of injection (Fig. 26k). These veins are truncated by several generations of frequent quartz veins, that are regularly replaced by chlorite (Fig. 26l), and by chlorite and hematite veins (Fig. 26b).

2.3.1.5 Pre-existing fabrics along the fault zone

The dominant, Precambrian, ductile foliation of the host rock gneisses strikes on average N-S to NNW-SSE, and dips more or less gently to the east (Fig. 22c). This fabric affects the entire area of the exposed damage zone of the Straumsbukta-Kvaløysletta fault zone (Fig. 22). This Precambrian fabric trends mostly parallel to the lithological boundaries, including the contact between the tonalitic and the amphibolitic gneisses, and might have helped the localization of the brittle fabric in Straumsbukta, which developed mostly N-S, i.e. parallel to the trend of the Precambrian foliation (Fig. 22a).

2.3.1.6 Summary and preliminary interpretations

The studied portion of the Straumsbukta-Kvaløysletta fault zone is marked by a well-defined network of brittle fractures, trending N-S and dipping moderately to the east, and distributed within an area at least 100 meters wide. The fractures seem to be concentrated along the lithological boundaries between tonalitic and amphibolitic gneisses (Fig. 22). The larger brittle fractures of the damage zone display an *en echelon* pattern in map view, and common listric and planar geometries in cross-sections (Fig. 25). Cataclastic fault rocks are abundant and they occur as protocataclasite in the western tonalitic gneisses, comprising a fine-grained matrix, and ultracataclasite in the eastern amphibolitic gneisses, containing a medium-grained to microscopic matrix probably implying an increasing deformation state towards the east (Fig. 26i & j). Very thin to millimeter-thick cataclastic veins seem injected in the host rocks (Fig. 26k). Late quartz, chlorite and hematite precipitations along the fracture surfaces truncate the cataclasites (Fig. 26b). These secondary mineral precipitations (chlorite, epidote) and the cataclastic fault rocks suggest greenschist metamorphic conditions, i.e. temperature of 350-500°C, and a formation depth of 5-10 km for the fault rocks (corresponding to a pressure range of 0.2-0.3 GPa; cf. Bucher & Grapes 2011). The N-S trending fractures exhibit dominant dip-slip normal kinematic indicators, and an additional dextral strike-slip movement component. Despite a dominant normal character, evidence for minor dip-slip reverse movement components and occasionally sinistral strike-slip

movements have also been observed in the field via offset of geological markers such as quartz and chlorite veins, and indicated by the slickenside data (Fig. 22b, 26d, e, f & g). An E-W extension direction has been inferred from elongated grains in quartz veins (Fig. 26h; Passchier & Trouw 2005). Regarding a possible control of the pre-existing fabrics, the N-S striking Precambrian foliation and lithological boundaries in the host rock gneisses typically trend parallel to the Straumsbukta-Kvaløysletta fault zone and the small-scale fractures. This suggests they have provided a preferential zone of weakness for the development of the Straumsbukta-Kvaløysletta fault zone.

2.3.2 Stonglandseidet fault zone

2.3.2.1 Large scale field relations and host rock characteristics

The southwest of Senja is marked by the Stonglandseidet fault zone, previously mentioned by Tveten & Zwaan (1993) and Olesen et al. (1993, 1997), that follows an overall ENE-WSW trend, shows a southeastern dip, and potentially continues eastward as the Solbergfjorden fault zone (Fig. 4 & 27). In the north of the probable fault trace, the footwall displays unaltered fine-grained granite very similar to the Ersfjord granite in Rekvika. This granitic host rock shows high contents in quartz, feldspar and alternatively white mica, biotite, chlorite and epidote (Fig. 28a). Southwards, a major, potentially up to 150 meters wide, calcite-rich, cataclastic zone characterizes the core of the Stonglandseidet fault zone. This turns into highly fractured protocataclastic granite in the hanging-wall (Fig. 28b) that looks progressively less deformed towards the south, and that defines a ca. 500 meters wide damage zone. The granite contains tens of centimeters to tens of meters wide, typically few meters wide lenses of cataclasite that trend NNE-SSW and ENE-WSW (Fig. 27 & 28c). These cataclastic zones are crosscut by high-frequency NNE-SSW, ENE-WSW and NW-SE trending fractures (Fig. 28b). The granite becomes more and more foliated approaching the lithological boundary with biotite-schist gneisses that crop out in the southeast of the Stonglandseidet fault zone. This fabric shows broad variations in attitude, bending from NE-SW to WNW-ESE, and up to a NNW-SSE strike (Fig. 27).

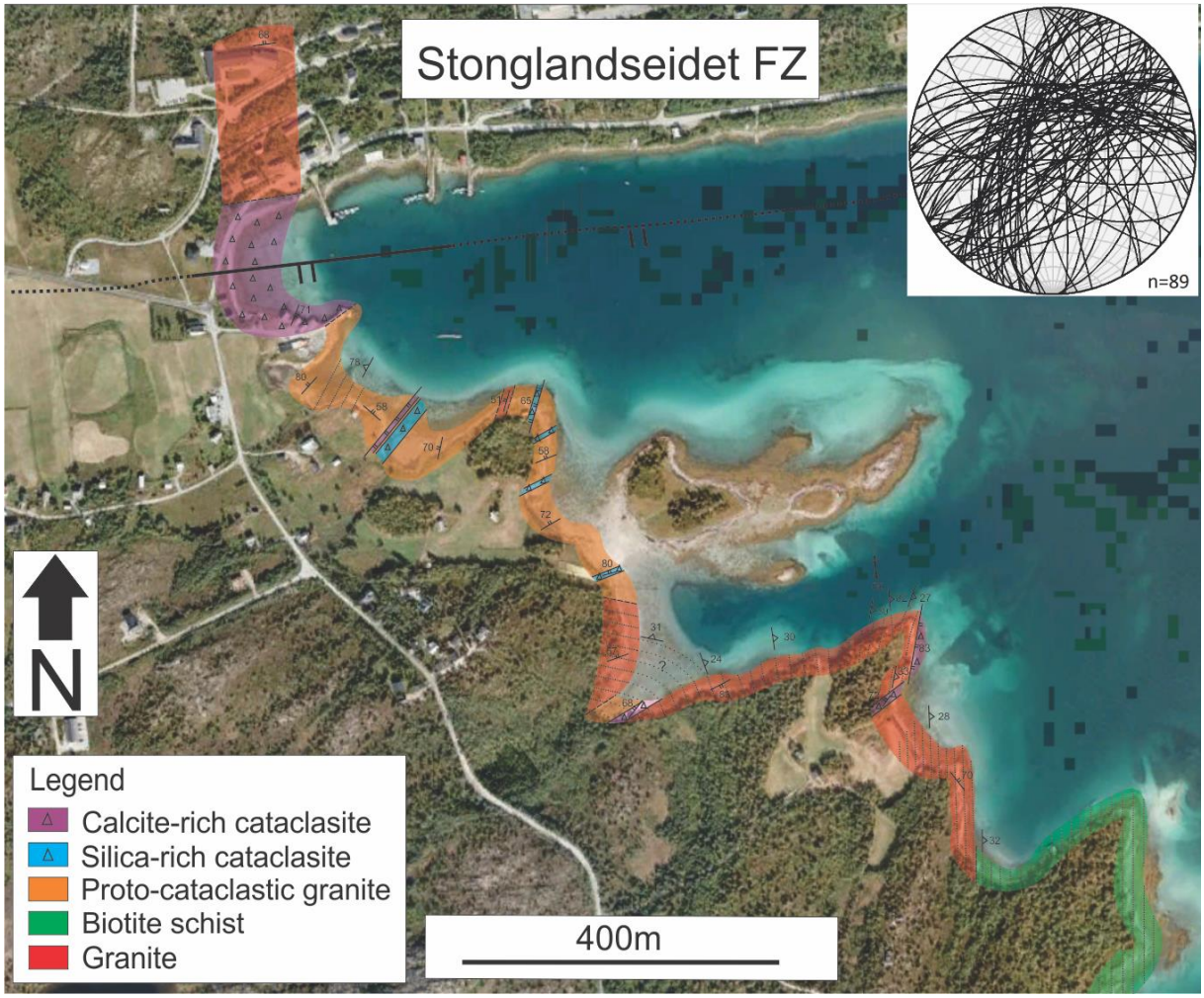

Figure 27: Structural and lithological map of the Stonglandseidet fault zone in south-western Senja. The granitic host-rock exhibits protocataclastic content in the hanging-wall of the ENE-WSW trending Stonglandseidet fault zone. Cataclastic lenses generally trend ENE-WSW or NNE-SSW in the fractured granite. The ductile foliation seems more developed around the contact between the granite and the biotite schist in the southwest, and shows broad variations in strike and dip potentially implying macrofolding. Note the stereonet plotting the orientation of the fractures observed along the Stonglandseidet fault zone. For structural legend see "common legend" in fig. 7.

2.3.2.2 Description of brittle fractures and associated structures in the fault zone

In Stonglandseidet, the major fault trace is believed to run ENE-WSW and dip steeply to the SE. It is defined by a possibly up to 150 meters wide calcite-rich, cataclastic core zone (Fig. 27). The structural study of the area led to the identification of three different sets of fractures (cf. stereonet in fig. 27). The most 2 prominent sets are made of high-frequency, ENE-WSW trending fractures that dip steeply to the north, and steep, high-frequency, NNE-SSW trending, NW-dipping fractures. These structures occasionally show *en echelon* and anastomosing geometries, and are commonly filled with quartz or calcite. These infill minerals do not show any timing difference from crosscutting relationships. Albeit these two fracture sets do not seem to offset each other, few NNE-SSW striking fractures bend

clockwise towards ENE-WSW trending fractures (Fig. 28b). The ENE-WSW and NNE-SSW trending fractures seem to curve clockwise and merge with subsidiary, high-frequency, steeply-dipping fractures that trend NW-SE to WNW-ESE (see fig. 28b).

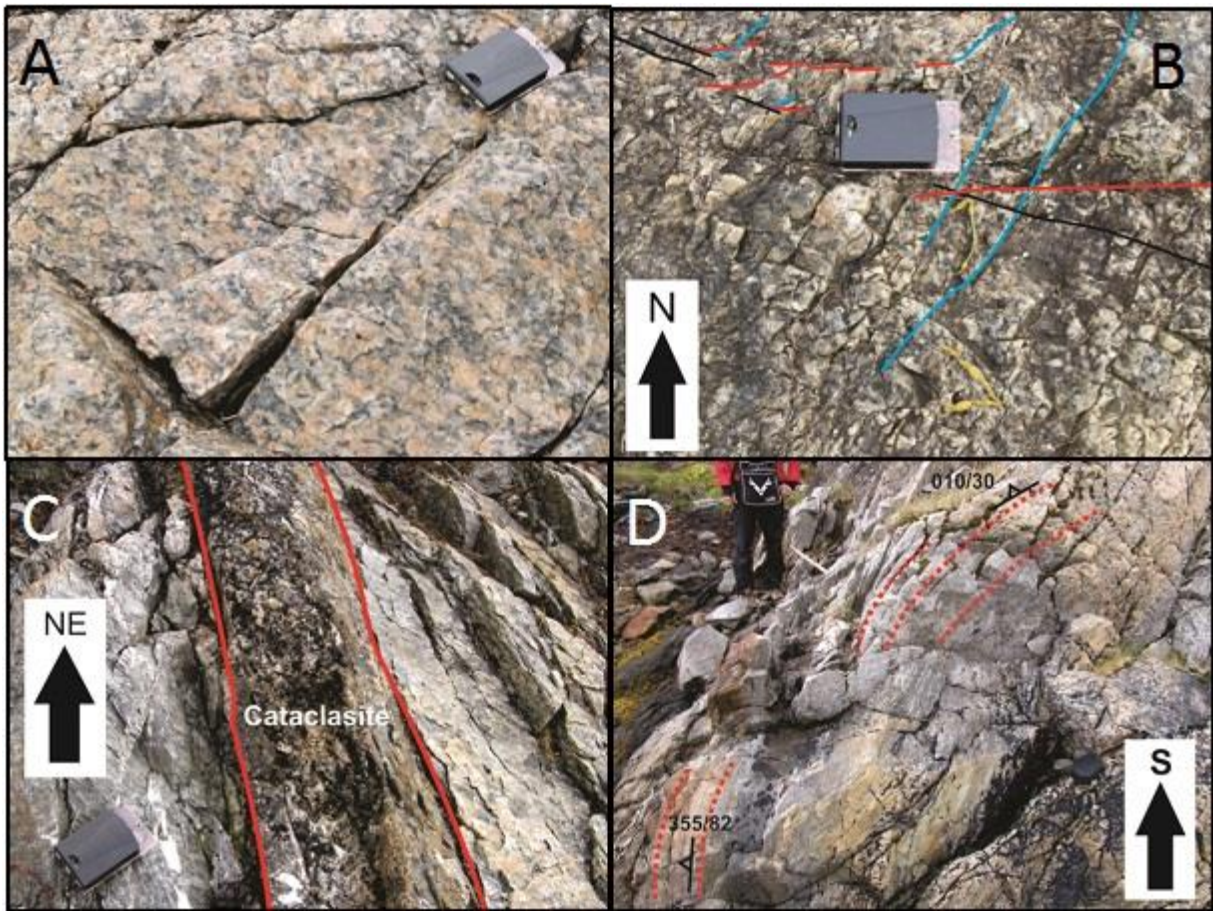

Figure 28: Outcrop photographs of the host and fault rocks, and associated structures in Stonglandseidet. (A) Relatively undeformed granite that dominates the lithology in the north of the main fault trace, and showing similarities with the Ersfjord granite in Rekvika (B) Highly-fractured, protocataclastic granite crosscut by NNE-SSW (blue), ENE-WSW (red) and NW-SE (black) trending fractures. NNE-SSW trending fracture apparently bend clockwise towards ENE-WSW and NW-SE to WNW-ESE trending fractures, whilst ENE-WSW striking fractures display a clockwise curving geometry at the intersection with NW-SE striking fractures. These clockwise bending geometries tend to indicate dextral displacement along the NW-SE fractures and possibly along few ENE-WSW trending fractures (C) 10 cm wide, calcite-rich lens of cataclasite that truncates the granitic hostrock (D) Foliation in the granite (dotted red) showing a varying dipping angle that may suggest subhorizontal mesoscale folding.

2.3.2.3 Description of kinematic data

The shear sense of the fault zone remains difficult to assess according to the lack of slickensided surfaces. Nevertheless, occasional clockwise curving geometries (in map view) of NNE-SSW trending fractures toward ENE-WSW trending fractures probably indicate dextral strike-slip movements (Fig. 28b; cf. chapter 3.1.2). In addition, ENE-WSW and NNE-SSW trending fractures apparently both bend clockwise toward steeply-dipping brittle faults

trending a NW-SE to WNW-ESE. This curving character also denotes probable dextral strike-slip motions along the subsidiary, NW-SE to WNW-ESE trending fracture set. The microstructural analysis did not reveal any evident offset along the microfractures. They still displayed numerous healed cracks along which mineral recrystallization did not enable the identification of any displacement though (Fig. 29a).

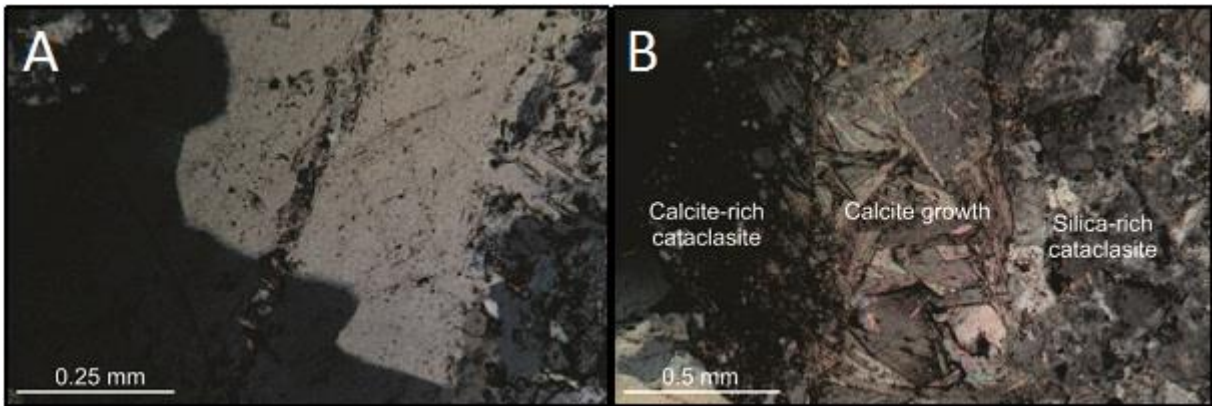

Figure 29: Microphotographs of fault rocks along the Stonglandseidet fault zone. (A) Healed crack in quartz characterized by mineral recrystallization along strike, and showing no apparent grain offset (B) Large crystals of calcite surrounded by a calcite-rich cataclasite showing a very fine-grained to microscopic matrix on the left, and a coarse-grained, silica-rich, cataclastic matrix on the right.

2.3.2.4 Description of fault rocks

A major calcite-rich, cataclastic zone has been identified in the north along the core of the Stonglandseidet fault zone, which width could reach up to 150 m (Fig. 27). The granite outcrops in the hanging-wall, in the south, contain protocataclastic material and seem truncated by major NNE-SSW and ENE-WSW trending faults showing 10's of centimeters to 10m wide lenses of protocataclasite and cataclasite (Fig. 27 & 28c). Toward the south the granite looks progressively less deformed as the frequency of fractures and lenses of cataclasite decreases. These lenses generally show high calcite or silica (quartz and feldspar) contents, as well as fewer amounts of chlorite and epidote. On a microscopic scale, two different kinds of cataclasite could be distinguished. The first is composed of a very fine-grained to microscopic matrix and shows enrichment in calcite (Fig. 29b). The second cataclastic matrix is coarse-grained and enriched in quartz and feldspar. Large crystals of calcite appear to have precipitated and superimposed over the 2 different kinds of cataclasites (Fig. 29b), potentially indicating a younger age for these crystals.

2.3.2.5 *Pre-existing fabrics along the fault zone*

The presumably Caledonian, ductile fabric observed in the granite and the biotite schists, in the south of the Stonglandseidet fault zone, trends parallel to the contact between these two lithologies but generally strikes obliquely to the brittle fractures (Fig. 27). This foliation/fabric is mostly composed of biotite crystals and shows a wide range of orientations and gentle dips, from NE-SW trending and NW-dipping, to an N-S strike associated with an eastern dip in the southeast. These changes in trend and dip direction may be related to subhorizontal macroscale folding, as suggested by subhorizontal mesoscale folds observed in the field that are mainly characterized by variations in the foliation dipping angle (Fig. 27 & 28d). Therefore the foliation may have locally favored the development of brittle fractures, providing suitable strike and dip e.g. for NNE-SSW trending fractures in the north, and for NW-SE trending fractures further south.

2.3.2.6 *Summary and preliminary interpretations*

The Stonglandseidet fault zone is characterized a major, up to 150m wide, calcite-rich cataclastic core zone and a 500 meters wide damage zone, which may be the results of relatively distributed deformation. The damage zone is composed of highly cracked, protocataclastic granite that includes typically several meters wide lenses of cataclasite and NW-dipping brittle fractures that trend NNE-SSW and ENE-WSW (Fig. 27 & 28b). The association of biotite, chlorite and epidote, although registered in low amounts, together with the cataclastic fault rocks suggest greenschist to upper greenschist metamorphic conditions, implying temperatures up to 350-550°C, and a depth of formation up to 10 km, (i.e. a pressure range of 0.2-0.3 GPa; Bucher & Grapes 2011). The NNE-SSW and ENE-WSW trending fractures seem to bend and merge into parallelism with subsidiary NW-SE to WNW-ESE trending faults that might, thus, have accommodated dextral strike-slip movements (Fig. 28b). The sense of shear of the Stonglandseidet fault zone remains albeit hard to define since no slickensides were found on the field and no displacement observed along the microfractures. Cataclastic lenses are composed of a very fine-grained, calcite-rich matrix and a coarse-grained, silica-rich matrix that do not show any significant timing difference (Fig. 29b). The local foliation shows variation in attitude which might be due to macrofolding (Fig. 27 & 28d). This ductile fabric may have locally provided preferential zones of weakness for the development of brittle fractures (cf. chapter 2.3.2.6).

3 Discussion

The studied fault segments in western Troms have been described individually, focusing on their structural characteristics and associated structures. The aim of the following chapter is to use the brittle fault and fracture characteristics, in conjunction with the fault rocks (cataclasites) and kinematic characters from field and microscale data, and the evaluation of relative and absolute timing constraints between the different fracture sets of the fault damage and core zones to propose a tentative correlation/linkage of the individual fault zones, by arguing that they belong to two major fault complexes: the Rekvika fault complex and the Vestfjorden-Vanna fault complex. Next, the formation and evolution of the cataclastic fault rocks and associated hydrothermal and secondary mineral precipitation, will be discussed from the perspective of mechanical deformation. The probable controlling effect of pre-existing fabrics in the basement host rock in order to localize the brittle fault zones will also be considered. Finally, the onshore fault systems in western Troms described in this work will be considered in a regional context in order to compare them to the structural elements of the SW Barents Sea and the Lofoten-Vesterålen Margins (cf. Indrevær et al. 2013).

3.1 Fault system characteristics, linkage and correlation

3.1.1 Rekvika fault system

This fault complex is composed of the Rekvika, Bremneset, Tussøya-Røkneset and Hillesøya fault zones that crop out in northwestern Kvaløya (Fig. 30). These individual faults mostly display a NNE-SSW trend with a dominant dip down to the SE. Their location and general attitude (Fig. 30) indicate they are part of a right-stepping *en echelon* fault complex that corresponds well with the major NNE-SSW trend of the fjords and glacial valleys and troughs in western Troms. If these faults are genetically related, they should likely be linked by ENE-WSW to E-W transfer faults as in Lofoten, in order to produce the complete zigzag network of faults and landscape features that characterizes both Lofoten, Vesterålen and western Troms (Fig. 30; Bergh et al. 2007a; Eig et al. 2008a; Hansen & Bergh 2012). Such transfer faults, however have not been observed onshore between the Rekvika, Bremneset,

Tussøya-Røkneset and Hillesøya faults, but they may be present in the fjords in between (Fig. 30). The Hillesøya fault zone has a more variable trend, from NNW-SSE to NE-SW, and dips to the NW/W (Fig. 18), which may be either an indication for a change in fault geometry to a transfer zone and/or associated with basement heterogeneities (see chapter 3.4).

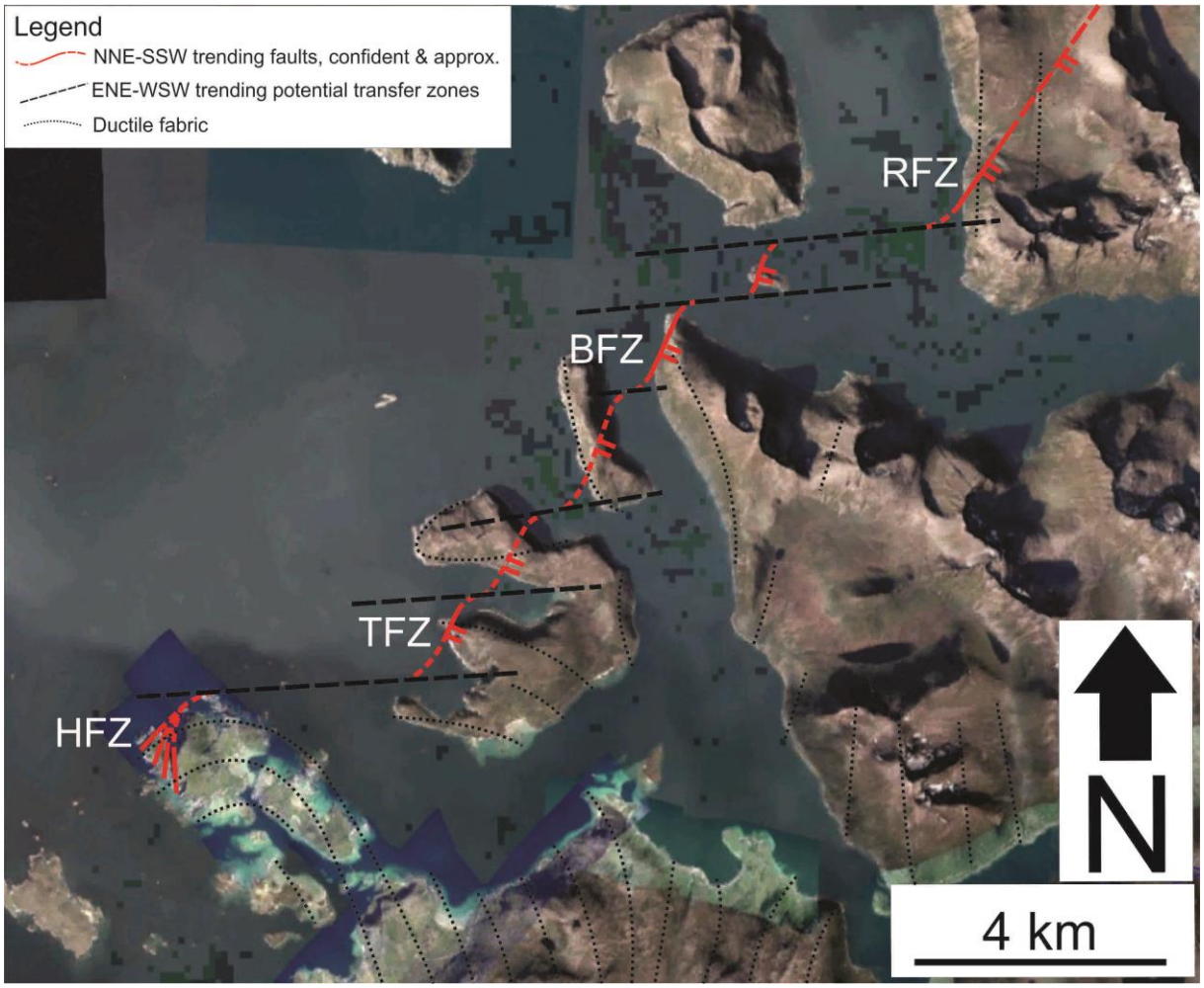

Figure 30: Satellite image of the Rekvika fault complex. The right-stepping, *en echelon*, NNE-SSW trending fault zones (red) are potentially linked by ENE-WSW to E-W striking transfer faults (dashed black). The ductile fabric data (dotted black) are from Bergh et al. (2010), this study, and unpublished data from Zwaan. Abbreviations: BFZ = Bremneset fault zone, HFZ = Hillesøya fault zone, RFZ = Rekvika fault zone, TFZ = Tussøya-Røkneset fault zone.

The individual fault segments display narrow, typically 50 meters wide damage zones comprising few meters thick core zones and show a limited length of a few 100's of meters (< 1 km). Since the width and the length of a fault zone are directly related to the amount of displacement accommodated by this fault (linear relations; cf. Watterson 1986; Kim & Sanderson 2005), it is suggested that brittle deformation was relatively localized and that the fault zones of the Rekvika fault complex only accommodated modest displacement. This has been confirmed by the study of a similar intra-horst fault zone in Skorelvvatn that shows a

minimum displacement of ca. 250m (Indrevær et al. 2013). An exception is the Rekvika fault zone, which can be traced few km towards the NE (Antonsdóttir 2006).

One way to test if any of the studied *en echelon* faults is linked with *transfer* type faults is to evaluate and compare the internal fault kinematics (dip-slip normal versus dip-slip oblique) and relative timing of the various fault-fracture sets. All the faults have damage zones that commonly include high-frequency, generally planar, right-stepping *en echelon* fractures showing steep to moderate dips to the SE. A second well-developed fracture set trending ENE-WSW often interacts closely with the dominant fracture pattern that strikes NNE-SSW, either by merging together into e.g. duplex-shaped structures composed of gash fractures (Fig. 11b, 12 & 16d), or by defining separate oblique-slip fault zones in between the NNE-SSW faults (Fig. 14). Some NNW-SSE trending, ESE-dipping brittle faults in Hillesøya rather follow the trend of the Svecofennian Senja Shear Belt (Zwaan 1995), and another potential explanation of the stepping geometry of the NNE-SSW trending faults might reside in basement related, NW-SE trending transfer zones (cf. chapter 3.4).

Oblique-normal movement, as would be expected within an *en echelon* stepping fault system with synchronous fault formation (Hansen & Bergh 2012), is largely supported by slickensided fault surfaces (Chapter 2 and 3.2; Fig. 7, 10, 14, 18, 22 & 27) that mostly indicate oblique dextral normal, down to the SE motions. This sense of shear has also been confirmed by the microstructural analysis (normal/dextral micro-offsets; e.g. fig. 17b, c & d) and occasionally by offset of geological markers such as pegmatite dykes (Fig. 11d). Despite the dominance of dextral strike-slip components, the Hillesøya fault zone shows oblique sinistral normal movements along strike (Fig. 18). On the other hand, slickensided surfaces observed along the ENE-WSW trending faults in Tussøya indicate dominant sinistral movements along these structures (Fig. 14b). Few slickensides and micro-offsets might also suggest minor dip-slip reverse overprint (Fig. 13b), implying a potential reactivation of the Rekvika fault complex individual fault zones and/or evolution in a more complex, local strain field, potentially NW-SE contraction.

Some sigmoidal curving geometry in cross-section in Tussøya and Bremneset have been interpreted as extensional duplexes and indicate normal dip-slip movements (Eig & Bergh 2011). On the contrary, other bending geometries in map view in Rekvika

(Antonsdóttir 2006) and Tussøya may indicate strike-slip displacement. Similar geometries have been described along NNE-SSW and ENE-WSW trending faults in Lofoten and Vesterålen by Hansen & Bergh (2012). Their models can be applied to the fault-fracture patterns and bending geometries observed in western Troms (Fig. 31). A first model implies a relatively older age for the ENE-WSW fractures that may have been dragged towards NNE-SSW faults (Fig. 31a), which would require sinistral strike-slip displacement, i.e. significant offset of older structures, and an increase in strain toward the NNE-SSW trending faults. A second model implies a possibly younger age for the ENE-WSW fractures that would have formed later or synchronously with the NNE-SSW trending fractures (Fig. 31b). Shear displacement would not be necessary since the curving geometry would result from stress perturbation around the NNE-SSW trending fractures (Hansen & Bergh 2012). In Rekvika, significant offsets have been observed by Antonsdóttir (2006), which would favor the interpretation of fig. 31a, implying sinistral movements along the NNE-SSW striking faults and a relatively younger age for these structures. In Tussøya, the NNE-SSW trending fractures show oblique slip kinematic indicators, comprising a sinistral movement component, and the ENE-WSW fractures bend anticlockwise toward the NNE-SSW striking fractures in map view. This would again support the interpretation of fig 31a, i.e. a younger age for the NNE-SSW trending faults. On the contrary in Tussøya, clockwise bending of NNE-SSW striking fractures towards ENE-WSW trending faults (Fig. 14) would indicate dextral strike-slip movements and a younger age for the ENE-WSW striking faults according to fig. 31c. These ENE-WSW trending fault, however, show evidence for sinistral strike-slip movements (cf. fig. 14), which may therefore indicate a younger age for the NNE-SSW trending fractures or a synchronous development of the two fracture sets. In this case the curving geometry would be the result of stress perturbation around the ENE-WSW trending fractures (Fig. 31d). Therefore, the NNE-SSW trending fractures may have formed later or synchronously with the ENE-WSW striking fractures in the fault zones along the Rekvika fault complex.

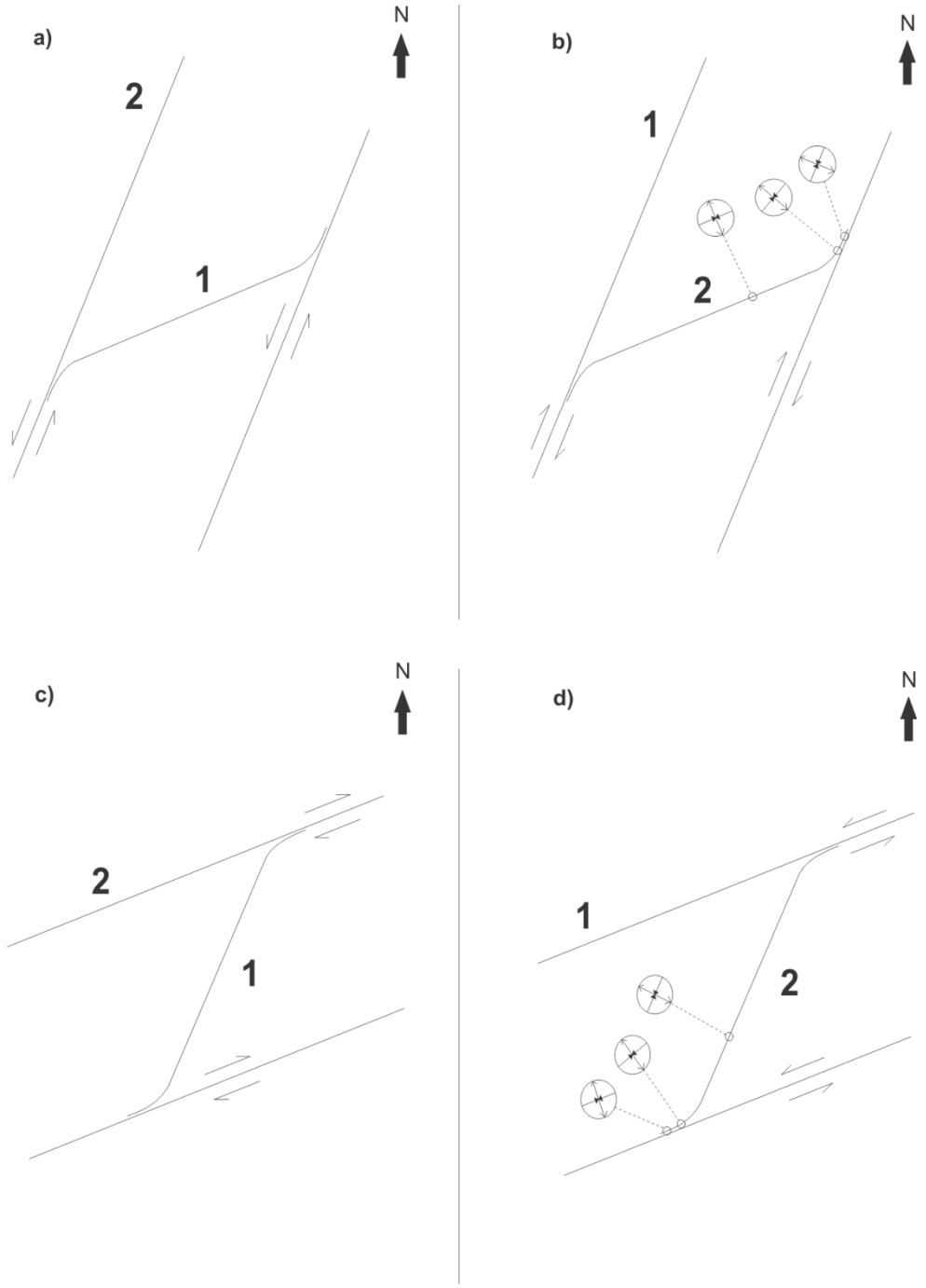

Figure 31 : Models showing two potential kinematic interpretations and relative timing (indicated by numbers) for NNE-SSW and ENE-WSW trending fracture sets. a) Anticlockwise sigmoidal curving of ENE-WSW fractures that formed earlier (1), and that have been dragged toward younger NNE-SSW striking faults (2) during sinistral shearing and due to material rotation along the NNE-SSW trending faults b) ENE-WSW trending fractures (2) are bent into parallelism with older or synchronous, NNE-SSW striking fractures (1). The anticlockwise curving is, here, due to local stress perturbation along the potentially dextral, NNE-SSW striking faults. Note that shearing along the NNE-SSW striking fractures is not necessary to produce the curving geometry c) Clockwise sigmoidal bending of NNE-SSW trending fractures that formed earlier (1), and that have been dragged toward younger ENE-WSW striking faults (2) during dextral shearing and due to material rotation along the ENE-WSW trending faults d) NNE-SSW trending fractures (2) merge into parallelism with older/synchronous ENE-WSW trending fractures (1). The clockwise curving is due to local stress perturbation along the potentially sinistral ENE-WSW striking faults. Shearing along ENE-WSW striking fractures is not required to bend the NNE-SSW trending fractures. Redrawn and modified after Dyer (1988) and Hansen & Bergh (2012).

The NW-SE striking fracture set present throughout the Rekvika fault complex fault zones seems unlikely related to the fault zones themselves since these NW-SE trending fractures truncate all the other brittle fractures and show mainly strike-slip kinematic indicators (Antonsdóttir 2006 and this study). This fracture set is believed to have formed due to NE-SW extension as suggested by quartz fiber growth along NW-SE trending fractures (Fig. 9e).

3.1.2 Vestfjorden-Vanna fault complex

The Vestfjorden-Vanna fault complex (Olesen et al. 1997), on a regional, scale displays a zigzag geometry, including fault segments running successively NNE-SSW and ENE-WSW. This study demonstrates that a correlation can be made between different segments of the NNE-SSW to ENE-WSW trending, SE-dipping Straumsbukta-Kvaløysletta fault zone in Kvaløya (Forslund 1988), the ENE-WSW trending, SSE-dipping Stonglandseidet fault zone in southwestern Senja, and the NNE-SSW trending Nybygda and Grasmyrskogen fault zones in Senja (Indrevær et al. 2013). The correlation is supported by the map pattern (Fig. 32) and internal fault characteristics, as outlined and discussed further below.

The damage zones of the individual fault zones typically are several 100's of meters wide (500m in Stonglandseidet; cf. fig. 27) and they show thick core zones from ca. 20m width in Straumsbukta (Forslund 1988), and 100-150m wide in Stonglandseidet (Fig. 27). The fault zones can actually be traced for 10's of km (Fig. 32; cf. Forslund 1988; Tveten & Zwaan 1993; Olesen et al. 1993, 1997). Watterson (1986) and Kim & Sanderson (2005) established linear relations linking the length and width of a fault zone to the amount of displacement along these faults. Moreover the Solbergfjorden fault zone (See fig. 4 for location), probable eastern continuation of the Stonglandseidet fault zone, shows a down to the SSE vertical displacement of at least 1000m (Tveten & Zwaan 1993). Hence, both the NNE-SSW and ENE-WSW trending fault segments of the Vestfjorden-Vanna fault complex seem to have accommodated large-magnitude (at least 1-3km) displacement, which is likely since the Vestfjorden-Vanna fault complex is considered as the boundary between the West Troms Basement Complex and the Caledonian nappes, i.e. supposed to have down-dropped the Caledonian nappes several km to the SE (Forslund 1988; Olesen et al. 1997; Indrevær et al.

2013). This similarity also suggests the two fault sets may be genetically related and formed synchronously; this will be further discussed in this section.

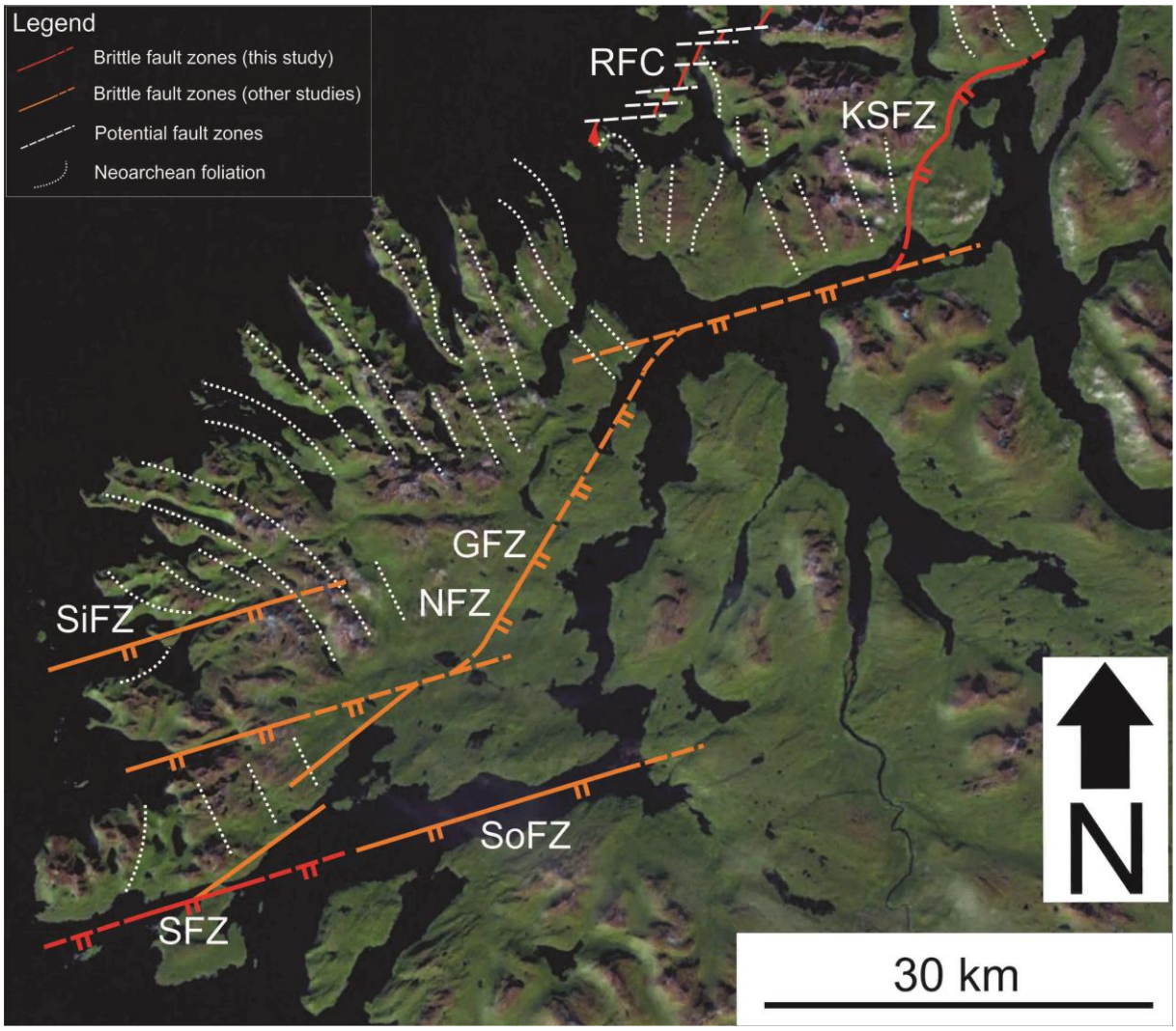

Figure 32: Satellite imaging of Senja and southern Kvaløya showing the zigzag fault pattern that defines the Vestfjorden-Vanna fault complex. The brittle faults plotted here are from this study (red), Forslund (1988), Gagama (2005) and Indrevær et al. (2013). The Precambrian foliation (dotted white) data are from Bergh et al. (2010). Abbreviations: GFZ = Grasmyrskogen fault zone, KSFZ = Kvaløysletta-Straumsbukta fault zone, NFZ = Nybygda fault zone, RFC = Rekvika fault complex, SFZ = Stonglandseidet fault zone, SiFZ = Sifjorden fault zone, SoFZ = Solbergfjorden fault zone.

On the outcrop scale, all of the studied faults comprise multiple minor fault-fracture sets that can be used to test at least fault correlation and relative timing on a smaller scale. For example in Straumsbukta, the damage zone comprises both listric and planar, right-stepping *en echelon*, N-S and locally NE-SW trending, E-dipping fractures that link or merge together, indicating close relative timing (Fig. 24). The same is apparent in Stonglandseidet where the core of the fault zone displays high-frequency, mainly planar, NNE-SSW and ENE-WSW trending fractures that show steep dips to the NW (Fig. 27).

The slickensides found on N-S to NE-SW trending fault surfaces in Straumsbukta indicate a dominant oblique normal dextral sense of shear (Fig. 22). This is supported by dextral and normal micro-offsets (Fig. 26d & e). Furthermore quartz fibers that developed along N-S trending fracture surfaces indicate an E-W directed extension (Fig. 26h). The NNE-SSW trending Nybygda and Grasmyrskogen fault zones both display internal zigzag fault zones with slickensides that favor oblique dextral normal and dip-slip normal movements respectively (Indrevær et al. 2013). On the contrary, the Stonglandseidet fault zone is characterized by a lack of slickensided surfaces and kinematic indicators, but presumably corresponds to a steep, mostly strike-slip fault with an undetermined sense of shear, based on the dome-like structure described in Tveten & Zwaan (1993) and Olesen et al. (1993). Since the Solbergfjorden fault zone displays a vertical movement of at least 1000m and is thought to correspond to the eastern continuation of the Stonglandseidet fault zone (cf. Tveten & Zwaan 1993), it is suggested that the Stonglandseidet fault zone also accommodated down to the SSE vertical displacement. In Straumsbukta, the slickenside data and the microstructural analysis comprise indications for minor dip-slip reverse overprint (slicks: 22b & 26f), which could suggest a later reactivation of the Straumsbukta-Kvaløysletta fault zone.

The NNE-SSW striking fractures in Stonglandseidet sometimes show clockwise bending towards ENE-WSW trending faults in map view (Fig. 28b). Similar geometries have earlier been described in Lofoten and Vesterålen by Hansen & Bergh (2012) and their model can also be considered for the curving geometries in Stonglandseidet (Fig. 31). The first model implies a younger age for the ENE-WSW trending fractures and dextral simple shear along these structures (Fig. 31c). This interpretation would imply offset of the NNE-SSW striking fractures and an increase in strain towards the ENE-WSW striking faults. The second model requires that the NNE-SSW trending fractures developed later or at the same time as the ENE-WSW trending fractures (Fig. 31d). The curving geometry would then be the result of stress perturbation along possibly sinistral, ENE-WSW trending fractures, although in this case shearing is not required to bend the NNE-SSW trending fractures. Since the NNE-SSW trending fractures do not seem offset in Stonglandseidet it seems more likely that the bending geometries developed due to a perturbed stress field along the ENE-WSW striking

fractures, and that the NNE-SSW trending fracture set developed later or synchronously with the ENE-WSW striking fractures (Fig. 31d).

In Stonglandseidet, a set of steep, high-frequency, NW-SE striking fractures, similar to the NW-SE trending fractures observed along the fault zones of the Rekvika fault complex, crosscuts the other fracture sets, sometimes bending them (Fig. 28b). This indicates a relatively younger age and possible dextral strike-slip movements along the NW-SE trending fractures. Therefore these structures are probably youngest and not related to the formation of the Stonglandseidet fault zone.

3.2 Fault rocks and fracture evolution

3.2.1 Rekvika fault complex

In order to estimate the depth of fault formation (P-T conditions) and further characterize the evolution of the Rekvika and Vestfjorden-Vanna fault complexes, we focus on the fault rocks, mineral assemblages and timing relationships of fracture sets in the fault zones. The core of all the studied fault zones located within the Rekvika fault complex are generally marked by proto to ultracataclastic granite that indicates greenschist facies conditions (from the presence of epidote and chlorite), i.e. temperature of ca. 350-500°C, and locally, upper prehnite-pumpellyite facies conditions along the Tussøya-Røkneset fault zone (Fig. 17a). The presence of diagnostic pumpellyite implies temperatures around 250-350°C. The cataclastic fault rocks potentially formed due to pressure of ca. 0.2-0.3 GPa and at depth of about 5-10km (Bucher & Grapes 2011). Injected vein material found in Tussøya (Fig. 16f) and in Rekvika (Antonsdóttir 2006), previously thought to be pseudotachylyte, now has been investigated to be composed of ultracataclastic fault rock (Fig. 17b; this study).

The fault rocks show at least two generations of cataclasites, the first displaying enrichment in epidote and the other in quartz and feldspar (Fig. 17f). The Hillesøya fault zone differs from the other fault segments of the Rekvika fault complex since it comprises calcite-rich cataclasite and breccias in the fault core (Fig. 20). These cataclasites comprise numerous healed micro-fractures characterized by recrystallized material (Fig. 13c) that may indicate rapid injection over a short period of time. According to Keulen et al. (2008) a single

tectonic event may lead to several generations of cataclasite in granitic host rocks since natural healing of fault rocks in granitoids can occur within one year.

The relative and absolute timing of the corresponding NNE-SSW to ENE-WSW trending fault sets within the major faults can be further evaluated from the nature of mineral precipitation on minor fractures. In Tussøya and Bremneset, both the NNE-SSW and ENE-WSW internal fracture surfaces display epidote and hematite precipitations (Fig. 16d) while epidote and calcite dominate in Hillesøya. In Rekvika, numerous fracture sets exist and they show pronounced quartz, calcite, chlorite, epidote and hematite precipitation in conjunction with intense quartz veining, suggesting injections of quartz-rich hydrothermal fluids (Antonsdóttir 2006). In general, the fractures with distinct and different secondary mineral precipitations do not show any consistent relative timing difference from crosscutting relationships. It is therefore suggested that the NNE-SSW and ENE-WSW trending fractures developed simultaneously. A good indicator of the synchronous development of the NNE-SSW and ENE-WSW striking faults-fractures is the interaction of the two sets to define extensional duplex-shaped structures (Gibbs 1984; Eig & Bergh 2011; Fig. 11b, 12, 16d & 17c). Moreover in Rekvika, Antonsdóttir (2006) proposed a relatively younger age for N-S trending fractures in comparison with NE-SW trending fractures, whereas Gagama (2005) proposed a contradicting interpretation in Senja along the Sifjorden fault zone: relatively older N-S and younger NE-SW trending fractures. This inconsistency may be an additional evidence for a synchronous formation of the two fault-fracture sets.

The NW-SE trending fracture set present throughout the fault zones, crosscuts all the other brittle fracture sets, displays mostly hematite coatings on fracture surfaces (cf. Antonsdóttir 2006) and does not seem to be associated with major faulting. These fractures must, therefore, be relatively younger than the NNE-SSW and ENE-WSW trending fracture sets. Noteworthy, they trend parallel to major ductile (Svecofennian) shear zones such as the Senja Shear Belt (Fig. 4; Zwaan 1995; Bergh et al. 2010; see chapter 3.4). The curving geometries they show towards ENE-WSW striking faults in Tussøya may just result from stress perturbation around older, ENE-WSW trending fractures, as inferred earlier from the model of Hansen & Bergh (2012) for NNE-SSW trending fractures in Tussøya (Fig. 31d; cf. chapter 3.1.1).

From the perspective of absolute ages of the studied brittle faults, the Tussøya-Røkneset fault zone has recently been dated by the Apatite Fission Track method (Hendriks et al. 2010) to yield an age of 205 ± 11 Ma (Davids et al. 2012b). Other recent K/Ar and $^{40}Ar/^{39}Ar$ dating from Davids et al. (2010) yielded an age of ca. 280 Ma for the Rekvika fault zone. Similar Permo-Triassic ages (minimum ages of 200 Ma) have been obtained for a number of brittle fault zones in western Troms (Davids et al. 2010, 2012b), whereas much younger Apatite Fission Track ages (mostly Jurassic-Cretaceous) were found for faults in Vesterålen and Lofoten (Hendriks et al. 2010). A Permian age was obtained for a major phase of hydrothermal activity: 280-250 Ma ages from K-feldspar $^{40}Ar/^{39}Ar$ dating (Davids et al. 2012b). This is consistent with the age of faulting and the intense hydrothermal veining in Rekvika. The consistent Permian ages for most radiometrically dated faults in western Troms (cf. Olesen et al. 1997) suggest only one stage of major faulting and coupled hydrothermal alteration, indicating that the faults may be genetically linked in time and space. This would also supports a synchronous formation of the major NNE-SSW and ENE-WSW trending faults onshore western Troms, and a similar age range for the mineral precipitations along the small-scale, brittle fracture surfaces.

3.2.2 Vestfjorden-Vanna fault complex

As for the Rekvika fault complex, the Straumsbukta-Kvaløysletta and Stonglandseidet fault zones (Vestfjorden-Vanna fault complex) in Kvaløya and southern Senja show well-developed protocataclastic host-rocks in the damage zone and more localized, cataclastic to ultracataclastic fault rocks (Fig. 28b & c) in the core zone (cf. Forslund 1988; Olesen et al. 1993, 1997). These cataclastic host rocks underwent greenschist to lower amphibolitic metamorphic conditions from the presence of epidote, chlorite and locally biotite, suggesting a temperature range of ca. 350-550°C, a pressure of about 0.2-0.3 GPa and a crustal depth of approximately 5-10km (Bucher & Grapes 2011).

Two types of cataclastic fault rocks have been described along the Stonglandseidet fault zone, and they display high concentration in calcite and in silica (quartz and feldspar) respectively (Fig. 29b). The complex cross-cutting relationships among discrete fault rocks and the high amount of healed fractures found in these rocks (Fig. 29a) may indicate

formation during the same faulting event since natural crack healing in granitoids can occur within one year (Keulen et al. 2008).

Relative timing constrains between the NNE-SSW and ENE-WSW trending fracture sets in the Stonglandseidet fault zone can be inferred from the fact that calcite and quartz/feldspar veins occur on both fracture sets. As along the Rekvika fault complex, crosscutting relationships do not indicate any relative timing difference between the quartz/feldspar and calcite veins in the Stonglandseidet fault zone, or between the chlorite and quartz filled-fractures in the Straumsbukta fault zone, and this may also indicate a simultaneous formation of the NNE-SSW and the ENE-WSW trending faults.

The NW-SE trending fractures in Stonglandseidet truncate and sometimes appear to bend the NNE-SSW and ENE-WSW trending fractures, suggesting a relatively younger age for these structures (Fig. 28b). As along the Rekvika fault complex, the NW-SE trending faults and fractures trend approximately parallel to major ductile shear zones (cf. Senja Shear Belt; see chapter 3.4) and are probably not associated to the main fault zones in the Vestfjorden-Vanna fault complex.

Regarding absolute ages of faulting, Olesen et al. (1993, 1997) and Davids et al. (2010, 2012b) constrained the faulting history along the Vestfjorden-Vanna fault complex to have occurred in a single Permian-Triassic event in western Troms, using paleomagnetic and geochronological studies. The same studies (Davids et al. 2012b) also yielded a Permian age for a pronounced hydrothermal activity implying that the faulting and hydrothermal events may have overlapped, and that the latter affected at least a major portion of the Vestfjorden-Vanna fault complex. This work demonstrates that quartz, calcite and feldspar minerals precipitated along all the fracture surfaces, and thus, that the NNE-SSW and ENE-WSW trending fractures may have developed simultaneously during the same faulting event.

3.3 Comparison of the studied fault complexes

The studied fault segments of the Rekvika and the Vestfjorden-Vanna fault complexes share many features in common, but also show some major difference, e.g. regarding attitude, fault rocks, hydrothermal veining, kinematics and internal timing relationships. Among the most important similarities are the dominant trends and geometries of the fault-

fracture sets. NNE-SSW, ENE-WSW and NW-SE trending fracture sets have been observed, showing high-frequency, *en-echelon* and listric/planar geometries. The dip directions are toward the SE for both the NNE-SSW and ENE-WSW trending faults-fractures of the Rekvika and Vestfjorden-Vanna fault complexes. The NW-SE trending fractures, widespread along the studied fault zones, are clearly unrelated to the main faulting event along the two fault complexes. Moreover, the NNE-SSW and ENE-WSW striking faults and fractures show a similar timing and probably developed synchronously, both in the Rekvika and Vestfjorden-Vanna fault complexes. Another similarity is the main oblique-slip normal dextral sense of shear, and the evidence for minor inversion of the normal brittle faults indicated by slickensides along these two fault complexes. The individual fault zones of the Rekvika and Vestfjorden-Vanna fault complexes also display well-developed cataclastic fault rocks along strike that largely indicate greenschist facies conditions (350-500°C) and comparable pressure (ca. 0.2-0.3 GPa) and depth (5-10 km), and similar hydrothermal veining principally made up of quartz, calcite, epidote, chlorite and hematite. A single event of faulting and overlapping hydrothermalism in the Permian-Early Triassic has, therefore, been inferred for both fault complexes (cf. chapter 3.2).

On the other hand, major differences include the width and the length of the individual fault segments composing the Rekvika and Vestfjorden-Vanna fault complexes. The Straumsbukta-Kvaløysletta and Stonglandseidet fault zones are actually much wider (ca. 500m damage zones) than the Rekvika, Bremneset, Tussøya-Røkneset and Hillesøya fault zones (ca. 100m damage zones). In addition, the Stonglandseidet and Straumsbukta-Kvaløysletta can be traced for 10's of km along the Vestfjorden-Vanna fault complex. On the contrary, the fault segments of the Rekvika fault complex crop out only for short distances (< 1km, locally few km in Rekvika). Furthermore, tectonic breccias are thought to be exposed in the core of the Straumsbukta-Kvaløysletta and Stonglandseidet fault zones (in addition with cataclasite; cf. Forslund 1988; Tveten & Zwaan 1993; Olesen et al. 1993) whereas the Rekvika fault complex is only characterized by cataclastic fault rocks (see chapter 3.2).

From the similarities and contrasts outlined above, it seems likely that the Vestfjorden-Vanna fault complex accommodated very large amounts of displacement (about 1-3km; cf. Forslund 1988). This is in accordance with this fault system bordering the West Troms Basement Complex and downdropping the Caledonian nappes several km to the SE.

The Rekvika fault complex however accommodated much less movements, in the order of only few 100's of meters (Indrevær et al. 2013). Based on displacement calculations along an apparent, intra-horst fault zone at Skorelvvatn on Kvaløya (see fig. 4 for location), the most likely interpretation is that the Rekvika fault complex is an intra-horst fault system. Considering the fault complexes in a regional frame and assuming a WNW-ESE extension direction (Wilson et al. 2006; Bergh et al. 2007a, 2008; Eig et al. 2008a; Hansen et al. 2009, 2012), the NNE–SSW-trending faults of the Rekvika and Vestfjorden-Vanna fault complexes may represent the main orthogonal, *en echelon* fault system that developed perpendicular to the trend of extension, whilst the ENE-WSW trending faults in between represent simultaneously-developed transfer zones (cf. Morley et al. 1990) linking the NNE–SSW striking fault arrays (cf. Hansen & Bergh 2012). The deep formation depth inferred for the fault rocks exposed along the Rekvika and Vestfjorden-Vanna fault complexes (5-10 km depth) implies that the West Troms Basement Complex has later been uplifted, probably during the late Cenozoic (Indrevær et al. 2013).

The Hillesøya fault zone locally shows a NNW-SSE trend, and a dominant northwestern dip, i.e. away from the basement horst, and an oblique sinistral normal slip which differs from the dominant oblique-dextral normal slip commonly observed along the Rekvika, Bremneset and Tussøya-Røkneset fault zones. Moreover the Hillesøya fault zone is characterized by calcite-rich cataclasite and breccias similar to the fault rocks found along the Vestfjorden-Vanna fault complex. These differences with the other fault segments of the Rekvika fault complex may indicate that the Hillesøya fault zone is located in the vicinity of a major transfer zone. The Hillesøya fault zone is actually split into four fault traces showing variable trends (Fig. 18). More particularly, NNW-SSE trending faults rather strike parallel to the NW-SE Senja Shear Belt and may reflect a change toward a NW-SE transfer zone or just a specific trend of the basement fabric (see chapter 3.4).

3.4 Basement control

Palaeoproterozoic (Svecofennian) and Caledonian (Silurian) structures and fabrics display local similarities in trend and dip with the various segments of the Rekvika and Vestfjorden-Vanna fault complexes described in this study, and may have acted as zones of weakness and contributed to the localization of the brittle faults. Hansen et al. (2009)

noticed "anomalous" fault orientations along the Lofoten-Vesterålen Margin that do not match with any major fault population, and they suggested that these anomalously oriented brittle faults following pre-existing basement weaknesses. In the study area, the pre-existing basement fabrics include variably steep lithological contacts, steep NW-SE trending Svecofennian foliations and ductile shear zones (Bergh et al. 2010), and NE-SW trending, mostly gently dipping NW and SE Caledonian foliations and thrusts (Zwaan et al. 1998; Roberts et al. 2007; Steltenpohl et al. 2011).

The Tussøya-Røkneset fault zone has developed along the contact between red-stained granite and the amphibolitic gneisses of the Kattfjord complex, which is NNE-SSW trending and gently dipping to the SE (Fig. 15). In Bremneset, the NNE-SSW to NE-SW trending fractures are locally parallel to the gently-dipping, down to the SE contact between the granitic intercalations and the Kattfjord complex gneisses (Fig. 12). In both localities, most of the brittle deformation seems actually localized around the lithological boundary where the brittle fractures commonly merge into duplex-like structures (Fig. 12 & 15).

The main Precambrian foliation in the Kattfjord complex gneisses is sometimes parallel with brittle fractures, suggesting that favorable attitudes may have, at least locally, helped brittle fault localization. For instance in the Straumsbukta fault zone, the predominant N-S trending fracture set trends parallel to the Svecofennian foliation and the contact delimiting the tonalitic and amphibolitic gneisses boundary, and may have used this pre-existing zone of weakness to develop N-S (Fig. 22). In Rekvika, the dominant ductile fabric corresponds to an N-S to NNE-SSW foliation striking parallel to the lithological contact between the Ersfjord granite and the Kattfjord complex. This foliation, which probably developed during the intrusion of the Ersfjord granite, shows the same trend than the NNE-SSW trending brittle fractures described along the Rekvika fault zone and consequently, they may have helped to localize the development of these structures (Fig. 7a). A similar relationship may be inferred for the formation of subsidiary NW-SE trending fractures in Bremneset, which strike parallel to the NW-SE Svecofennian foliation in the NW in the Bremneset fault zone (Fig. 10). In Tussøya as well, high-frequency NNE-SSW trending fractures in the core zone developed sub-parallel to the NE-SW trending, SE-dipping Precambrian foliation (Fig. 14), whereas further west the foliation turns into an ENE-WSW trend, i.e. sub-parallel to the ENE-WSW trending fractures. It is therefore proposed that this

NE-SW to ENE-WSW striking Precambrian foliation has played a key role in the localization of the NNE-SSW and ENE-WSW striking fracture sets in Tussøya.

In Rekvika, the structural data indicate two sets of minor Svecofennian ductile shear zone trending NE-SW and NW-SE, and dipping respectively to the SE and the NE (Fig. 7c). Moreover, the major NW-SE trending shear zone observed in the NW of the Rekvika fault zone shows an anticlockwise ductile bending towards the brittle Rekvika fault zone. It is then suggested that the Rekvika fault zone formed along a major dextral, NE-SW trending, SE-dipping Svecofennian shear zone. This is supported by the remnant, S-C shaped, chlorite foliation found along the core zone (Fig. 9a). In Tussøya, the foliation bends towards a minor NNE-SSW striking, sinistral, ductile shear zone (Fig. 14), and also toward the brittle, NNE-SSW trending Tussøya-Røkneset fault zone. This could indicate ductile shearing along the lithological contact between the granite and the amphibolitic gneisses in Tussøya and, therefore, a preferential zone of weakness for the development of the Tussøya-Røkneset fault zone.

Forslund (1988) recorded stretching lineations and asymmetric feldspar porphyroclasts along the Straumsbukta-Kvaløysletta fault zone that indicate a top to the SE transport direction along mylonitic shear zones located close to the contact between the Caledonian nappes and the West Troms Basement Complex. In addition, the Stonglandseidet, Nybygda and Grasmyrskogen fault zones (Indrevær et al. 2013) are located close to the lithological boundary between the Caledonian nappes and the basement horst (Fig. 4). This suggests the Caledonian thrust contact bounding the Caledonian nappes in the SE and the West Troms Basement Complex in the NW may have been reactivated as normal brittle faults, probably in the Permian-Triassic during the formation of the individual fault segments along the Vestfjorden-Vanna fault complex. Steltenpohl et al. (2011) also evidenced the reactivation of Caledonian thrusts as low-angle normal faults in Vesterålen, and particularly in Eidsfjorden and Fiskefjorden. These faults were suggested to be responsible for the exhumation of metamorphic core complexes in the Devonian and Permian such as the Lofoten Ridge (Osmundsen et al. 2005; Eig et al. 2008b)

The Hillesøya fault zone is located on the steeply-dipping western limb of a sub-vertical macrofold previously identified by Thorstensen (2011), where the foliation trend is

approximately parallel to the brittle fault zone. Thus, the macro-scale fold may have controlled the development and variation in trend of the Hillesøya fault zone from NNW-SSE in the east to NE-SW in the NW (Fig. 33). Macro-scale folding also seems likely in Stonglandseidet considering the variation in attitude of the foliation. In this case, the foliation changes from a NE-SW trend and a NW dip in the NW, to an N-S strike and an eastern dip in the SE, defining a sub-horizontal macrofold (Fig. 27). Therefore in Stonglandseidet, the northwestern limb of this macro-scale fold might have helped the development of similarly oriented, ENE-WSW trending, NW-dipping fractures, whereas the southeastern limb might have acted as a weakness zones for the development of NNE-SSW trending fractures.

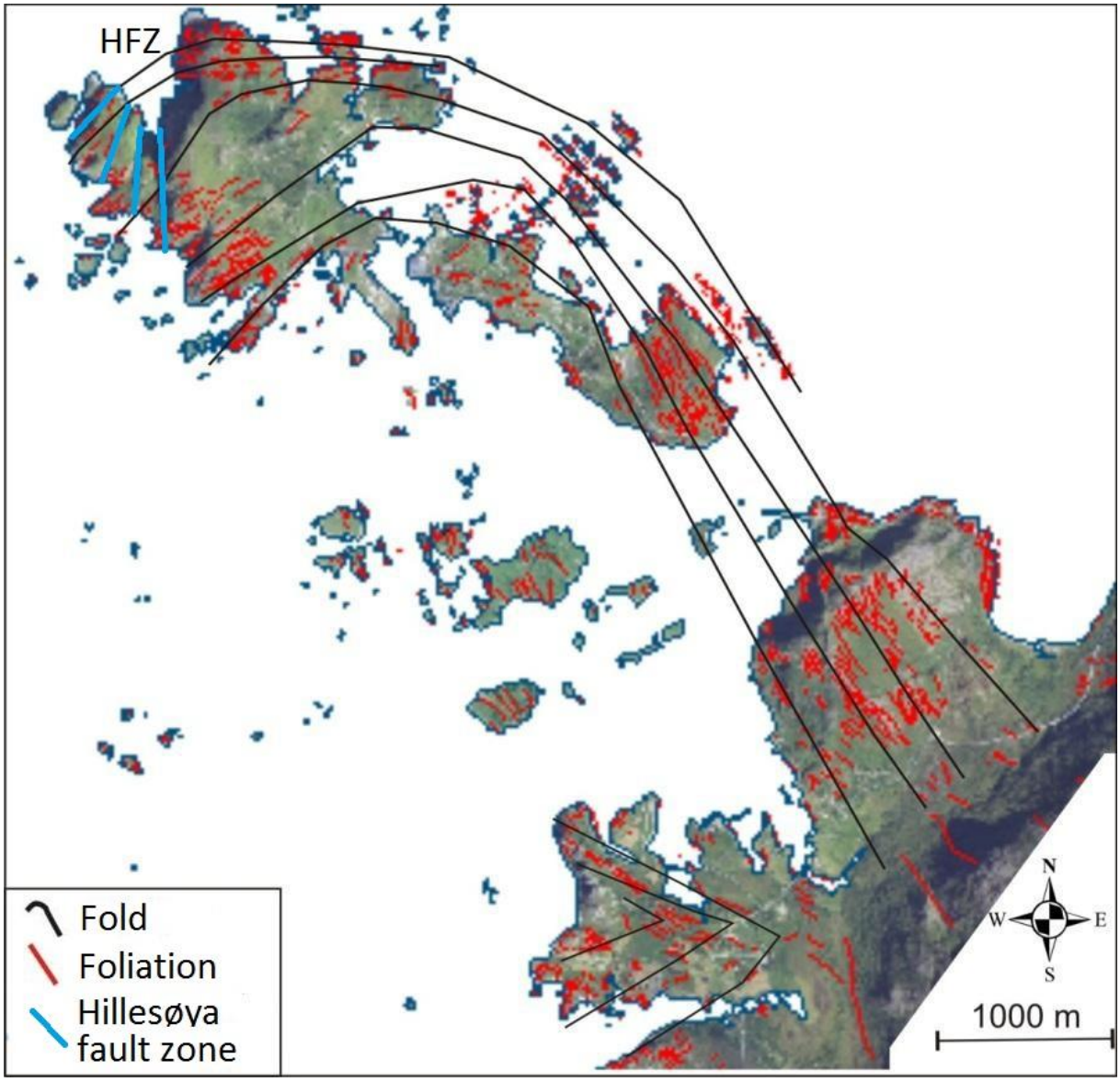

Figure 33: Aerial photograph over Hillesøya showing the regional bending of the Svecofennian foliation defining a macro-scale fold. Abbreviation: HFZ = Hillesøya fault zone. Modified after Thorstensen (2011).

Alternatively, the NW-SE striking, Svecofennian Senja Shear Belt may have influenced the trend of the NNW-SSE trending faults observed within the Hillesøya fault zone and led to the formation of this anomalous trend of brittle fractures. Therefore, the four fault segments defining the Hillesøya fault zone may possibly represent a splay of the Hillesøya fault zone towards a NW-SE trending transfer zone: the Senja Shear Belt. The right-stepping geometry shown by the NNE-SSW striking fault segments of the Rekvika fault complex was previously correlated with ENE-WSW trending transfer zones (cf. chapter 3.1). A secondary model, however, implies a set of basement seated, NW-SE to WNW-ESE trending transfer faults that could also explain the right-stepping geometry of the NNE-SSW trending fault zones. This interpretation is supported by the WNW-ESE trend of the fjords in this area (Fig. 30), and by unpublished bathymetric data from Indrevær et al. (2013; fig. 34) that show NW-SE trending lineaments intercalated between the individual NNE-SSW trending fault zones of the Rekvika fault complex in the northwest of Kvaløya.

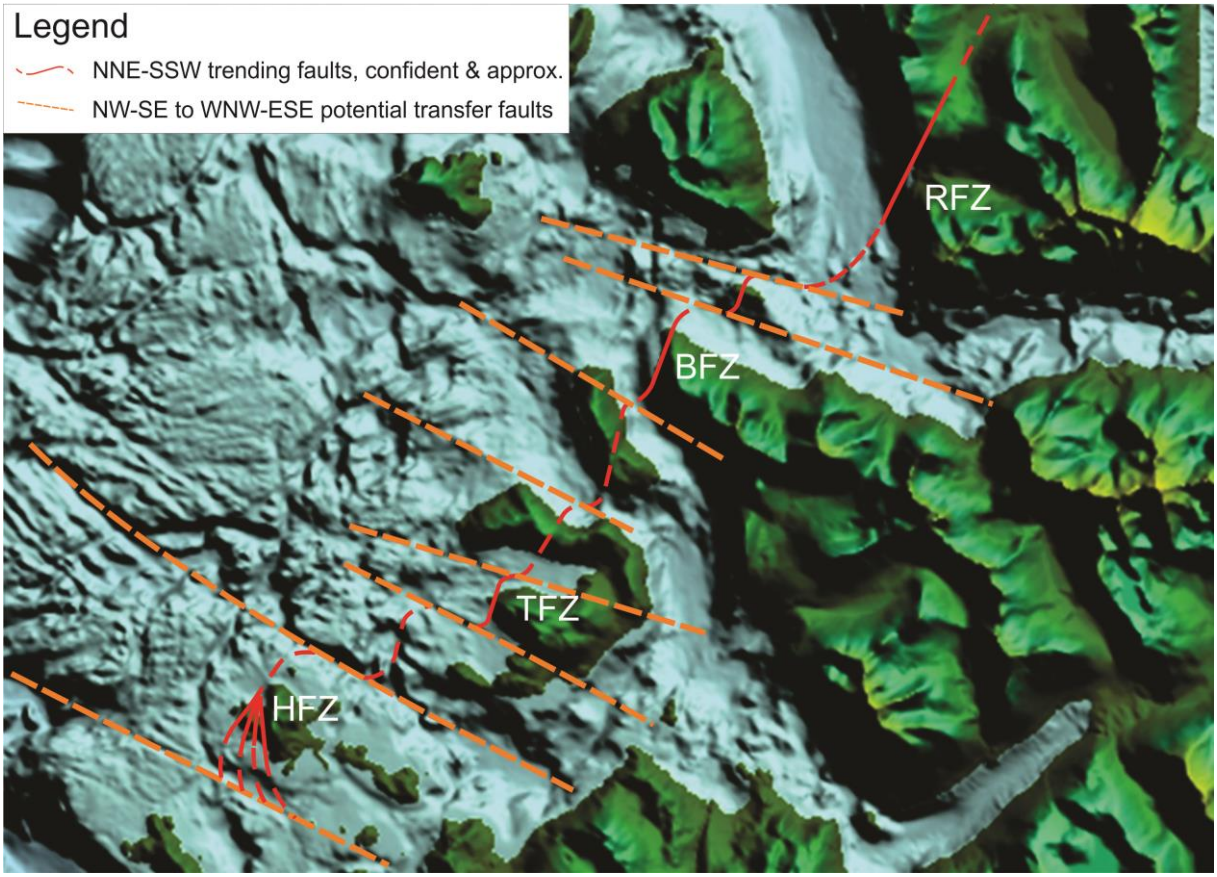

Figure 34: Bathymetric map of the northwest of Kvaløya showing prominent NW-SE trending lineaments (dotted orange) that possibly link the right-stepping, *en echelon*, NNE-SSW trending faults (red); see text for further discussion. Abbreviations: BFZ = Bremneset fault zone, HFZ = Hillesøya fault zone, RFZ = Rekvika fault zone, TFZ = Tussøya-Røkneset fault zone. Unpublished map from Indrevær.

3.5 Implications for the North Norwegian passive margin evolution

During the Paleozoic and Mesozoic Periods, the North Norwegian margin experienced multiple rifting episodes that started in the Late Devonian with large-scale block faulting via reactivation of Caledonian thrusts (Gabrielsen et al. 1990; Doré et al. 1997; Bergh et al. 2007a, 2008; Eig et al. 2008a; Hansen et al. 2009, 2011, 2012; Steltenpohl et al. 2011). Offshore, major sedimentary basins including the Harstad, Tromsø, Hammerfest, Bjørnøya, Sørvestnaget and Nordkapp basins on the SE Barents Sea Margin, and Vestfjorden, Ribban and Træna basins on the Lofoten-Vesterålen Margin started to develop due to regional subsidence during a presumed early stage of rifting that took place from the mid-Carboniferous to the Early Triassic (Fig. 1; Faleide et al. 2008). This period of time includes the timing constraints obtained for onshore faulting in western Troms in the Permian-Early Triassic (Olesen et al. 1997; Davids et al. 2010, 2012a, 2012b; Hansen et al. 2011). These major basins are bounded by prominent fault systems such as the NE-SW trending Troms-Finnmark fault complex that defines the southwestern flank of the Harstad basin and the southern border of the Hammerfest basin toward the Finnmark platform, or the East and West Lofoten Border Faults that border the Lofoten Ridge basement horst towards the Vestfjorden and the Ribban basins respectively (Fig. 1 & 6; Gabrielsen et al. 1990; Blystad et al. 1995; Bergh et al. 2007a; Barrère et al. 2009; Indrevær et al. 2013). These fault complexes are formed by alternating, *en echelon*, NNE-SW and ENE-WSW trending fault segments and delineate zigzag patterns (Bergh et al. 2007a, 2008; Indrevær et al. 2013), which is pretty similar to the presently studied Rekvika and Vestfjorden-Vanna fault complexes geometry. These major offshore fault complexes have obviously remained active throughout successive rifting pulses in the Mid/Late Jurassic to earliest Cretaceous and in the latest Cretaceous-Paleocene in order to accommodate regional subsidence, until the final break-up of Pangea in the Eocene (Gabrielsen et al. 1990; Faleide et al. 1993, 2008; Blystad et al. 1995; Knutsen & Larsen 1997; Gudlaugsson et al. 1998; Larssen et al. 2002; Bergh et al. 2007a, 2008; Hansen et al. 2012; Indrevær et al. 2013). Major faulting activity seems also likely onshore Lofoten-Vesterålen and Finnmark (Roberts & Lippard 2005; Bergh et al. 2007a; Eig et al. 2008a). On the contrary, no tectonic activity has been evidenced along the onshore, zigzag-shaped Rekvika and Vestfjorden-Vanna fault complexes in western Troms and this is the

reason why a potential shift of the extension to the west and northwest is considered for western Troms in the Early Triassic (Olesen et al. 1993, 1997; Davids et al. 2010, 2012b).

The NNE-SSW and ENE-WSW trending fault segments in western Troms display major similitudes with brittle faults onshore Lofoten and Vesterålen, e.g. dominant ENE-WSW and NNE-SSW trends, sigmoidal curving geometries, occurrence of cataclastic fault rocks along the fault cores, and oblique-slip kinematics (Eig et al. 2008a; Hansen & Bergh 2012). Hansen & Bergh (2012) proposed that the ENE-WSW trending faults in Lofoten-Vesterålen originated as joints and were later reactivated as sinistral transfer faults (cf. Morley et al. 1990) linking subsequent NNE-SSW trending fault arrays. The NNE-SSW faults are thought to represent the main, right-stepping *en echelon*, orthogonal fault system that apparently developed perpendicular to a WNW-ESE directed crustal extension in the Early Triassic (Hansen et al. 2012; Hansen & Bergh 2012). Regarding the relative timing of these two fault-fracture sets, Hansen & Bergh (2012) proposed that the ENE-WSW striking joints formed first or at the same time as the NNE-SSW trending faults based on the sigmoidal bending geometries of the faults and fractures in Lofoten-Vesterålen (cf. chapter 3.1 and fig. 31). Considering the faults in western Troms along the Rekvika and Vestfjorden-Vanna fault complexes, the interpretation of Hansen & Bergh (2012) supports a simultaneous formation of both sets of faults-fractures rather than a formation in 2 distinct faulting event since the ENE-WSW and NNE-SSW striking fracture surfaces show similar mineral precipitations along strike. Another argument in favor of a synchronous development would be that onshore faulting in western Troms, and more particularly in Rekvika and Tussøya, has been constrained to a single tectonic event in the Permian-Early Triassic by absolute age dating (cf. Davids et al. 2010, 2012b).

The faulting activity in the Late Cretaceous-Paleocene is marked by the formation of NE-SW trending, NW-dipping faults offshore Lofoten-Vesterålen, by a minor inversion of some extensional brittle faults, and by the development of NW-SE trending fractures onshore the North Norwegian margin (Gabrielsen et al. 1990, 1997; Faleide et al. 1993; Blystad et al. 1995; Knutsen & Larsen 1997; Eig et al. 2008a; Aftab 2011; Eig & Bergh 2011; Hansen & Bergh 2012). Forslund (1988) and paleomagnetic studies from Olesen et al. (1993, 1997) also identified a late stage of faulting in the Late Cretaceous-Paleocene onshore western Troms. In addition, the present work evidenced NW-SE trending fractures and few

micro-offsets and slickensides indicating a reverse sense of shear (Fig. 7b, 13b, 18b & 26f). Bergh et al. (2007a) and Eig et al. (2008a) argued for a major change in the extension direction, switching from WNW-ESE to NNW-SSE in the Late Cretaceous, in order to explain the formation of the NW-SE trending fractures. However recent studies reveal that such a shift in the extension direction is not necessary to form these structures (Eig & Bergh 2011; Hansen & Bergh 2012). Instead, it has been proposed that the NW-SE trending fractures developed as post break-up neotectonic joints due to ridge-push forces and NE-SW directed extension. This is supported by elongated quartz fibers along NW-SE fracture surfaces in Rekvika that indicate a NE-SW trending extension direction (Fig. 9e). This model could also explain the inversion of extensional structures along the North Norwegian margin via NW-SE directed contraction during the opening of the North Atlantic Ocean. Another possible interpretation of the NW-SE trending joints implies stress perturbation within NW-SE trending transfer zones (Eig & Bergh 2011), which would, however, not account for the inversion of extensional structures. Hence, the reverse kinematic indicators and the NW-SE trending fractures found onshore western Troms are thought to be the result of NW-SE contraction and NE-SW crustal extension due to ridge-push forces. Indrevær et al. (2013) suggested that the ridge-push forces partly helped uplifting the West Troms Basement Complex horst, which could explain the exposure of deeply-formed fault rocks along the Rekvika and Vestfjorden-Vanna fault complexes (see chapter 3.2).

The onshore and offshore fault systems of the North Norwegian margin are thought to be segmented by NW-SE trending transfer zones trending parallel to the Precambrian basement fabrics. This results in fault stepping and/or shifts in polarity across these transfer zones (Olesen et al. 1997; Doré et al. 1997; Tsikalas et al. 2001, 2005; Bergh et al. 2007a; Indrevær et al. 2013). The Troms-Finnmark fault complex e.g. displays a different behavior along its southern and northern segments. It actually shows a displacement of 5 to 10 km along the eastern flank of the Harstad basin whereas it downdrops the southern Hammerfest basin of only 3km (Indrevær et al. 2013). This spatial change of throw corresponds with the intersection of the Troms-Finnmark fault complex and the Ringvasøy-Loppa fault complex with the recently discovered NW-SE to N-S trending Fugløya transfer zone that corresponds to the northwestern continuation of the Bothnian-Kvænangen fault complex (Fig. 35). The Vestfjorden-Vanna fault complex displays a change of polarity across

the Fugløya transfer zone, from SE-dipping in the SW to a northwestern dip in the NE (Fig. 35), and merges with the NE-SW trending Måsøy fault complex offshore in the NE (Aftab 2011; Indrevær et al. 2013), whereas in Senja it steps up across the Senja Shear Belt (Fig. 32; Olesen et al. 1997) and continues further south across the Vesterålen transfer zone where it links up with the East Lofoten Border Fault along the Lofoten Ridge (Doré et al. 1997; Olesen et al. 1997; Tsikalas et al. 2001, 2005; Wilson et al. 2006; Bergh et al. 2007a). In western Kvaløya, the southwestern tip of the Rekvika fault complex (i.e. the Hillesøya fault zone) shows W-dipping, occasionally NNW-SSE trending faults approaching the NW-SE striking Senja Shear Belt. This may indicate a potential shift in polarity for the SE-dipping Rekvika fault complex across the Senja Shear Belt (Fig. 34). Indrevær et al. (2013) suggested that the Rekvika fault complex links up with the offshore Nysleppen fault complex in the NE (Fig. 35).

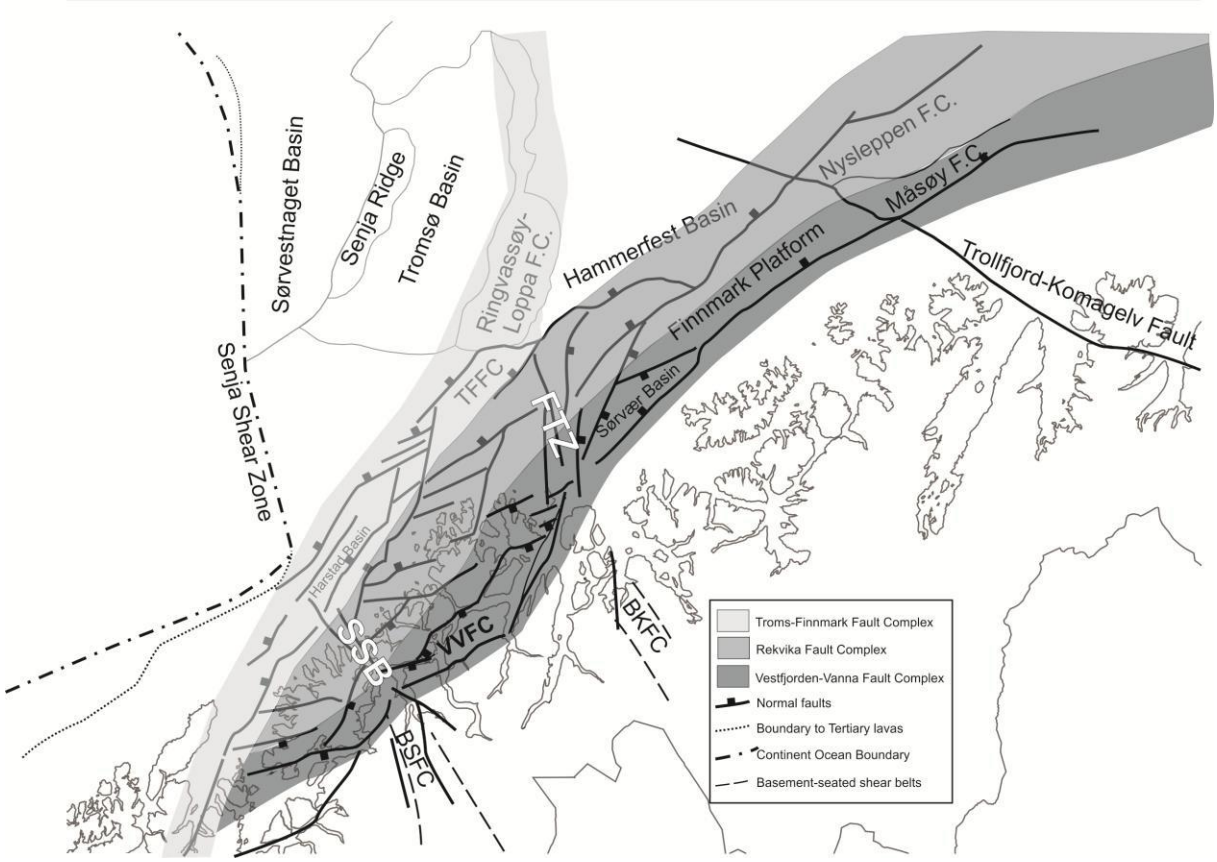

<u>Figure 35:</u> Tectonic map of the SW Barents Sea Margin linking and correlating the onshore NE-SW trending Rekvika and Vestfjorden-Vanna fault complexes to potential offshore continuations in the NE: the Nysleppen and the Måsøy fault complexes respectively. Note the two NW-SE striking transfer zones: the Senja Shear Belt and the Fugløya transfer zone that define the continuation of the Bothnian-Senja and the Bothnian-Kvænangen fault complexes respectively. Abbreviations: BKFC = Bothnian-Kvænangen fault complex, BSFC = Bothnian-Senja fault complex, FTZ = Fugløya transfer zone, SSB = Senja Shear Belt, TFFC = Troms-Finnmark fault complex, VVFC = Vestfjorden-Vanna fault complex. Picture from Indrevær et al. (2013).

4 Conclusions

The present study focuses on onshore brittle fault zones located within the gneisses and granitic intrusions of the West Troms Basement Complex, on the islands of Kvaløya and Senja, North Norway. DEM satellite images, structural field observations and a microstructural analysis provide the bases for the characterization of the geometry, kinematics and fault rock of individual fault zones that have been used to get a better understanding of the regional structural character. The following conclusions can be drawn combining regional, outcrop-scale and micro-scale analyses.

- Two major sets of faults exist in western Troms. They trend NNE-SSW and ENE-WSW, defining a zigzag pattern, dip steeply to moderately and have been gathered into two, NE-SW trending fault complexes: the Rekvika fault complex and the Vestfjorden-Vanna fault complex. These fault complexes strike parallel to the offshore Troms-Finnmark fault complex that borders major Late Paleozoic sedimentary basins in the NW (Fig. 35). Subsidiary NW-SE trending fractures truncate all the other structures and therefore do not seem associated to the Rekvika and Vestfjorden-Vanna fault complexes.
- The Vestfjorden-Vanna fault complex (Fig. 32) defines the boundary between the Caledonian nappes in the south-east and the West Troms Basement Complex in the north-west. This fault system is characterized by wide fault zones (ca. 500m): e.g. the Straumsbukta-Kvaløysletta and the Stonglandseidet fault zones that display dominantly oblique dextral normal slips, and cataclastic to brecciated fault rocks that probably accommodated major displacement (ca. 1-3km).
- The Rekvika fault complex (Fig. 30) appears to be an intra-horst fault system that is composed of narrow (ca. 100m), NNE-SSW trending, SE-dipping fault zones: the Rekvika, Bremneset, Tussøya-Røkneset and Hillesøya fault zones. These fault zones show mainly oblique dextral normal kinematic indicators and cataclastic fault rocks that have probably accommodated minor displacement (> 250 m). The Hillesøya fault zone differs slightly from the other fault zones since it displays a northwestern dip, a dominant oblique sinistral normal sense of shear and brecciated fault rocks. Therefore, it is suggested that the Hillesøya fault zone development has been

controlled by a major, basement-related, NW-SE trending transfer zone: the Senja Shear Belt.

- The basement is thought to have locally helped the localization of brittle faulting along pre-existing zones of weakness. The brittle fault zones indeed show similarities attitude (trend and dip) with the NE-SW trending Caledonian and NW-SE trending Svecofennian fabrics such as ductile foliations and shear zones in Rekvika, lithological boundaries in Bremneset, Tussøya and Straumsbukta, and macrofolding in Hillesøya and Stonglandseidet.
- A temperature range of 350-500°C, and pressure of ca. 0.2-0.3 GPa and a 5 to 10km depth have been inferred from the mineral assemblages and the deformation mechanism (cataclastic flow) for the formation of the fault rocks. Such a deep formation of the fault rocks suggests large-scale uplift of the West Troms Basement Complex from 5-10km deep to the present level, which has probably occurred during the Late Cenozoic.
- The NNE-SSW and ENE-WSW trending fault zones composing the Rekvika and Vestfjorden-Vanna fault complexes likely developed synchronously due to WNW-ESE crustal extension. The NNE-SSW faults are thought to represent the main orthogonal fault system perpendicular to the extension direction, and the ENE-WSW striking faults possibly correspond to transfer zones that developed oblique to the extension direction and that link the right-stepping, NNE-SSW trending fault arrays (Fig. 30 & 32). An alternative model implies NW-SE to WNW-ESE trending transfer faults to link the NNE-SSW trending faults (Fig. 34).
- Regarding the absolute timing of the Rekvika and the Vestfjorden-Vanna fault complexes, new geochronological studies constrain their formation in the Permian-Early Triassic during an early rifting episode well-established along the Lofoten-Vesterålen and the SW Barents Sea Margins.
- A late stage of NW-SE contraction and NE-SW directed extension is believed to be responsible for a minor reverse reactivation of the NNE-SSW and ENE-WSW trending faults and for the development of NW-SE trending fractures via ridge-push forces during the opening of the North Atlantic Ocean in the Eocene.

References

Aftab, M. 2011. “Structural Analysis of the Måsøy Fault Complex in the SW Barents Sea.” *Unpublished Master Thesis, University of Oslo*.

Anderson, M. W., A. J. Barker, D. G. Bennett, and R. D. Dallmeyer. 1992. “A Tectonic Model for Scandian Terrane Accretion in the Northern Scandinavian Caledonides.” *Journal of the Geological Society* 149 (5): 727–741.

Andresen, A. 1988. “Caledonian Terranes of Northern Norway and Their Characteristics.” *Trabajos de Geologia, Univ. de Oviedo* 17: 103–118.

Andresen, A., and T. Forslund. 1987. “Post-Caledonian Brittle Faults in Troms: Geometry, Age and Tectonic Significance (Abstract).” *The Caledonian and Related Geology of Scandinavia. Symposium Cardiff, Sept. 1987*.

Andresen, A., and M. G. Steltenpohl. 1994. “Evidence for Ophiolite Abduction, Terrane Accretion and Polyorogenic Evolution of the North Scandinavian Caledonides.” *Tectonophysics* 231: 59–70.

Antonsdóttir, V. 2006. “Structural and Kinematic Analysis of the Rekvika Fault Zone, Kvaløya, Troms.” *Unpublished Master Thesis, University of Tromsø*.

Barrère, C., J. Ebbing, and L. Gernigon. 2009. “Offshore Prolongation of Caledonian Structures and Basement Characterisation in the Western Barents Sea from Geophysical Modelling.” *Tectonophysics* 470 (1-2): 71–88.

Bergh, S. G., G. Corner, and F. Corfu. 2008. “Proterozoic Igneous and Metamorphic Rocks: a Template for Mesozoic-Cenozoic Brittle Faulting and Tectonic Inherited Landscapes in Lofoten-Vesterålen, North Norway.” *33 IGC Excursion Guidebook* 38 (IGC The Nordic Countries): 71.

Bergh, S. G., K. Eig, O. S. Kløvjan, T. Henningsen, O. Olesen, and J-A Hansen. 2007a. “The Lofoten-Vesterålen Continental Margin: a Multiphase Mesozoic-Palaeogene Rifted Shelf as Shown by Offshoreonshore Brittle Fault-fracture Analysis.” *Norwegian Journal of Geology* 87: 29–58.

Bergh, S. G., K. Kullerud, P. E. B. Armitage, K. B. Zwaan, F. Corfu, E. J. K. Ravna, and P. I. Myhre. 2010. “Neoarchaean to Svecofennian Tectono-magmatic Evolution of the West Troms Basement Complex, North Norway.” *Norwegian Journal of Geology* 90: 21–48.

Bergh, S. G., K. Kullerud, F. Corfu, P. E. B. Armitage, B. Davidsen, H. W. Johansen, T. Pettersen, and S. Knudsen. 2007b. “Low-grade Sedimentary Rocks on Vanna, North Norway: a New Occurrence of a Palaeoproterozoic (2.4-2.2 Ga) Cover Succession in Northern Fennoscandia.” *Norsk Geologisk Tidsskrift* 87 (3): 301.

Bjørlykke, A., and S. Olaussen. 1981. “Silurian Sediements, Volcanics and Mineral Deposits in the Agelvvatn Area, Troms, Northern Norway.” *Norges Geologiske Undersøkelse* 365: 39–54.

Blystad, P., H. Brekke, R. B. Færseth, B. T. Larsen, J. Skogseid, and B. Tørudbakken. 1995. “Structural Elements of the Norwegian Continental Shelf, Part II. The Norwegian Sea Region.” *Norwegian Petroleum Directorate Bulletin* 8: 45.

Bøe, R., H. Fossen, and M. Smelror. 2010. “Mesozoic Sediments and Structures Onshore Norway and in the Coastal Zone.” *Norges Geologiske Undersøkelse Bulletin* 450: 15–32.

Braathen, A., P. T. Osmundsen, and R. H. Gabrielsen. 2004. “Dynamic Development of Fault Rocks in a Crustal-scale Detachment: An Example from Western Norway.” *Tectonics* 23 (4): 21.

Breivik, A. J., J. I. Faleide, and S. T. Gudlaugsson. 1998. “Southwestern Barents Sea Margin: Late Mesozoic Sedimentary Basins and Crustal Extension.” *Tectonophysics* 293 (1): 21–44.

Brekke, H. 2000. “The Tectonic Evolution of the Norwegian Sea Continental Margin, with Emphasis on the Voring and More Basins.” *Geological Society, London, Special Publications* 167: 327–378.

Bucher, K., and R. H. Grapes. 2011. *Petrogenesis of Metamorphic Rocks*. Springerverlag Berlin Heidelberg.

Caine, J. S., J. P. Evans, and C. B. Forster. 1996. “Fault Zone Architecture and Permeability Structure.” *Geology* 24 (11): 1025.

Corfu, F. 2004. “U-Pb Age, Setting and Tectonic Significance of the Anorthosite-Mangerite-Charnockite-Granite Suite, Lofoten-Vesterålen, Norway.” *Journal of Petrology* 45 (9): 1799–1819.

Corfu, F., P. E. B. Armitage, K. Kullerud, and S. G. Bergh. 2003a. “Preliminary U-Pb Geochronology in the West Troms Basement Complex, North Norway: Archaean and Palaeoproterozoic Events and Younger Overprints.” *Norges Geologiske Undersøkelse Bulletin* 441: 61–72.

Corfu, F., K. Kullerud, and S. G. Bergh. 2006. “U-Pb Constraints on the Late Palaeoproterozoic Evolution of the West Troms Basement Complex, Northern Norway (Abstract).” *Geological Society of Finland Bulletin, Special Issue 1*: 23.

Corfu, F., E. J. K. Ravna, and K. Kullerud. 2003b. “A Late Ordovician U-Pb Age for the Tromsø Nappe Eclogites, Uppermost Allochthon of the Scandinavian Caledonides.” *Contributions to Mineralogy and Petrology* 145 (4): 502–513.

Corfu, F., R. J. Roberts, T. H. Torsvik, L. D. Ashwal, and D. M. Ramsay. 2007. “Peri-Gondwanan Elements in the Caledonian Nappes of Finnmark, Northern Norway: Implications for the Paleogeographic Framework of the Scandinavian Caledonides.” *American Journal of Science* 307 (2): 434–458. doi:10.2475/02.2007.05.

Dalland, A. 1981. “Mesozoic Sedimentary Succession at Andøya, Northern Norway, and Relation to Structural Development of the North Atlantic Area. In: Geology of the North Atlantic Borderlands (edited by Kerr, J. W. & Fergusson, A. J.).” *Canadian Society of Petroleum Geologist Memoir* 7: 563–584.

Dallmeyer, R. D. 1988. “Polyphase Tectonothermal Evolution of the Scandinavian Caledonides.” *Geological Society, London, Special Publications* 38 (1): 365–379.

Dallmeyer, R. D. 1992. “40Ar/39Ar Mineral Ages Within the Western Gneiss Terrane, Troms, Norway: Evidence for Polyphase Proterozoic Tectonothermal Activity (Svecokarilian and Sveconorwegian).” *Precambrian Research* 57: 195–206.

Davids, C., J. A. Benowitz, and P. Layer. 2012a. “Constraining the Caledonian Tectonic Overprint in a Precambrian Gneiss Terrane in Northern Norway.” *Thermo 2012, 13th International Conference on Thermochronology 2012-08-24 - 2012-08-28*

Davids, C., S. G. Bergh, K. Wemmer, and P. Layer. 2010. “K-Ar and 40Ar/39Ar Dating of Post Caledonian Brittle Faults in Northern Norway.” *Thermo 2010, 12th International Conference on Thermochronology, Glasgow, UK, 16-20 August 2010*.

Davids, C., F. Kohlmann, J-A Hansen, J. A. Benowitz, P. Layer, and J. Jacobs. 2012b. “Post-Caledonian Onshore Exhumation History of Troms, Northern Norway, as Constrained by K-feldspar 40Ar/39Ar and Apatite Fission Track Thermochronology.” *Abstract and Proceedings of the Geological Society of Norway. Onshore-Offshore Relationship*

on the North Atlantic Margin, Trondheim, October 17-18, 2012. NGF. Number 2, 2012.

Davidsen, B., A. Sommaruga, and R. Bøe. 2001. "Final Report: Sedimentation, Tectonics and Uplift in Vesterålen. Phase 1 - Localizing Near-shore Faults and Mesozoic Sediment Basins." *NGU Report* 111: 16.

Doré, A. G., E. R. Lundin, C. Fichler, and O. Olesen. 1997. "Patterns of Basement Structure and Reactivation Along the NE Atlantic Margin." *Journal of the Geological Society* 154 (1): 85–92.

Dyer, R. 1988. "Using Joint Interactions to Estimate Paleostress Ratios." *Journal of Structural Geology* 10 (7): 685–699.

Eig, K., and S. G. Bergh. 2011. "Late Cretaceous–Cenozoic Fracturing in Lofoten, North Norway: Tectonic Significance, Fracture Mechanisms and Controlling Factors." *Tectonophysics* 499 (1-4): 190–205.

Eig, K., S. G. Bergh, T. Henningsen, O. S. Kløvjan, and O. Olesen. 2008a. "Kinematics and Relative Timing of Brittle Faults and Fractures in Lofoten, North Norway: Constraint s on the Structural Development of the Lofoten Margin." *Unpublished PhD-thesis, University of Tromsø.*

Eig, K., T. Henningsen, O. Olesen, S. G. Bergh, and J-A Hansen. 2008b. "Crustal Scale Inherited Late Caledonian and Devonian Structures as a Framework for Mesozoic to Cenozoic Development of the Lofoten-Vesterålen Margin, North Norway." *Unpublished PhD-thesis, University of Tromsø.*

Faleide, J. I., F. Tsikalas, A. J. Breivik, R. Mjelde, O. Ritzmann, O. Engen, J. Wilson, and O. Eldholm. 2008. "Structure and Evolution of the Continental Margin Off Norway and the Barents Sea." *Episodes* 31 (1): 82.

Faleide, J. I., E. Vågnes, and S. T. Gudlaugsson. 1993. "Late Mesozoic-Cenozoic Evolution of the South-western Barents Sea in a Regional Rift-shear Tectonic Setting." *Marine and Petroleum Geology* 10: 186–214.

Forslund, T. 1988. "Post-Kaledonske Forkastninger i Vest-Troms, Med Vekt På Kvaløyslettaforkastningen, Kvaløya." *Hovedfagsoppgave i Geologi, Universitetet i Tromsø.*

Fürsich, F. T., and E. Thomsen. 2005. "Jurassic Biota and Biofacies in Erratics from the Sortland Area, Vesterålen, Northern Norway." *Geological Survey of Norway Bulletin* 443: 37–53.

Gabrielsen, R. H., R. B. Færseth, L. N. Jensen, J. E. Kalheim, and F. Riis. 1990. "Structural Elements of the Norwegian Continental Shelf — Part I: The Barents Sea Region." *Norwegian Petroleum Directorate Bulletin* 6: 33.

Gabrielsen, R. H., I. Grunnaleite, and E. Rasmussen. 1997. "Cretaceous and Tertiary Inversion in the Bjørnøyrenna Fault Complex, South-western Barents Sea." *Marine and Petroleum Geology* 14 (2): 165–178.

Gagama, M. F. V. 2005. "Strukturell Analysa Av Post-kaledonske Lineamenter Ved Sifjorden, Vest-Senja, Troms." *Unpublished Master Thesis, University of Tromsø.*

Gibbs, A. D. 1984. "Structural Evolution of Extensional Basin Margins." *Journal of the Geological Society* 141 (4): 609–620.

Griffin, W. L., P. N. Taylor, J. W. Hakkinen, K. S. Heier, I. K. Iden, E. J. Krogh, O. Malm, K. I. Olsen, D. E. Ormaasen, and E. Tveten. 1978. "Archaean and Proterozoic Crustal Evolution in Lofoten–Vesterålen, N Norway." *Journal of the Geological Society* 135 (6): 629–647.

Gudlaugsson, S. T., J. I. Faleide, S. E. Johansen, and A. J. Breivik. 1998. "Late Palaeozoic Structural Development of the South-western Barents Sea." *Marine and Petroleum Geology* 15 (1): 73–102.

Hansen, J-A, and S. G. Bergh. 2012. “Origin and Reactivation of Fracture Systems Adjacent to the Mid-Norwegian Continental Margin on Hamarøya, North Norway: Use of Digital Geological Mapping and Morphotectonic Lineament Analysis.” *Norwegian Journal of Geology* 92: 391–403.

Hansen, J-A, S. G. Bergh, and T. Henningsen. 2012. “Mesozoic Rifting and Basin Evolution on the Lofoten and Vesterålen Margin, North-Norway; Time Constraints and Regional Implications.” *Norwegian Journal of Geology* 91: 203–228.

Hansen, J-A, S. G. Bergh, O. Olesen, and T. Henningsen. 2009. “Onshore and Offshore Fault Correlation on the Lofoten and Vesterålen Margin – Architecture, Evolution and Basement Control.” *Unpublished PhD-thesis, University of Tromsø.*

Hansen, J-A, C. Davids, and S. G. Bergh. 2011. “Brittle Fault Zones in North Norway: Onshore – Offshore Link and Regional Implications.” *Unpublished Poster, University of Tromsø.*

Hendriks, B. W. H., P. T. Osmundsen, and T. F. Redfield. 2010. “Normal Faulting and Block Tilting in Lofoten and Vesterålen Constrained by Apatite Fission Track Data.” *Tectonophysics* 485 (1-4): 154–163.

Indrevær, K. 2011. “The Tromsø Nappe Contact with the Nakkedal Nappe Complex NE of Tromsdalstind: Shear Kinematics and Relationship with Metamorphism.” *Unpublished Master Thesis, University of Tromsø.*

Indrevær, K., S. G. Bergh, J-B Koehl, J-A Hansen, E. Schermer, and A. Ingebrigtsen. 2013. “Onshore-Offshore Correlation of post-Caledonian Brittle Fault Zones on the Hyper-extended SW Barents Sea Margin: New Insights into the Margin Architecture.” *Norwegian Journal of Geology, Onshore-Offshore Relationships*.

Keulen, N., H. Stünitz, and R. Heilbronner. 2008. “Healing Microstructures of Experimental and Natural Fault Gouge.” *Journal of Geophysical Research* 113 (B6).

Kim, Y-S, and D. J. Sanderson. 2005. “The Relationship Between Displacement and Length of Faults: a Review.” *Earth-Science Reviews* 68 (3-4): 317–334.

Knutsen, M. L. 2012. “Polymetamorphic Evolution of Nepheline Normative Rocks in the Skattøra Migmatite Complex, Tromsø, North Norway.” *Unpublished Master Thesis, University of Tromsø.*

Knutsen, S. M., and K. I. Larsen. 1997. “The Late Mesozoic and Cenozoic Evolution of the Ssrvestsnaget Basin: A Tectonostratigraphic Mirror for Regional Events Along the Southwestern Barents Sea Margin?” *Marine and Petroleum Geology* 14 (1): 27–54.

Krogh, E. J., A. Andresen, I. Bryhni, T. M. Broks, and S. E. Kristensen. 1990. “Eclogites and Polyphase P–T Cycling in the Caledonian Uppermost Allochthon in Troms, Northern Norway.” *Journal of Metamorphic Geology* 8: 289–309.

Kullerud, K., F. Corfu, S. G. Bergh, B. Davidsen, and E. J. K. Ravna. 2006. “U-Pb Constraints on the Archaean and Early Proterozoic Evolution of the West Troms Basement Complex, North Norway (Abstract).” *Bulletin of the Geological Society of Finland Special Issue I*: 79.

Kullerud, K., K. P. Skjerlie, F. Corfu, and J. D. de la Rosa. 2006b. “The 2.40Ga Ringvassøy Mafic Dykes, West Troms Basement Complex, Norway: The Concluding Act of Early Palaeoproterozoic Continental Breakup.” *Precambrian Research* 150 (3-4): 183–200.

Larssen, G. B., G. Elvebakk, L. B. Henriksen, S. E. Kristensen, I. Nilsson, T. J. Samuelsberg, T. A. Svånå, L. Stemmerik, and D. Worsley. 2002. “Upper Palaeozoic Lithostratigraphy of the Southern Norwegian Barents Sea.” *Norwegian Petroleum Directorate Bulletin* 9.

Lindstrøm, M., and A. Andresen. 1992. “Early Caledonian High-grade Metamorphism Within Exotic Terranes of the Troms Caledonides?” *Norsk Geologisk Tidsskrift* 72 (4): 375–379.

Lister, G. S., and G. A. Davis. 1989. “The Origin of Metamorphic Core Complexes and Detachment Faults Formed During Tertiary Continental Extension in the Northern Colorado River Region, USA.” *Journal of Structural Geology* 11 (1): 65–94.
Løseth, H., and E. Tveten. 1996. “Post-Caledonian Structural Evolution of the Lofoten and Vesterålen Offshore and Onshore Areas.” *Norsk Geologisk Tidsskrift* 76: 215–230.
Maddock, R. H., J. Grocott, and M. Van Nes. 1987. “Vesicles, Amygdales and Similar Structures in Fault-generated Pseudotachylytes.” *Lithos* 20 (5): 419–432.
McGrath, A. G., and I. Davison. 1995. “Damage Zone Geometry Around Fault Tips.” *Journal of Structural Geology* 17 (7): 1011–1024.
Morley, C. K., R. A. Nelson, T. L. Patton, and S. G. Munn. 1990. “Transfer Zones in the East African Rift System and Their Relevance to Hydrocarbon Exploration in Rifts.” *The American Association of Petroleum Geologists Bulletin* 74 (8): 1234–1253.
Mosar, J., E. A. Eide, P. T. Osmundsen, A. Sommaruga, and T. H. Torsvik. 2002. “Greenland-Norway Separation: a Geodynamic Model for the North Atlantic.” *Norsk Geologisk Tidsskrift* 82 (4): 281–298.
Motuza, G. 1998. “Description to the Geological Map of the Eastern Part of Kvaløya, Troms County, Northern Norway.” *NGU Report* 111: 18.
Motuza, G., V. Motuza, B. Beliatsky, and E. Savva. 2001. “Volcanic Rocks of the Ringvassoya Greenstone Belt (North Norway): Implication for the Stratigraphy and Tectonic Setting (Abstract).” *Journal of Conference EUG XI, 6(1), 578.*
Myhre, P. I., and F. Corfu. 2008. “Titanite Versus Zircon U-Pb-systematics; Tracing Multiple Episodes of Metamorphism and Intrusion in Precambrian Rocks of the West Troms Basement Complex (abstract).” *33rd International Geological Congress, Oslo.*
Myhre, P. I., F. Corfu, and S. G. Bergh. 2009. “The Palaeoproterozoic (1995-1950 Ma) Pre-Orogenic Supracrustal Sequences in the West Troms Gneiss Region, Arctic Norway.” *Eos Trans. AGU, 90(22), GA74A-07.*
Olesen, O., J. Ebbing, E. Lundin, E. Mauring, J. R. Skilbrei, T. H. Torsvik, E. K. Hansen, T. Henningsen, P. Midbøe, and M. Sand. 2007. “An Improved Tectonic Model for the Eocene Opening of the Norwegian–Greenland Sea: Use of Modern Magnetic Data.” *Marine and Petroleum Geology* 24 (1): 53–66.
Olesen, O., T. H. Torsvik, E. Tveten, and K. B. Zwaan. 1993. “The Lofoten-Lopphavet Project - an Integrated Approach to the Study of a Passive Continental Margin.” *NGU Report* 93. 129: 54.
Olesen, O., T. H. Torsvik, E. Tveten, K. B. Zwaan, H. Løseth, and T. Henningsen. 1997. “Basement Structure of the Continental Margin in the Lofoten-Lopphavet Area, Northern Norway: Constraints from Potential Field Data, On-land Structural Mapping and Palaeomagnetic Data.” *Norsk Geologisk Tidsskrift* 77: 15–30.
Oliver, G. J. H., and E. J. Krogh. 1995. “U–Pb Zircon Age of 469±5 Ma for the Kjosen Unit of the Lyngen Magmatic Complex, Northern Norway.” *Norges Geologiske Undersøkelse Bulletin* 426: 27–33.
Osmundsen, P. T., A. Braathen, A. Sommaruga, J. R. Skilbrei, Ø. Nordgulen, D. Roberts, T. B. Andersen, O. Olesen, and J. Mosar. 2005. “Metamorphic Core Complexes and Gneiss-cored Culminations Along the Mid-Norwegian Margin: An Overview and Some Current Ideas.” *Norwegian Petroleum Society Special Publications* 12: 29–41.
Passchier, C. W., and R. A. J. Trouw. 2005. *Microtectonics*. Berlin; New York: Springer.
Peacock, D. C. P., R. J. Knipe, and D. J. Sanderson. 2000. “Glossary of Normal Faults.” *Journal of Structural Geology* 22 (3): 291–305.
Roberts, D. 2003. “The Scandinavian Caledonides: Event Chronology, Palaeogeographic Settings and Likely Modern Analogues.” *Tectonophysics* 365 (1-4): 283–299.

Roberts, D., and S. J. Lippard. 2005. “Inferred Mesozoic Faulting in Finnmark: Current Status and Offshore Links.” *Norges Geologiske Undersøkelse Bulletin, 55* 60.

Roberts, D., Ø. Nordgulen, and V. Melezhik. 2007. “The Uppermost Allochthon in the Scandinavian Caledonides: From a Laurentian Ancestry through Taconian Orogeny to Scandian Crustal Growth on Baltica.” *Geological Society of America Memoirs* 200: 357–377.

Root, K. G. 1990. “Extensional Duplex in the Purcell Mountains of Southeastern British Columbia.” *Geology* 18 (5): 419.

Selbekk, R. S., K. P. Skjerlie, and R. B. Pedersen. 2000. “Generation of Anorthositic Magma by H2O-fluxed Anatexis of Silica-undersaturated Gabbro: An Example from the North Norwegian Caledonides.” *Geological Magazine* 137 (06): 609–621.

Steltenpohl, Mark G., David Moecher, Arild Andresen, Jacob Ball, Stephanie Mager, and Willis E. Hames. 2011. “The Eidsfjord Shear Zone, Lofoten–Vesterålen, North Norway: An Early Devonian, Paleoseismogenic Low-angle Normal Fault.” *Journal of Structural Geology* 33 (5) (May): 1023–1043.

Steltenpohl, Mark G., Brad T. Carter, Arild Andresen, and Daniel L. Zeltner. 2009. “Ar Thermochronology of Late- and Postorogenic Extension in the Caledonides of North-Central Norway.” *The Journal of Geology* 117 (4) (July): 399–414.

Thorstensen, L. 2011. “Land-sokkel Korrelasjon Av Tektoniske Elementer i Ytre Del Av Senja Og Kvaløya i Troms.” *Unpublished Master Thesis, University of Tromsø*.

Tsikalas, F., O. Eldholm, and J. I. Faleide. 2005. “Crustal Structure of the Lofoten–Vesterålen Continental Margin, Off Norway.” *Tectonophysics* 404 (3-4): 151–174.

Tsikalas, F., J. I. Faleide, and O. Eldholm. 2001. “_____Lateral Variations in Tectono-magmatic Style Along the Lofoten-Vesterålen Volcanic Margin Off Norway.” *Marine and Petroleum Geology* 18: 807–832.

Tsikalas, F., J. I. Faleide, and N. J. Kusznir. 2008. “Along-strike Variations in Rifted Margin Crustal Architecture and Lithosphere Thinning Between Northern Vøring and Lofoten Margin Segments Off mid-Norway.” *Tectonophysics* 458 (1-4): 68–81.

Tveten, E., and K. B. Zwaan. 1993. “Geology of the Coast Region from Lofoten to Loppa, with Special Emphasis on Faults, Joints and Related Structures.” *NGU Report* 93. 083: 25.

Watterson, J. 1986. “Fault Dimensions, Displacements and Growth.” *Pure and Applied Geophysics* 124 (1-2): 365–373.

Wilson, R. W., K. J. W. McCaffrey, R. E. Holdsworth, J. Imber, R. R. Jones, A. I. F. Welbon, and D. Roberts. 2006. “Complex Fault Patterns, Transtension and Structural Segmentation of the Lofoten Ridge, Norwegian Margin: Using Digital Mapping to Link Onshore and Offshore Geology.” *Tectonics* 25 (4): 28.

Woodcock, N. H., and M. Fischer. 1986. “Strike-slip Duplexes.” *Journal of Structural Geology* 8 (7): 725–735.

Zwaan, K. B. 1995. “Geology of the West Troms Basement Complex, Northern Norway, with Emphasis on the Senja Shear Belt: a Preliminary Account.” *Norges Geologiske Undersøkelse, Bulletin* 427: 33–36.

Zwaan, K. B., E. Fareth, and P. W. Grogan. 1998. “Geologiske Kart over Norge, Berggrunnskart TROMSØ, M: 1:250000.” *Norges Geologiske Undersøkelse*.


UNIVERSITY
OF TROMSØ